The importance of regulating neurite dynamics during cortical neuron migration

By
Russell J. Taylor

A dissertation submitted in partial fulfillment of
The requirements for the degree of

Doctor of Philosophy
(Neuroscience Training Program)

At the
UNIVERSITY OF WISCONSIN-MADISON
2021

Date of final oral examination: 6/2/21

The dissertation is approved by the following members of the Final Oral Committee:
Erik Dent, Professor, Neuroscience
Anjon Audhya, Professor, Genetics
William Bement, Professor, Integrative Biology
Anita Bhattacharyya, Assistant Professor, Cell and Regenerative Biology
Timothy Gomez, Professor, Neuroscience

Table of Contents

Acknowledgements

No one completes graduate school alone, and I have certainly been no exception. There have been many people who helped me along my path, starting in childhood and continuing through to today. I cannot adequately thank them, but I can at least in part acknowledge their contributions here.

Thank you to my friend and mentor, Erik Dent. He has been everything I could ask for - kind, curious, understanding, crazy smart. Erik has always managed to walk a difficult tightrope - he has provided fantastic amounts of leeway in project design, while simultaneously being ever-present for advice, congratulations and commiserations. I cannot think of anyone else who I would have rather worked under for the last five years.

Thank you to my thesis committee. Jon Audhya, Bill Bement, Anita Bhattacharyya, Tim Gomez and Kate O'Connor-Giles have been wonderfully helpful and have done a great job of guiding me throughout graduate school. You have provided much needed pushback and guidance, and I have relied upon all of you to accomplish what I have done.

Thank you to all the wonderful people and personalities of the Dent Lab. The lab would not have been a place I continued to enjoy if not for all the people I interacted with every day. Kendra Taylor taught me so much more than she will ever admit. Lauren and Lizzi have been my allies and friends through this final slog, and put up with a lot, probably more than was appropriate. Karl and Tanner have both been people I look forward to seeing every day, as well as people I look forward to leaving every day. Matt, Chandra, Kara and Derek have all been unofficial mentors, and I have learned large and small lessons from each of you.

Thank you to all the labs of the fifth floor. Gomez, Huang, Roopra, Moore and Murphy labs are made up of the most friendly, helpful people I could have asked for.

Thank you to Maeve, Justin and Leah, my OG army. You guys were amazing people to mentor, and I got so much more back than I ever put in.

Thank you to Connor, Emily and Rory. I haven't spent as much time with any of you as I would have liked to have, but I relied on all of you, and you have all done amazing work.

Thank you to all the people who helped me get into research, and all the people who helped me stay into research. Ms. Lee, Mr. Weisner, Mrs. Howard, Mr. O'Neal, Mr. Sprague, Mr. Affeldt were all instrumental in developing my love for science. Dan Kaufman, Xingui Tian, Tom Reh and Olivia Bermingham-McDonogh took that love, and taught me the tools and confidence required to thrive.

Thanks to my family - Mom and Dad, Ann and Wayne, Christie and Joe, Kenny and Jen, and all the rest. You guys haven't always understood what I'm doing, but you have always supported me because you believed in me. I love you all.

Thank you Leon. You are the keeper of all my happiness, I have never had a bad day when I am with you. I love you.

Thank you Ingrid. You have been incredibly loving and supportive, and we only survived this by being together. I am so proud of you, of us. I would do it all over again, as long as you are with me. That being said, let's never do this again. I love you.

Abstract

Development and differentiation of mammalian excitatory cortical neurons is a highly complex process, involving extreme morphological alterations and requiring close coordination of the actin cytoskeleton and plasma membrane. This process has been well studied *in vitro*, but *in vivo* studies are lagging significantly due to technical limitations. Here, I introduce a significant improvement (Double UP) to an already existing technique (*in utero* electroporation), to allow for internal controls, while reducing variability and the number of animals required. This improvement has simultaneously increased statistical strength and decreased difficulty of analysis. I then implement this new technique to examine the effects of modulating expression of the F-BAR protein CIP4 on neuronal migration and differentiation *in vivo*. CIP4 is unusual in that it is only expressed in the cortex prenatally and coordinates the actin cytoskeleton and plasma membrane to repress neurite formation *in vitro*. However, the role of CIP4 in radial neuron migration and differentiation *in vivo* is unclear, including the timing and manner of neurite repression. Relying heavily on Double UP, I show that either knockdown or overexpression of CIP4 results in the marked disruption of radial neuron migration, by increasing or decreasing neurite number and length, respectively. Based on these results I propose a new model whereby CIP4 is critical for cortical neurite retraction, which allows neurons to exit the multipolar phase and resume radial migration as bipolar neurons.

Chapter 1:

Introduction to Cortical Neuronal Migration

Introduction

A fully developed human brain is comprised of almost one hundred billion neurons, and almost one hundred billion non-neuronal cells as well (Herculano-Houzel, 2012). The development of this most-critical organ is very structured and stereotyped, as reflected by the high degree of anatomical similarity between humans. This process of brain development begins as early as the third gestational week, with the development of the neural tube, and is not considered complete until around 20 years after birth. How the brain matures is of great interest, as departures from normal development result in a wide range of disorders, including lissencephaly, autism, cerebral palsy and schizophrenia, to name a few. Some disorders are the result of individual genes or individual chromosomes being altered, like Lissencephaly (Reiner et al., 1993) or Down Syndrome (Lejeune, Gautier, & Turpin, 1959), respectively. Understanding the genetic cause of disorders relating to neuronal migration is a powerful way to identify genes important for normal neuronal migration. Identification of key genes is more straightforward when the mutations are located within individual genes, as is common with Lissencephaly. Study of individuals with Lissencephaly has led to identification of critical neurodevelopmental genes, including both LIS1 (Reiner et al., 1993) and DCX (Gleeson, Lin, Flanagan, & Walsh, 1999). LIS1 is important for coordination of the nucleus and centrosome during migration (Shu et al., 2004; Tanaka et al., 2004), whereas loss of DCX leads to a decrease in progenitor proliferation and subsequent decrease in cortical thickness (Gleeson et al., 1999). Other disorders, like autism spectrum disorders and attention deficit hyperactivity disorder result from a wide range of genetic and environmental contributions, with no single or dominant cause identifiable (Chaste & Leboyer, 2012; Faraone et al., 2015). To

systematically address disorders with many contributing factors, it is essential to understand how typical development progresses.

Normal Cortical Development

To be able to address and treat neurodevelopmental disorders we need a greater understanding of how neurodevelopment typically occurs. Only by first understanding the intricacies of normal development can the greater scientific and medical community systematically address, treat and potentially cure neurodevelopment gone awry.

If a major goal of studying neuronal development is to develop therapeutics to prevent or lessen the impacts of developmental disorders in humans, it seems logical that studies should focus primarily on humans. There is an increasing body of research involving newborn infants and functional magnetic resonance imaging (Ellis & Turk-Browne, 2018; Morita, Asada, & Naito, 2016; Seghier, Lazeyras, & Huppi, 2006), but studies in neurodevelopment in humans are limited primarily to descriptive analysis and postmortem studies. These types of studies can be highly informative, but are limited in scope. To compliment and inform these studies, researchers use *in vitro* culture systems and model organisms, each with their distinctive advantages and disadvantages, to study neuronal development. There are many to choose from, but some of have gained prominence through a combination of historical momentum (tools being developed early on to allow for easier research), relevance to human development, and issues relating to cost and rate of reproduction. Some of the most popular model organisms, from most simple to most complex, include: *C. elegans, Drosophila*, zebrafish, *Xenopus laevis*, mice, rats, non-human

primates and humans. As one climbs the ladder of complexity from *C. elegans* to humans, there are tradeoffs that must be considered. Organisms more closely related to humans are more directly relevant to human conditions, and both genetic and protein structure is more similar between more closely related organisms. However, this is offset by greater cost, longer gestational periods and more complex scientific procedures. As such, careful consideration should be given when determining the appropriate organism for undertaking a research study.

Each of 302 neurons present with *Caenorhabditis elegans* (*C. elegans*) has been described and mapped (White, Southgate, Thomson, & Brenner, 1986), and more recently the connectivity of each neuron to each other neuron has also been mapped (Cook et al., 2019). Understanding the lifespan and connectivity of each individual neuron is a great tool for studying circuits, but at the expense of fewer cells, a vastly more simple brain and correspondingly much more simple behaviors than higher order animals. *Drosophila* have a nervous system orders of magnitude larger than *C. elegans*, have an easily manipulatable genome and fast breeding time, allowing it to be a powerful tool in linking genetics and behavior of individual neurons and circuits. Zebrafish and larval *Xenopus laevis* are translucent, allowing for high resolution imaging at both temporal and spatial scales. Mice are much more similar to humans than any of the above-mentioned species, and the smallest of the commonly used research models to have a cerebral cortex. Getting more “human-like” than mice, the order of commonly used models would be rats, non-human primates and of course, humans. Rats are larger than mice and have a much richer suite of behavioral characteristics, allowing for more targeted surgery and behavioral outcomes. Non-human primates are larger and much more complex, more closely mimicking humans in many regards. Study of neuronal development in humans is largely limited to descriptive studies and

clinical trials. Each model outlined here has risen to prominence due to occupying a niche of usefulness and relevance. The work presented here focuses on cell migration and the behavior of individual neurons in the developing somatosensory cortex, and therefore relies entirely on mice, as the development of an individual neuron is roughly comparable between mice and humans.

Cortical neuron development can be studied in monolayer cultures (Bartlett and Banker, 1984), in organoid cultures (Lancaster & Knoblich, 2014), or in *in vivo* (Saito & Nakatsuji, 2001; Tabata & Nakajima, 2001), and again there are tradeoffs and limitations. Dissociated neurons, whether from primary cultures or derived from either embryonic stem cells (ESCs) or induced pluripotent stem cells (iPSCs) are easier to work with, manipulate and image over time, but with that simplification comes a loss of something important, the cellular environment, and thus directional information and cues that are present in an intact brain. Organoids recapitulate the three dimensionality and some of the cellular environment of a brain, but can be variable, difficult to grow, expensive to use, and are unable to expand to a size comparable to an actual brain. Neurons in an intact developing brain are harder to study because manipulating individual cells is much more complex. Additionally, the very dense nature of neurons in the brain can make it challenging or impossible to distinguish one neuron from another, or to track the entirety of an elongated neuron through three dimensions. However, several key features are completely absent from *in vitro* studies, including directed migration and spatial cues relating to axon targeting and/or dendritic branching. These phenomena can be recapitulated to a limited and artificial degree *in vitro*, but for a full picture must be studied *in vivo*.

Thus, each research model serves as an approximation of human development, but none recapitulate it. Non-human primates and human ESC/iPSCs are the closest equivalent, but the ability to manipulate individual neurons in non-human primates is limited and both two and three-dimensional culture of ESCs and iPSCs are still only approximations of the intricacy of intact brains.

Mice were determined to be the appropriate organism for this study, as they have a cerebral cortex, well-established techniques allow for manipulation of individual neurons within live animals, and they are inexpensive relative to other organisms with a cerebral cortex. This combination of factors allows for thorough examination of the role of individual genes through overexpression or knockout studies at a moderate throughput level.

Cortical Development *in vitro* and *in vivo*

Many commonalities remain between development of mouse neurons *in vitro* and *in vivo*. Stages of primary hippocampal neuron development were first carefully delineated *in vitro* by Dotti and colleagues (Dotti, Sullivan, & Banker, 1988). Subsequently, it was determined that neocortical neurons also progress through these stereotyped stages of development *in vitro* (de Lima,

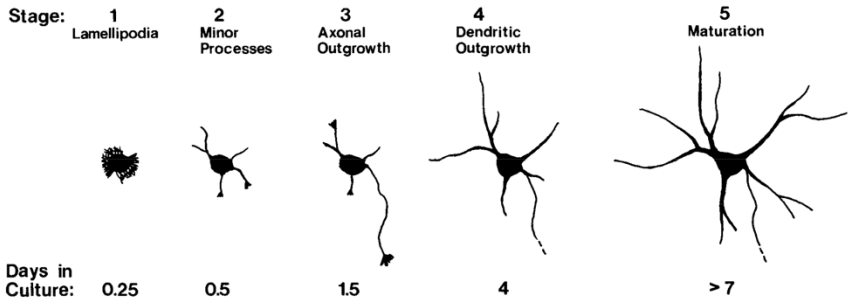

Figure 1. Neuronal Development *in vitro*. Within about six hours of a neuron being plated on a permissive substrate, lamellipodia expand around much of the cell body. These lamellipodia coalesce into neurites, then one neurite becomes longer and dominant, which is the presumed axon. Following axonal specification, the other processes become dendrites. Diagram from Dotti, 1988

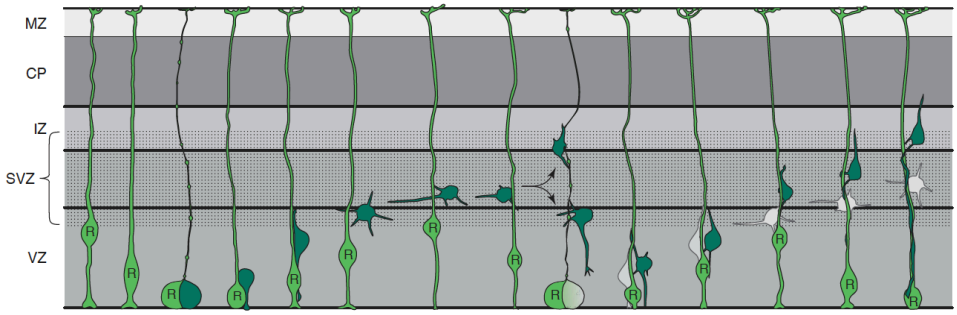

Figure 2. Generation of a new neuron *in vivo*. Time advances on the Y-axis. A radial glia (R) makes contact with the ventricle, and divides into two cells. Depicted is the most common division, an asymmetric division. The radial glia (light green) remains in place as the newly born neuron (dark green) extends a leading process, and moves from the ventricular zone (VZ) into the subventricular (SVZ) and intermediate zone (IZ). Here, it enters into a multipolar phase, extending neurites. Upon exiting this multipolar phase, it can either continue traversing towards the cortical plate (CP), or it can return towards the ventricle, before ultimately beginning its trip to the cortical plate. Diagram from Noctor, 2004

Merten, & Voigt, 1997). Newly dissociated neurons start out as round cells partially surrounded by flat, veil like structures termed lamellipodia (Intro Figure 1). These neurons then break symmetry by extending a prominent extension called a neurite (also referred to as a minor process), followed by several more neurites. After extending several neurites, one neurite begins to grow rapidly and becomes the axon, while the others develop into dendrites over several days (Intro Figure 1). Exact timing varies from cell to cell, and use of different culture techniques can alter timing of events, but this is the general time-course of development of hippocampal or cortical excitatory neurons. This progression of neuronal development *in vitro* appears morphologically similar to neuronal development *in vivo* (Intro Figure 2), but lacks the spatial context. *In vivo*, excitatory pyramidal neurons in the cortex are born as round cells at the ventricular surface, which break symmetry by extending a neurite (Intro Figure 2) (Miyata, Kawaguchi, Okano, & Ogawa, 2001; Noctor, Martinez-Cerdeno, Ivic, & Kriegstein, 2004). However, this neurite is attached to a radial glia cell (progenitor cell), is oriented towards the pial surface, and acts to pull the neuron towards the pial surface and cortical plate. Once the cell has migrated away from the ventricle, it enters the subventricular zone and intermediate zone. Here,

it enters a multipolar phase, in which the neuron extends and retracts multiple neurites (Tabata & Nakajima, 2003). While the exact purpose of this multipolar phase remains unclear, it has been proposed that the neuron may be searching for environmental cues (Tabata & Nakajima, 2003), as each of the multiple neurites behave in a manner similar to that seen in axonal growth cones (Halloran & Kalil, 1994). Following the multipolar phase, one of two things happens. Either the cell continues migrating towards the cortical plate, or it returns to the ventricle, makes contact, and then begins its journey towards the cortical plate (Intro Figure 2) (Noctor et al., 2004). Both of these types of migration patterns occur through contact with radial glial cells.

Neurite Formation

As outlined above, much of our understanding of early neuronal development involves analysis of neurites. Neurites are clearly important, as they become both an axon and dendrites and are involved in migration. Additionally, the ease with which neurites can be observed and measured has meant that historically they were the first clear morphological component that could be measured as a neuron developed (Dotti et al., 1988). As such, there is a good understanding of the nature of neurite development *in vitro*. Newly plated cells form broad, segmented, actin-rich lamellipodia, tipped by filopodia. If these filopodia are prevented from forming by genetic means or treatment with drugs, the neuron does not develop neurites, and instead remains as a spherical cell surrounded by lamellipodia (Dent et al., 2007). Over time, lamellipodia coalesce and form much more stable neurites, which are both actin rich and contain microtubules (Dehmelt, Smart, Ozer, & Halpain, 2003). There is not a definitive definition at which point a protrusion

becomes a neurite, but the general consensus is that a protrusion containing either stable microtubules or a distal growth cone is a neurite (Dent et al., 2007).

Many of the proteins involved in neurite formation either directly interact with the cytoskeleton, or are signaling molecules that act one step removed from the cytoskeleton, as neurites form from either actin-rich lamellipodia or filopodia (Dent et al., 2007). Additionally, the two hallmarks of neurite formation (having an actin-rich growth cone and/or stable microtubules) are by definition cytoskeletal elements. As a consequence, perturbations to normal cytoskeletal dynamics often result in disruptions to neurite initiation or formation. Cytoskeletal-associated proteins that influence neurite formation include the family of small Rho-GTPases, especially Rac1 (de Curtis, 2008; Govek, Newey, & Van Aelst, 2005) and Cdc42 (Kozma, Sarner, Ahmed, & Lim, 1997), which define regions of activity in large and small regions of cells. There are also more local actors, like srGAP2 (Guerrier et al., 2009; Ma et al., 2013) which localizes to filopodia and prevents neurite branching, lamellipodin (Krause et al., 2004; Pinheiro et al., 2011) which is necessary for Arp2/3-mediated lamellipodia to form, and the Ena/Vasp family of proteins (Dent et al., 2007; Kwiatkowski et al., 2007), which prevent the capping of actin barbed ends and promote filopodia formation. These proteins, along with many others, are generally thought to promote neurite outgrowth.

In contrast, there are very few proteins intrinsic to newly born neurons that are known to function to delay and inhibit neurites either *in vitro* (Saengsawang et al., 2012) or *in vivo* (Nakamura et al., 2006). This may be because initiating and extending neurites seems to be one of, if not the, primary undertaking of a newly born neuron. Thus, there have been few studies of proteins that inhibit early neurite development. Nevertheless, it is likely that neurons contain

both neurite promoting proteins and neurite inhibiting proteins to control the spatial and temporal timing of neurite formation. A prime candidate for a protein that inhibits early neurite formation is the F-BAR protein CIP4 (Aspenstrom, 1997). It is worth noting that several proteins, such as the inverse F-BAR (iF-BAR) protein srGAP2, have been reported to inhibit neurites in cell lines, such as PC-12 cells which are "neuron like" (Ma et al., 2013). However, srGAP2 induces neurites in primary neurons (Guerrier et al., 2009), indicating that primary neurons and "neuron like" cells, such as PC-12 cells, differ in their mode of neurite formation.

CIP4 inhibits neurites

F-BAR proteins act at the interface of the cytoskeleton and plasma membrane. They are named due to the F-BAR region on the (typically) N-terminus of the protein, which can sense and alter membrane curvature. When F-BAR proteins dimerize the F-BAR region forms a banana-shaped structure that binds via the concave surface to curved membrane, and is often found interacting with endocytic vesicles (Henne et al., 2007). The CIP4 family of proteins (CIP4, FBP17 and Toca-1) also have an HR-1 domain, capable of interacting with small Rho-GTPases, and an SH3 domain, capable of interacting with actin-associated proteins, such as N-WASP or WAVE (Ahmed, Bu, Lee, Maurer-Stroh, & Goh, 2010). As such, this family of proteins can be thought of as bridge proteins. They connect the signaling pathways with actin-associated proteins, while also directly binding and affecting the curvature of the plasma membrane. These proteins were discovered and classically understood to function in endocytosis, which they do in most cells (Shimada et al., 2007). However, one family member, CIP4, functions differently in one cell type, neurons. Rather than elongating endocytosing vesicles by forming end-to-end polymers around the vesicle as

does another family member FBP17 (K. L. Taylor et al., 2019), CIP4 localizes specifically to protruding plasma membrane (Saengsawang et al., 2012). Overexpression of CIP4 delays neurite initiation by forming veils between filopodia, effectively decreasing filopodia number and length (Saengsawang et al., 2012; Saengsawang et al., 2013). However, the molecular mechanism by which it acts in protrusions is still unclear. Overexpression of CIP4 results in large lamellipodia extending around the periphery of newly differentiating neurons, with CIP4 localizing to the protruding edges and preventing any neurites from forming. Conversely, knockout of CIP4 results in neurites being formed precociously *in vitro*, as much as 12 hours before wildtype counterparts (Saengsawang et al., 2012). CIP4 is expressed most highly in early mouse cortex (E10.5), decreasing to almost undetectable levels around birth (Saengsawang et al., 2012).

These *in vitro* findings, combined with the cortical expression timeline, have made CIP4 a prime candidate to study the nature and consequences of inhibiting neuritogenesis *in vivo*. Understanding the time-course of expression in newly born neurons presents an opportunity to examine the time at which neurite inhibition is critical in the life of an individual neuron. Moreover, study of the location of endogenous or expressed CIP4 protein can shed light on the molecular mechanism of neurite inhibition. By addressing the when and where of neurite inhibition, we hope to gain insight into the <u>why</u> of neurite inhibition, and in so doing gain an improved understanding of the mechanisms of neuronal migration and differentiation.

To determine the role neurite inhibition plays in cortical migration, I have utilized *In Utero* Electroporation (IUE), a surgical technique to simultaneously fluorescently label cells and manipulate genes in newly born neurons and progenitors in the developing brain (Saito & Nakatsuji, 2001; Tabata & Nakajima, 2001). First, however, I established that this technique was

highly variable, and developed a novel methodology (Double UP) to reduce this variability (R. J. Taylor et al., 2020) (Chapter 2). With this accomplished, I then used Double UP to address the migration and morphological phenotypes of perturbing CIP4 levels in developing neurons. These studies identified a novel role of CIP4 in neurite retraction, as loss of CIP4 stalled the exit of neurons from the multipolar phase of neuronal migration (Chapter 3). To determine the endogenous expression levels and localization of CIP4 I have developed a transgenic mouse through CRISPR/Cas9 technology in which endogenous CIP4 is tagged with an mScarlet protein. This work has led to the preliminary finding that CIP4 is expressed in regions of the cortex associated with progenitors and multipolar neurons, but is absent from the upper intermediate zone and cortical plate, the regions of the brain where neurons re-enter bipolar migration, and develop axons and dendrites, respectively.

Retraction of neurites in the developing cortex is a little studied phenomenon, but that does not mean it is unimportant. By undertaking these studies, I hope to improve understanding of neurite retraction in migrating neurons, and in so doing develop a more complete model of the cellular intricacies involved in neuronal migration. Understanding the ways in which normal migration occurs will better position us for determining how migration goes awry in disorders of cortical development.

References

Ahmed, S., Bu, W., Lee, R. T., Maurer-Stroh, S., & Goh, W. I. (2010). F-BAR domain proteins: Families and function. *Commun Integr Biol, 3*(2), 116-121. doi:10.4161/cib.3.2.10808

Aspenstrom, P. (1997). A Cdc42 target protein with homology to the non-kinase domain of FER has a potential role in regulating the actin cytoskeleton. *Curr Biol, 7*(7), 479-487. doi:10.1016/s0960-9822(06)00219-3

Chaste, P., & Leboyer, M. (2012). Autism risk factors: genes, environment, and gene-environment interactions. *Dialogues Clin Neurosci, 14*(3), 281-292. Retrieved from https://www.ncbi.nlm.nih.gov/pubmed/23226953

Cook, S. J., Jarrell, T. A., Brittin, C. A., Wang, Y., Bloniarz, A. E., Yakovlev, M. A., . . . Emmons, S. W. (2019). Whole-animal connectomes of both Caenorhabditis elegans sexes. *Nature, 571*(7763), 63-71. doi:10.1038/s41586-019-1352-7

de Curtis, I. (2008). Functions of Rac GTPases during neuronal development. *Dev Neurosci, 30*(1-3), 47-58. doi:10.1159/000109851

de Lima, A. D., Merten, M. D., & Voigt, T. (1997). Neuritic differentiation and synaptogenesis in serum-free neuronal cultures of the rat cerebral cortex. *J Comp Neurol, 382*(2), 230-246. doi:10.1002/(sici)1096-9861(19970602)382:2<230::aid-cne7>3.0.co;2-4

Dehmelt, L., Smart, F. M., Ozer, R. S., & Halpain, S. (2003). The role of microtubule-associated protein 2c in the reorganization of microtubules and lamellipodia during neurite initiation. *J Neurosci, 23*(29), 9479-9490. Retrieved from https://www.ncbi.nlm.nih.gov/pubmed/14573527

Dent, E. W., Kwiatkowski, A. V., Mebane, L. M., Philippar, U., Barzik, M., Rubinson, D. A., . . . Gertler, F. B. (2007). Filopodia are required for cortical neurite initiation. *Nat Cell Biol, 9*(12), 1347-1359. doi:10.1038/ncb1654

Dotti, C. G., Sullivan, C. A., & Banker, G. A. (1988). The establishment of polarity by hippocampal neurons in culture. *J Neurosci, 8*(4), 1454-1468. Retrieved from https://www.ncbi.nlm.nih.gov/pubmed/3282038

Ellis, C. T., & Turk-Browne, N. B. (2018). Infant fMRI: A Model System for Cognitive Neuroscience. *Trends Cogn Sci, 22*(5), 375-387. doi:10.1016/j.tics.2018.01.005

Faraone, S. V., Asherson, P., Banaschewski, T., Biederman, J., Buitelaar, J. K., Ramos-Quiroga, J. A., . . . Franke, B. (2015). Attention-deficit/hyperactivity disorder. *Nat Rev Dis Primers, 1*, 15020. doi:10.1038/nrdp.2015.20

Gleeson, J. G., Lin, P. T., Flanagan, L. A., & Walsh, C. A. (1999). Doublecortin is a microtubule-associated protein and is expressed widely by migrating neurons. *Neuron, 23*(2), 257-271. doi:10.1016/s0896-6273(00)80778-3

Govek, E. E., Newey, S. E., & Van Aelst, L. (2005). The role of the Rho GTPases in neuronal development. *Genes Dev, 19*(1), 1-49. doi:10.1101/gad.1256405

Guerrier, S., Coutinho-Budd, J., Sassa, T., Gresset, A., Jordan, N. V., Chen, K., . . . Polleux, F. (2009). The F-BAR domain of srGAP2 induces membrane protrusions required for neuronal migration and morphogenesis. *Cell, 138*(5), 990-1004. doi:10.1016/j.cell.2009.06.047

Halloran, M. C., & Kalil, K. (1994). Dynamic behaviors of growth cones extending in the corpus callosum of living cortical brain slices observed with video microscopy. *J Neurosci, 14*(4), 2161-2177. Retrieved from https://www.ncbi.nlm.nih.gov/pubmed/8158263

Henne, W. M., Kent, H. M., Ford, M. G., Hegde, B. G., Daumke, O., Butler, P. J., . . . McMahon, H. T. (2007). Structure and analysis of FCHo2 F-BAR domain: a dimerizing and membrane recruitment module that effects membrane curvature. *Structure, 15*(7), 839-852. doi:10.1016/j.str.2007.05.002

Herculano-Houzel, S. (2012). The remarkable, yet not extraordinary, human brain as a scaled-up primate brain and its associated cost. *Proc Natl Acad Sci U S A, 109 Suppl 1*, 10661-10668. doi:10.1073/pnas.1201895109

Kozma, R., Sarner, S., Ahmed, S., & Lim, L. (1997). Rho family GTPases and neuronal growth cone remodelling: relationship between increased complexity induced by Cdc42Hs, Rac1, and acetylcholine and collapse induced by RhoA and lysophosphatidic acid. *Mol Cell Biol, 17*(3), 1201-1211. doi:10.1128/mcb.17.3.1201

Krause, M., Leslie, J. D., Stewart, M., Lafuente, E. M., Valderrama, F., Jagannathan, R., . . . Gertler, F. B. (2004). Lamellipodin, an Ena/VASP ligand, is implicated in the regulation of lamellipodial dynamics. *Dev Cell, 7*(4), 571-583. doi:10.1016/j.devcel.2004.07.024

Kwiatkowski, A. V., Rubinson, D. A., Dent, E. W., Edward van Veen, J., Leslie, J. D., Zhang, J., . . . Gertler, F. B. (2007). Ena/VASP Is Required for neuritogenesis in the developing cortex. *Neuron, 56*(3), 441-455. doi:10.1016/j.neuron.2007.09.008

Lancaster, M. A., & Knoblich, J. A. (2014). Organogenesis in a dish: modeling development and disease using organoid technologies. *Science, 345*(6194), 1247125. doi:10.1126/science.1247125

Lejeune, J., Gautier, M., & Turpin, R. (1959). [Study of somatic chromosomes from 9 mongoloid children]. *C R Hebd Seances Acad Sci, 248*(11), 1721-1722. Retrieved from https://www.ncbi.nlm.nih.gov/pubmed/13639368

Ma, Y., Mi, Y. J., Dai, Y. K., Fu, H. L., Cui, D. X., & Jin, W. L. (2013). The inverse F-BAR domain protein srGAP2 acts through srGAP3 to modulate neuronal differentiation and neurite outgrowth of mouse neuroblastoma cells. *PLoS One, 8*(3), e57865. doi:10.1371/journal.pone.0057865

Miyata, T., Kawaguchi, A., Okano, H., & Ogawa, M. (2001). Asymmetric inheritance of radial glial fibers by cortical neurons. *Neuron, 31*(5), 727-741. doi:10.1016/s0896-6273(01)00420-2

Morita, T., Asada, M., & Naito, E. (2016). Contribution of Neuroimaging Studies to Understanding Development of Human Cognitive Brain Functions. *Front Hum Neurosci, 10*, 464. doi:10.3389/fnhum.2016.00464

Nakamura, K., Yamashita, Y., Tamamaki, N., Katoh, H., Kaneko, T., & Negishi, M. (2006). In vivo function of Rnd2 in the development of neocortical pyramidal neurons. *Neurosci Res, 54*(2), 149-153. doi:10.1016/j.neures.2005.10.008

Noctor, S. C., Martinez-Cerdeno, V., Ivic, L., & Kriegstein, A. R. (2004). Cortical neurons arise in symmetric and asymmetric division zones and migrate through specific phases. *Nat Neurosci, 7*(2), 136-144. doi:10.1038/nn1172

Pinheiro, E. M., Xie, Z., Norovich, A. L., Vidaki, M., Tsai, L. H., & Gertler, F. B. (2011). Lpd depletion reveals that SRF specifies radial versus tangential migration of pyramidal neurons. *Nat Cell Biol, 13*(8), 989-995. doi:10.1038/ncb2292

Reiner, O., Carrozzo, R., Shen, Y., Wehnert, M., Faustinella, F., Dobyns, W. B., . . . Ledbetter, D. H. (1993). Isolation of a Miller-Dieker lissencephaly gene containing G protein beta-subunit-like repeats. *Nature, 364*(6439), 717-721. doi:10.1038/364717a0

Saengsawang, W., Mitok, K., Viesselmann, C., Pietila, L., Lumbard, D. C., Corey, S. J., & Dent, E. W. (2012). The F-BAR protein CIP4 inhibits neurite formation by producing lamellipodial protrusions. *Curr Biol, 22*(6), 494-501. doi:10.1016/j.cub.2012.01.038

Saengsawang, W., Taylor, K. L., Lumbard, D. C., Mitok, K., Price, A., Pietila, L., . . . Dent, E. W. (2013). CIP4 coordinates with phospholipids and actin-associated proteins to localize to the protruding edge and produce actin ribs and veils. *J Cell Sci, 126*(Pt 11), 2411-2423. doi:10.1242/jcs.117473

Saito, T., & Nakatsuji, N. (2001). Efficient gene transfer into the embryonic mouse brain using in vivo electroporation. *Dev Biol, 240*(1), 237-246. doi:10.1006/dbio.2001.0439

Seghier, M. L., Lazeyras, F., & Huppi, P. S. (2006). Functional MRI of the newborn. *Semin Fetal Neonatal Med, 11*(6), 479-488. doi:10.1016/j.siny.2006.07.007

Shimada, A., Niwa, H., Tsujita, K., Suetsugu, S., Nitta, K., Hanawa-Suetsugu, K., . . . Yokoyama, S. (2007). Curved EFC/F-BAR-domain dimers are joined end to end into a filament for membrane invagination in endocytosis. *Cell, 129*(4), 761-772. doi:10.1016/j.cell.2007.03.040

Shu, T., Ayala, R., Nguyen, M. D., Xie, Z., Gleeson, J. G., & Tsai, L. H. (2004). Ndel1 operates in a common pathway with LIS1 and cytoplasmic dynein to regulate cortical neuronal positioning. *Neuron, 44*(2), 263-277. doi:10.1016/j.neuron.2004.09.030

Tabata, H., & Nakajima, K. (2001). Efficient in utero gene transfer system to the developing mouse brain using electroporation: visualization of neuronal migration in the developing cortex. *Neuroscience, 103*(4), 865-872. doi:10.1016/s0306-4522(01)00016-1

Tabata, H., & Nakajima, K. (2003). Multipolar migration: the third mode of radial neuronal migration in the developing cerebral cortex. *J Neurosci, 23*(31), 9996-10001. Retrieved from https://www.ncbi.nlm.nih.gov/pubmed/14602813

Tanaka, T., Serneo, F. F., Higgins, C., Gambello, M. J., Wynshaw-Boris, A., & Gleeson, J. G. (2004). Lis1 and doublecortin function with dynein to mediate coupling of the nucleus to the centrosome in neuronal migration. *J Cell Biol, 165*(5), 709-721. doi:10.1083/jcb.200309025

Taylor, K. L., Taylor, R. J., Richters, K. E., Huynh, B., Carrington, J., McDermott, M. E., . . . Dent, E. W. (2019). Opposing functions of F-BAR proteins in neuronal membrane protrusion, tubule formation, and neurite outgrowth. *Life Sci Alliance, 2*(3). doi:10.26508/lsa.201800288

Taylor, R. J., Carrington, J., Gerlach, L. R., Taylor, K. L., Richters, K. E., & Dent, E. W. (2020). Double UP: A Dual Color, Internally Controlled Platform for in utero Knockdown or Overexpression. *Front Mol Neurosci, 13*, 82. doi:10.3389/fnmol.2020.00082

White, J. G., Southgate, E., Thomson, J. N., & Brenner, S. (1986). The structure of the nervous system of the nematode Caenorhabditis elegans. *Philos Trans R Soc Lond B Biol Sci, 314*(1165), 1-340. doi:10.1098/rstb.1986.0056

Chapter 2:

Double UP: A Dual Color, Internally Controlled Platform for *in utero* Knockdown or Overexpression

This chapter was published as the following journal article:

Taylor, R. J., Carrington, J., Gerlach, L. R., Taylor, K. L., Richters, K. E., & Dent, E. W. (2020). Double UP: A Dual Color, Internally Controlled Platform for in utero Knockdown or Overexpression. *Front Mol Neurosci, 13*, 82. doi:10.3389/fnmol.2020.00082

*RT and ED conceived the project. RT, JC, LG, KT and KR executed the experiments. RT and ED wrote the manuscript with input from all authors. ED supervised all aspects of the work.

Abstract

In utero electroporation is a powerful tool for testing the role of genes in neuronal migration and function, but this technique suffers from high degrees of variability. Such variability can result from inconsistent surgery, developmental gradients along both rostral-caudal and medial-lateral axes, differences within littermates and from one litter to another. Comparisons between control and experimental electroporations rely on section matching, which is inherently subjective. These sources of variability are cumulative, leading to difficult to interpret data and an increased risk of both false positives and false negatives. To address these limitations, we developed two tools: (1) a new plasmid, termed Double UP, which combines LoxP-flanked reporters and limiting Cre dosages to generate internal controls and (2) an automated program for unbiased and precise quantification of migration. In concert, these tools allow for more rigorous and objective experiments, while decreasing the mice, time and reagents required to complete studies.

Introduction

The method of *in utero* electroporation (IUE) (Saito & Nakatsuji, 2001; Tabata & Nakajima, 2001) has contributed greatly to our understanding of neuronal differentiation and migration in the central nervous system. Indeed, it is the *de facto* technique to determine how neuronal function and migration are disrupted in the central nervous system after genetic manipulation or in disease models.

However, this technique relies on “section matching” to generate controls, an approach which suffers from a high degree of variability due to a multitude of inherent challenges, including inconsistent surgeries, developmental differences within and between litters, gradients

of maturation within multiple axes in the developing brain (Bayer & Altman, 1991) and inconsistent section matching between control and experimental conditions. These sources of variability are cumulative, leading to difficult to interpret data and an increased risk of both false positives and false negatives.

To overcome these limitations inherent in IUE we have developed a novel plasmid containing LoxP-flanked reporters termed Double UP, designed to generate optimal internal controls. By titrating the amount of Cre transfected with Double UP we are able to label approximately half of the neurons with a green reporter, which serves as a control, and the other half of neurons with both a red reporter and an experimental manipulation, either protein overexpression or shRNA-mediated knockdown. Thus, both green (control) and red (experimental) neurons are present throughout the electroporated area. When the electroporated area of cortex is sectioned and imaged, green and red cells can be quantified in a single slice, greatly reducing the dependency on section matching.

Results

Introducing an internal control to *in utero* electroporation

To address and mitigate the variabilities inherent to IUE, as well as the additional confounds of studies utilizing mixed genetic backgrounds, we have developed a dual-fluorescent plasmid, designed to generate an internal control. This plasmid, termed “Double UP”, uses the strong ubiquitous CAG (CMV enhancer/beta-Actin promoter and rabbit Globin PolyA tail) promoter (Kootstra & Verma, 2003). The CAG promoter is followed by a LoxP-flanked cassette (Kilby, Snaith, & Murray, 1993) consisting of the green fluorescent protein mNeon-Green (Shaner et al.,

2013), a stop codon and the rabbit-globin PolyA tail (Lanoix & Acheson, 1988). Following the second LoxP site is the red fluorescent protein mScarlet (Bindels et al., 2017), with an identical stop codon and rabbit-globin PolyA tail **(Fig. 1a)**. In the absence of Cre, cells containing this plasmid produce mNeon-Green **(Fig. 1b)**. However, if Cre is present in a cell, the mNeon-Green is excised, and replaced in the exact same locus by mScarlet. Co-injection with a limiting dose of pCAG-Cre (Matsuda & Cepko, 2007) plasmid allows rough control of the ratio of green cells to red cells. For cortical IUE, we titrated the amounts of Cre plasmid from 1ng/µL to 1 µg/µL, and found that 15ng/µL of Cre plasmid results in roughly half green cells and half red cells **(Fig. 1b')** and have used that concentration throughout the manuscript, unless otherwise noted. Greater than 200 embryos have been transfected with pCag-Cre at 15ng/µL, the large majority have had roughly equivalent numbers of green and red cells, with fewer than 10% having had at least twice as many cells of one color as the other. This Cre concentration will likely vary depending on usage, based on region targeted, timing of electroporation, amount of DNA being injected and the exact pulse sequence used during IUE. The same promoter (CAG) is used in both Double UP and Cre, so no preferential cell selection should occur, a hypothesis rigorously tested below.

Automated quantification of data

It became clear as we were developing Double UP that having a more precise and quantitative way of measuring differences in migration between control and experimental conditions would provide a more robust measure of migratory changes after protein overexpression or knockdown. Prior approaches to IUE analysis typically relied on linear bins to separate different regions of cortex, so that data could be easily combined and compared across brains. With the

ability to generate control and experimental cells within the same hemisphere, we set out to develop an automated method of quantification, designed to give exact positional information for each cell. To accomplish this, we developed a program which allows for automated quantification of distance from the nearest point on any user-defined region of interest, as well as location and brightness. This Java-based program, entitled "TRacking Overlapping Neurons" (TRON) utilizes simple processing steps, followed by a modified version of the Fiji plugin 3D Object Counter (Bolte & Cordelieres, 2006). TRON identifies the center of mass of every fluorescently-labeled neuronal cell body and calculates the distance to any user defined region of interest (ROI) **(Fig. 2a-g).** This approach eliminates the need for linear binning and manual counting, avoiding both data compression and user bias. For comparison with historical data, TRON does have the option to present data in automatically generated bins, with curvature that conforms to the actual curvature of cortical sections **(Fig. 2h-j)**. This process is highly automated, reducing the prevalence of bias, while simultaneously simplifying labor intensive data analysis. The only manual steps in this analysis program are demarcating regions of interest and optional "quality control" of neuronal location. The individual processing steps are available in Online Methods. The TRON program, a sample image and associated instructions are downloadable at https://go.wisc.edu/tron. We implement this program throughout the rest of the manuscript.

Confirming that green and red neurons behave similarly

To test the validity of Double UP, we needed to determine if the green and red fluorophores were either differentially affecting neuronal migration in the absence of overexpression/knockdown, or were labelling dissimilar populations of cells. If both mNeon and mScarlet are inert and labeling

unbiased populations of cells, the green and red population of neurons should migrate similarly. To test this assumption we performed surgery and imaged every section containing fluorescent cells from four embryos (n=61 sections, 4 embryos, from 2 pregnant mice). Sections were collected and mounted sequentially and aligned across brains according to the first section which contained an uninterrupted corpus callosum (CC). This matching scheme corresponded well with other common landmarks. Section matching refers to the comparison of all fluorescent cells (mNeon or mScarlet) between matched sections from two different brains. “Double UP” refers to the comparison between both mNeon and mScarlet cells within one section of one brain. Implementing the TRON program, referred to above, we were able to determine that mNeon-Green and mScarlet-labeled neurons migrate in statistically similar fashions in embryonic brain **(Fig. 1c, full data set, Supplemental Fig. 1)**. We decided to analyze migration as the distance from the top of the cortical plate, defined by the end of the DAPI labeled cell dense region. At the timepoints we examined, this is a measure of distance remaining to travel, as neurons will continue to migrate until they reach the top of the cortical plate. We also analyzed the distance of neurons from the ventricular surface, but ultimately decided to use the distance from the top of the cortical plate, to better isolate radial migration as opposed to the combination of radial and tangential migration. In control situations, measuring distance from the ventricular surface does not result in significantly different migration patterns between green and red cells (data not shown). Any cells located beyond an ROI were included in analysis and resulted in a negative value. Binned data was also collected and analyzed, but not used because binning inherently requires compression of data and therefore loss of information. Because all data from Double UP consists of matching sets of green and red cells, more powerful statistical tests (two-way ANOVA)

can be used to determine if red and green neurons are behaving differently. Together, these data indicate that Double UP is appropriately generating internal controls, and allows for its use to compare control and experimental conditions in single brain sections.

Comparing traditional IUE and Double UP

One confounding variable in traditional IUE is the requirement of using matched sections in control and experimental brains. It is well established that embryonic cortical development proceeds along both rostral-caudal and medial-lateral gradients (Bayer & Altman, 1991). However, the degree to which these gradients cause variabilities to IUE has not been well documented. To determine the validity of section matching in light of these gradients, we re-examined the data from Figure 1c. Neuronal migration data was compared in two ways. First, to perform section matching, all sections were aligned using the first slice within each brain to contain an uninterrupted corpus callosum as a landmark. After alignment, all fluorescent cells from each section were compared with all fluorescent cells from matching sections from the other brains **(see large box spanning Supplemental Fig. 1a and 1b as an example)**. We believe this is more rigorous than what is typically considered section matching, however publications that implement IUE often do not typically report the methodology used to section match, or even if section matching was implemented. Second, to compare with Double UP, each section that had at least one matching section was then also analyzed. **(see small box in Supplemental Fig. 1b as an example)**. The mean migration distance of green cells and red cells were compared within each section **(Fig. 1d)**. Between matched sections, we found an absolute variance of 80.8+/-6.7 μm (SEM). Utilizing Double UP, we found an absolute variance of 18.6+/-1.9μm. Within Double

UP, there was negligible bias towards either color migrating further, with green cells migrating 2.6+/-3.0μm further than red cells. If even precise section matching has high degrees of variability, it calls into question the practice of using matching sections from separate electroporations as a methodology to compare control and experimental conditions.

Testing for Leakiness

The intent of Double UP is to introduce overexpression or knockdown in combination with the red fluorophore to distinguish if and how the red experimental cells differ from the green control cells. It was expected that some red cells would be dimly green, and this was observed **(dashed circles, Fig. 3a)**. Red cells that were dimly green were expected because both Double UP and Cre share the same CAG promoter and therefore mNeon will be transcribed simultaneously with Cre prior to Cre-mediated recombination of Double UP. Examining seven brains electroporated with Double UP and pCAG-Cre, 1.0% of red cells had a green signal bright enough to be identified as both red and green cells by the TRON program. We have introduced a test in TRON to detect and disregard double positive cells, which was implemented for all studies other than those testing for leakiness. We believe double positive cells to be a result of rare instances when either Cre plasmids/protein transcribe or translate slowly, or when one or more copies of Double UP are slow to recombine for reasons that are unclear. Because it is expected that the first fluorophore will always be expressed at least briefly, any overexpression or knockdown is always associated with the second fluorophore.

It is acceptable, and likely unavoidable, for red (Cre-positive) cells to express mNeon. However, for the success of Double UP, it is vitally important that green (Cre-negative) cells do

not express any mScarlet **(solid oval, Fig. 3a)** or any associated overexpression or knockdown; a potential problem we are defining as “leakiness”. If Double UP was leaky, putative control cells would have either overexpressed protein or shRNA, and therefore be inappropriate controls. The design of Double UP also allows for delayed activation of both the red fluorescent protein and overexpression or knockdown, by transfecting limiting doses of CreER and timed administration of tamoxifen. We therefore also tested the system for leakiness using pCAG-ERT2-Cre-ERT2 (Matsuda & Cepko, 2007) (pCAG-CreER), without administration of tamoxifen. To test for leakiness, we undertook multiple tests. First, IUE was performed with Double UP (2 μg/μL) and either no Cre, pCAG-CreER (15ng/μL) or pCAG-Cre (15ng/μL). Sections from the pCAG-Cre brains were used to establish settings such that a few pixels were saturated, and then unchanged between conditions. Rather than using automatic thresholding for the TRON program, images for this set of experiments were artificially thresholded at 1000 gray values, out of 65535 possible. This gray value was an artificially low threshold, designed to detect even very dim cells. In the absence of Cre, there was a single red cell slightly above this threshold across four sections from four different brains **(Fig. 3b, column 4)**. IUE of Double UP and pCAG-CreER resulted in 3-4 red cells in each section (compared with several hundred green cells) **(Fig. 3b, column 6)**, and IUE of Double UP and pCAG-Cre resulted in roughly equal populations of green and red cells **(Fig. 3b, columns 1 and 2)**. These results demonstrate that in Cre negative cells, there is virtually no recombination of Double UP. It was not a surprise that Double UP with CreER was more leaky than Double UP with Cre, as CreER has been previously shown to have a low level of activity in the absence of exogenous tamoxifen/estrogen (Matsuda & Cepko, 2007). This is a known but acceptable tradeoff for the ability to have temporal control of activation.

Absence of visibly red cells in the no-Cre condition suggests that the loxP sites within Double UP are not recombining. However, this result does not establish whether green cells had below visible expression of mScarlet, or any associated manipulation. To test this, we needed to quantify the intensity of the red signal in individual green cells. Using the same images that were used in the previous leakiness test, fluorescent intensity measures were collected for 90 green cells in no-Cre and CreER conditions, and from 90 red cells in a +Cre condition, from three different brains per condition. In both no-Cre and CreER conditions, the brightness in the red channel was unchanged between green cells and background levels **(Fig. 3c)**, also indicating that Double UP is not leaky.

Finally, we performed Western blotting to detect any protein associated with mScarlet. To accomplish this, we used Double UP 3x-HA, in which 3x-HA was fused with the mScarlet fluorophore **(Fig. 3d)**. Western blotting analyses, performed in a mouse catecholaminergic cell line (CAD cells), demonstrated that in the presence of very little Cre plasmid (1ng), HA protein is readily detectable, but in the absence of Cre there is absolutely no detectable HA protein **(Fig. 3e, f)**. Together, these data suggest that in the absence of Cre no mScarlet or associated protein is produced, and therefore that Double UP is not leaky.

Replicating previous findings: Overexpression

In the absence of protein overexpression, red and green neurons migrate equivalently **(Fig. 1C)**. This allows for including overexpression of a protein of interest with the red fluorophore and examining the effects of this overexpression relative to the control green neurons. Thus, we set out to determine if using Double UP recapitulated previously published findings from multiple

groups. Interestingly, both constitutively active Rac1 (Rac1-V12) and dominant negative Rac1 (Rac1-N17) have been shown previously to inhibit neuronal migration (Kawauchi, Chihama, Nabeshima, & Hoshino, 2003; Konno, Yoshimura, Hori, Maruoka, & Sobue, 2005). Rac1-V12 and Rac1-N17 were separately cloned downstream of mScarlet, following a P2A peptide **(Fig. 4a, b)**. The P2A causes a ribosomal skip during translation, so that equimolar ratios of both mScarlet and either Rac1-V12 or Rac1-N17 are generated. Cells receiving both Double UP Rac1-V12 or Double UP Rac1-N17 and at least one Cre plasmid will now produce mScarlet and an untagged Rac1-V12 or Rac1-N17. Based on the leakiness experiments completed above, cells receiving only Double UP will produce only mNeon. IUE was performed at E14.5 and collected four days later (E14.5+4). Red neurons expressing either Double UP Rac1-V12 or Double UP Rac1-N17 fail to migrate, while green neurons migrate normally **(Fig. 4c-f, full data Supplemental Fig. 2a-c)**, indicating that Double UP replicates previous findings. Importantly, green neurons in each condition are not significantly different from green neurons in each other condition (one way ANOVA, $p=0.33$), further demonstrating that Double UP is not leaky, while also suggesting that Rac1-V12 and Rac1-N17 both act in a cell-autonomous manner.

Replicating previous Findings: Knockdown

The second common manipulation performed via IUE is knockdown, and there are already existing multiple Cre-dependent knockdown strategies (Coumoul, Li, Wang, & Deng, 2004; Ventura et al., 2004). After multiple rounds of design and experimentation, we determined that pSico PGK-Puro (Ventura et al., 2004) provided the strongest and most reliable Cre-dependent

knockdown. This plasmid has also been demonstrated previously to absolutely require Cre to generate knockdown (Ventura et al., 2004).

RapGEF2 knockdown has previously been shown to cause a decrease in migration (Ye, Ip, Fu, & Ip, 2014). We were able to recapitulate this phenotype using pSico PGK-Puro RapGEF2, to the same extent seen with pSuper RapGEF2, utilizing identical shRNA sequences **(Fig. 5a-c, Full data Supplemental Fig. 3)**. Importantly, we saw no significant difference between migration of green and red cells when a scrambled shRNA was used **(Fig. 5c, Full data Supplemental Fig. 3a)**. These findings indicate that Double UP and pSico PGK-Puro can replicate previous findings, to the same extent as pSuper. As with overexpression, the green cells receiving pSico Scrambled were not significantly different than the green cells receiving pSico RapGEF2 ($p=0.8890$, Student's t-test). This suggests that pSico is not leaky, and that the effects of knocking down RapGEF2 are cell autonomous.

Discussion

In utero electroporation has been a viable experimental technique for almost 20 years, with minimal alterations to the original protocols. However, the robustness of an experiment is dependent on the reliability of the controls used. Overreliance on section matching is a problem with traditional IUE, as variations between electroporations or between embryos can lead to significant shifts in migratory patterns. Section matching may also compromise other measures not tested here, including cell fate decisions, axonal targeting or dendritic branching. Many publications utilizing IUE neither refer to section matching nor littermate controls, which potentially introduces new confounds, since available measures to reduce variability may not

have been appropriately undertaken. The technique of IUE is challenging, requiring a dedicated teacher and patient researchers to master. Migration profiles can vary 80 µm on average and as much as 220µm even between precisely matched sections **(Fig. 1d)**. It is for these reasons that implementing Double UP, with or without pSico, will quantitatively improve an already powerful technique.

The concept of a green/red plasmid dependent on Cre expression is not in itself novel. A green/red plasmid termed "Stoplight" was first introduced in 2001(Yang & Hughes, 2001), and has been used in many lineage tracing studies. Double UP is essentially a "modernization" of Stoplight, using the same basic design, but with brighter and more stable fluorophores, and a stronger promoter. Other groups have used LoxP-based green/red plasmids as markers for labelling cells before or after Cre expression (D'Astolfo et al., 2015; Fernandez-Chacon et al., 2019). These techniques and approaches have been used for lineage tracing, or as reporters for Cre expression within floxed alleles. The novelty of Double UP resides in the simple but critical technique of using limiting dosages of non-selective Cre to pseudorandomly select cells to be either control or experimental, and thus generating internal controls.

Development and validation of Double UP was remarkably quick and efficient. In contrast, development and validation of a suitable Cre-dependent knockdown was slow and arduous. We attempted four different versions of plasmids which would constitutively express a scrambled shRNA/miRNA, to be replaced by a gene-of-interest targeting shRNA/miRNA following Cre recombination. All attempts knocked down gene expression *in vitro*, however none were capable of reliably reproducing phenotypes *in utero*. Following these attempts, we began using pSico PGK-Puro (Ventura et al., 2004) as a Cre inducible shRNA. pSico does not constitutively express

an shRNA or miRNA, and so does not produce ideal internal controls. However, as only pSico reliably replicated *in utero* phenotypes, we selected it despite this caveat. It is unclear why the other strategies failed, though it is possible that production of shRNA interfered with Cre recombination, or vice-versa.

With traditional IUE, it is often unclear if an effect is cell-autonomous or cell non-autonomous. Untransfected cells are not fluorescently labeled, and in an extremely crowded cortex it can be exceedingly difficult to determine the morphology of non-fluorescent cells. Groups have previously attempted to address these concerns by performing sequential IUE, first introducing control plasmids and after some time experimental plasmids or vice-versa. The interval between these sequential electroporations has been as little as 15 minutes (Baek et al., 2015) to as long as 24 hours (Zhang et al., 2012). However, in this context it can be difficult to determine if cells have overlapping expression of control and experimental plasmids at short time windows, and at longer time windows it is no longer possible to test for cell-autonomy in neurons born at similar times. Use of Double UP provides a tool to address the question of cell autonomy. As leakiness has been rigorously tested in Double UP (Figure 3), researchers can say with confidence that a green cell does not contain any scarlet or associated manipulation. In this manuscript, we tested three different experimental conditions (Rac1-V12 overexpression, Rac1-N17 overexpression and RapGEF2 knockdown). In each experimental condition the migration pattern of green (control) cells was not significantly different than the migration pattern of green cells in control conditions (empty or scrambled RNAi), suggesting that all experimental manipulations were cell-autonomous effects. Thus, comparing green cells in control and

experimental conditions could address questions of cell autonomy/non-autonomy for overexpression or knockdown of any protein of interest.

An additional means of decreasing protein expression is to utilize transgenic animals containing two floxed alleles of a gene of interest. IUE of Double UP and limiting dosages of Cre plasmids would label presumed knockout cells red, and wildtype cells green. However, there are concerns of incomplete recombination with low dosages of Cre and floxed alleles (Liu et al., 2013). Use of Double UP will not eliminate those concerns. Thus, to allow for combinatorial experiments utilizing transgenic mice and Double UP, we have generated and tested an additional plasmid (Double UP-FRT), which utilizes FLPe-FRT recombination (Akbudak & Srivastava, 2011) to achieve the same results as Double UP, while not interfering with Cre-based systems (data not shown). While this plasmid is not utilized in this manuscript, it has been deposited along with Double UP to Addgene.

IUE is a technique that has been used in a broad range of scientific studies, not limited to cortical neuron migration. Examples include studies focused on ganglion cell projections (Soares & Mason, 2015), spine formation in the hippocampus (Awad et al., 2018) and perturbations of the circadian clock (Noda et al., 2019). Furthermore, electroporation as a technique to introduce DNA has been used in species from chickens (Muramatsu, Mizutani, Ohmori, & Okumura, 1997) to ferrets (Borrell, 2010). However, for our studies, we opted to validate our system using phenotypes previously shown to cause cortical radial migration defects in mice. The reasoning for this is as follows. First, mouse cortical IUE is one of the most heavily studied areas of neuronal development. Secondly, we felt that if Double UP was going to have problems replicating previous findings, it would be in early phenotypes because Cre would need to: be transcribed, be

translated, locate Double UP, recombine and then for the overexpression/shRNA yield a result. We reasoned that of established phenotypes, migration deficits would be amongst those requiring the shortest amount of time for manipulation to have the desired effect.

It is important to emphasize that this manuscript has focused on migration. While no apparent differences were present in cell morphology, this was not examined closely and other metrics such as axon elongation or targeting were not tested. It will be important that anyone using Double UP confirms that for the metric being examined, green and red neurons behave similarly. While it has likewise not been tested, Double UP should work equally well in establishing internal controls for organoids, which are notoriously variable from one organoid to another.

By introducing an internal control and testing the validity of that control in several ways, we believe we have developed an easier to use, more rigorous version of IUE. Dependence on section matching is greatly reduced and variations in surgical technique will matter far less. Furthermore, other experimental paradigms are now much more feasible. For example, IUE can be performed on embryos from heterozygous-by-heterozygous crosses of mice because each embryo, whether it be wild type, heterozygous or homozygous, operates as its own control, no longer requiring well-matched electroporations from a matching genotype. Additionally, by introducing a tailored method of automated analysis with the TRON program, we have further reduced variability and bias in analysis. Implementation of Double UP and the TRON program allows the use of more rigorous statistical tests, which increases statistical power. Together, using Double UP and the TRON program allows for much faster collection of more reliable data.

In utero electroporation is a powerful and widely used technique, but is traditionally dependent upon extremely accurate and insufficient section matching. Brains have strong developmental gradients acting along multiple axes, increasing the difficulty of accurate section matching with regards to traditional IUE. By employing Double UP, experiments can now be performed within a single embryo, from a single surgery. Animal to animal variation is no longer an issue, inconsistencies in surgical technique are made inconsequential and section matching is greatly reduced. Thus, implementation of Double UP can provide more rigorous data, while simultaneously reducing the number of animals, reagents, and time to complete experiments.

References

Akbudak, M. A., & Srivastava, V. (2011). Improved FLP recombinase, FLPe, efficiently removes marker gene from transgene locus developed by Cre-lox mediated site-specific gene integration in rice. *Mol Biotechnol, 49*(1), 82-89. doi:10.1007/s12033-011-9381-y

Awad, P. N., Amegandjin, C. A., Szczurkowska, J., Carrico, J. N., Fernandes do Nascimento, A. S., Baho, E., . . . Di Cristo, G. (2018). KCC2 Regulates Dendritic Spine Formation in a Brain-Region Specific and BDNF Dependent Manner. *Cereb Cortex, 28*(11), 4049-4062. doi:10.1093/cercor/bhy198

Baek, S. T., Copeland, B., Yun, E. J., Kwon, S. K., Guemez-Gamboa, A., Schaffer, A. E., . . . Gleeson, J. G. (2015). An AKT3-FOXG1-reelin network underlies defective migration in human focal malformations of cortical development. *Nat Med, 21*(12), 1445-1454. doi:10.1038/nm.3982

Bayer, S., & Altman, J. (1991). *Neocortical Development*. New York, New York: Raven Press.

Bindels, D. S., Haarbosch, L., van Weeren, L., Postma, M., Wiese, K. E., Mastop, M., . . . Gadella, T. W., Jr. (2017). mScarlet: a bright monomeric red fluorescent protein for cellular imaging. *Nat Methods, 14*(1), 53-56. doi:10.1038/nmeth.4074

Bolte, S., & Cordelieres, F. P. (2006). A guided tour into subcellular colocalization analysis in light microscopy. *J Microsc, 224*(Pt 3), 213-232. doi:10.1111/j.1365-2818.2006.01706.x

Borrell, V. (2010). In vivo gene delivery to the postnatal ferret cerebral cortex by DNA electroporation. *J Neurosci Methods, 186*(2), 186-195. doi:10.1016/j.jneumeth.2009.11.016

Coumoul, X., Li, W., Wang, R. H., & Deng, C. (2004). Inducible suppression of Fgfr2 and Survivin in ES cells using a combination of the RNA interference (RNAi) and the Cre-LoxP system. *Nucleic Acids Res, 32*(10), e85. doi:10.1093/nar/gnh083

D'Astolfo, D. S., Pagliero, R. J., Pras, A., Karthaus, W. R., Clevers, H., Prasad, V., . . . Geijsen, N. (2015). Efficient intracellular delivery of native proteins. *Cell, 161*(3), 674-690. doi:10.1016/j.cell.2015.03.028

Fernandez-Chacon, M., Casquero-Garcia, V., Luo, W., Francesca Lunella, F., Ferreira Rocha, S., Del Olmo-Cabrera, S., & Benedito, R. (2019). iSuRe-Cre is a genetic tool to reliably induce and report Cre-dependent genetic modifications. *Nat Commun, 10*(1), 2262. doi:10.1038/s41467-019-10239-4

Kawauchi, T., Chihama, K., Nabeshima, Y., & Hoshino, M. (2003). The in vivo roles of STEF/Tiam1, Rac1 and JNK in cortical neuronal migration. *EMBO J, 22*(16), 4190-4201. doi:10.1093/emboj/cdg413

Kilby, N. J., Snaith, M. R., & Murray, J. A. (1993). Site-specific recombinases: tools for genome engineering. *Trends Genet, 9*(12), 413-421. Retrieved from https://www.ncbi.nlm.nih.gov/pubmed/8122308

Konno, D., Yoshimura, S., Hori, K., Maruoka, H., & Sobue, K. (2005). Involvement of the phosphatidylinositol 3-kinase/rac1 and cdc42 pathways in radial migration of cortical neurons. *J Biol Chem, 280*(6), 5082-5088. doi:10.1074/jbc.M408251200

Kootstra, N. A., & Verma, I. M. (2003). Gene therapy with viral vectors. *Annu Rev Pharmacol Toxicol, 43*, 413-439. doi:10.1146/annurev.pharmtox.43.100901.140257

Lanoix, J., & Acheson, N. H. (1988). A rabbit beta-globin polyadenylation signal directs efficient termination of transcription of polyomavirus DNA. *Embo J, 7*(8), 2515-2522. Retrieved from https://www.ncbi.nlm.nih.gov/pubmed/2847921

Liu, J., Willet, S. G., Bankaitis, E. D., Xu, Y., Wright, C. V., & Gu, G. (2013). Non-parallel recombination limits Cre-LoxP-based reporters as precise indicators of conditional genetic manipulation. *Genesis, 51*(6), 436-442. doi:10.1002/dvg.22384

Matsuda, T., & Cepko, C. L. (2007). Controlled expression of transgenes introduced by in vivo electroporation. *Proc Natl Acad Sci U S A, 104*(3), 1027-1032. doi:10.1073/pnas.0610155104

Muramatsu, T., Mizutani, Y., Ohmori, Y., & Okumura, J. (1997). Comparison of three nonviral transfection methods for foreign gene expression in early chicken embryos in ovo. *Biochem Biophys Res Commun, 230*(2), 376-380. doi:10.1006/bbrc.1996.5882

Noda, M., Iwamoto, I., Tabata, H., Yamagata, T., Ito, H., & Nagata, K. I. (2019). Role of Per3, a circadian clock gene, in embryonic development of mouse cerebral cortex. *Sci Rep, 9*(1), 5874. doi:10.1038/s41598-019-42390-9

Saito, T., & Nakatsuji, N. (2001). Efficient gene transfer into the embryonic mouse brain using in vivo electroporation. *Dev Biol, 240*(1), 237-246. doi:10.1006/dbio.2001.0439

Shaner, N. C., Lambert, G. G., Chammas, A., Ni, Y., Cranfill, P. J., Baird, M. A., . . . Wang, J. (2013). A bright monomeric green fluorescent protein derived from Branchiostoma lanceolatum. *Nat Methods, 10*(5), 407-409. doi:10.1038/nmeth.2413

Soares, C. A., & Mason, C. A. (2015). Transient ipsilateral retinal ganglion cell projections to the brain: Extent, targeting, and disappearance. *Dev Neurobiol, 75*(12), 1385-1401. doi:10.1002/dneu.22291

Tabata, H., & Nakajima, K. (2001). Efficient in utero gene transfer system to the developing mouse brain using electroporation: visualization of neuronal migration in the developing cortex. *Neuroscience, 103*(4), 865-872. doi:10.1016/s0306-4522(01)00016-1

Ventura, A., Meissner, A., Dillon, C. P., McManus, M., Sharp, P. A., Van Parijs, L., . . . Jacks, T. (2004). Cre-lox-regulated conditional RNA interference from transgenes. *Proc Natl Acad Sci U S A, 101*(28), 10380-10385. doi:10.1073/pnas.0403954101

Yang, Y. S., & Hughes, T. E. (2001). Cre stoplight: a red/green fluorescent reporter of Cre recombinase expression in living cells. *Biotechniques, 31*(5), 1036, 1038, 1040-1031. doi:10.2144/01315st03

Ye, T., Ip, J. P., Fu, A. K., & Ip, N. Y. (2014). Cdk5-mediated phosphorylation of RapGEF2 controls neuronal migration in the developing cerebral cortex. *Nat Commun, 5*, 4826. doi:10.1038/ncomms5826

Zhang, L., Song, N. N., Chen, J. Y., Huang, Y., Li, H., & Ding, Y. Q. (2012). Satb2 is required for dendritic arborization and soma spacing in mouse cerebral cortex. *Cereb Cortex, 22*(7), 1510-1519. doi:10.1093/cercor/bhr215

METHODS

Materials Availability

Double UP, Double UP Rac1-V12, Double UP Rac1-N17, are available through Addgene (#125139, #125136 and #125137 respectively).

Though not utilized in this manuscript, we have generated additional versions of Double UP that have been validated and are also available at Addgene. These plasmids are: Double UP superfolderGFP-to-mScarlet (Addgene #120261), Double UP mClover3-to-mScarlet (Addgene #120262), Double UP Halotag-to-mScarlet (Addgene #125138), Double UP mScarlet-to-mNeon (Addgene #125139). Double UP-FRT (Addgene #141111).

pCAG-Cre and pCAG-ERT2-Cre-ERT2 were gifts from Connie Cepko (Addgene #13375, #13777). pCAG-iCre was a gift from Wilson Wong (Addgene plasmid #89573). pSico PGK Puro was a gift from Tyler Jacks (Addgene plasmid #11586)

For the internal control to be valid, it is essential that both Double UP and Cre plasmids contain the same promoter, and so these Cre plasmids are highly recommended for use in combination with Double UP.

Further information and requests for resources and reagents should be directed to and will be fulfilled by the Lead Contact, Erik Dent (ewdent@wisc.edu).

Cell Culture Studies

CAD Cell lines were purchased from Sigma Aldrich (08100805). Cells were cultured in Dulbecco's Modified Eagle Medium/Nutrient Mixture F-12 (1056018, ThermoFisher Scientific) with 8% heat-

inactivated Fetal Bovine Serum (Wicell) and 1% Penicillin-Streptomycin (15140122, ThermoFisher Scientific) in a humidified incubator at 37°C and 5% CO_2.

For leakiness experiments (Fig. 3D, E) CAD cells were transfected using Lipofectamine 3000, following manufacturer instructions. This resulted in an estimated 60% transfection rate, based on fluorescence.

Animal Models

All mouse procedures were approved by the University of Wisconsin Committee on Animal Care and were in accordance with NIH guidelines. Timed matings were performed, and pregnant dams were used at embryonic day 14.5 (E14.5). Day E0.5 is the morning of sperm plug visualization. IUE was performed at E14.5, with embryos perfused either three or four days later, as specified in the text. Gender of embryos was not recorded. Pregnant females were housed individually. Prior to becoming pregnant, females were housed with 3-4 other females.

In Utero Electroporation (IUE)

Plasmid DNA was mixed before injection. For most studies (Figs 1, 2a-c, 3a, 4c-f, Supplementary Figs 1-3) either no Cre, or 15ng/µL of either pCAG-Cre or pCAG-CreER was mixed with 2µg/µL of Double UP, Double UP Rac1-V12 or Double UP Rac1-N17. For knockdown studies (Fig. 5 a-c), 15ng/µL pCAG-iCre was mixed with 1µg/µL Double UP and 2µg/µL of either pSico RapGEF2 or pSico scrambled. Plasmid DNA was then combined with Fast Green FCF to a final concentration of 0.05% Fast Green FCF, and loaded into pulled capillary needles. The dam was anesthetized with isoflurane, and a laparotomy was performed, exposing the embryos. The embryos were

gently pulled out of the abdominal cavity. The capillary needles were inserted into the lateral ventricles, and approximately 0.25-0.5 µL DNA/Fast Green FCF was injected using a PicoSpritzer II (Parker Instrumentation). Electrical current was passed across the head, in five pulses of 40 volts each lasting 100ms on and 900ms off using a CUY21 Electroporator (Bex Co. LTD). After the last embryo was electroporated, the embryos were inserted back into the mother, and the laparotomy was sutured closed. Embryos were allowed to develop normally for 3 or 4 days, depending on experiment (E14.5+3 or E14.5+4). Surgeries were performed on embryos from at least two different pregnant females for each experiment.

Tissue Collection

Embryos were again exposed via laparotomy on the mother after deep anesthesia with isoflurane. Embryos were removed from the uterus one by one, chest cavity was opened, a small incision was made in the right atrium and a needle was inserted into the left ventricle. Through this needle, the animal was perfused with approximately 1 mL of sterile saline and 3 mL of 4% paraformaldehyde (PFA) using an Instech perfusion pump, at the rate of approximately 1.25mL per minute. Following perfusion, heads were removed and left in PFA at 4°C overnight before dissection. After the last embryo was perfused, the dam was euthanized. Following dissection, embryos were screened for positive signal using the mScarlet signal, which is easily visible in an intact, dissected brain. All brains containing mScarlet signal were further processed.

Fixed Tissue Sectioning

After 16 hours in PFA at 4°C, heads were transferred to PBS and brains were dissected. Brains were placed in 3% low melt agarose for 10 minutes at 42°C, then moved into 6% low melt agarose and allowed to set on ice. After the agarose hardened, the brains were sectioned on a Leica VT1000S vibratome at 100µm in PBS. Sections were stored for less than one week in PBS+0.2% sodium azide before being stained with 4',6-diamidino-2-phenylindole (DAPI) and imaged.

Section Preparation

DAPI was diluted to a final concentration of 2.4 nM in 0.4% Triton/PBS, and left on sections for one hour on a gently rotating platform at room temperature. After one hour, the sections were washed three times in PBS before being mounted in Aqua-Poly Mount (Polysciences). Slides were allowed to dry for at least one hour and then imaged within two days.

Section Matching

When section matching was used (Figure 1c, d, Supplemental Fig 1), every 100µm section was collected and stored sequentially. All sections were treated with DAPI and mounted. The first slice to contain an uninterrupted corpus callosum was identified, and set as slice 0. All sections containing fluorescent signal were imaged and analyzed. One brain contained fluorescent signal in sections located before the first slice to contain an uninterrupted corpus callosum, but these sections were not analyzed as there was no matching section in the other brains examined in this way.

Imaging

Confocal imaging was performed on a Zeiss LSM 800. Unless otherwise noted, all images were acquired at 12 optical sections, each 1µm apart. 2x2 tiles were collected with a 20x/0.8NA Plan Apochromat objective, with 2x averaging, and presented as maximum projections. Figure 3a was acquired at 47 optical sections, each 0.24 µm apart, with a 63x/1.4NA Plan Apochromat oil objective, with 4x averaging, and presented as a maximum projection. Unless otherwise specified, gain/laser power were altered between each image set to optimize image quality. Tiles were stitched together using the stitching tool in Zen 2.3 (Zeiss), and resulting images were analyzed using the TRON Program software described elsewhere in this manuscript.

Western Blot Analysis

For leakiness experiments (Fig. 3e) cells were transfected at 60% confluency with 10µg of Double UP and either no pCAG-Cre or 1ng pCAG-Cre using Lipofectamine 3000 (Invitrogen) following the manufacturer's protocol. 48 hours after transfection, cells were washed once with cold PBS before being lysed with 300µl NP-40 Lysis Buffer (Invitrogen) with Complete Mini (Roche) at 48 hours post-transfection. Lysate was spun at 21,000g for 10 minutes, and supernatants were flash-frozen and stored at -80°C until use. Samples were thawed and loaded onto a 4%-10% SDS-Page gel, then transferred to PVDF membrane (Millipore). Membranes were blocked in 5% milk in 0.1% TBS-T, incubated with primary antibody overnight at 4°C, and blotted with a HRP-conjugated secondary antibody for 1 hour. Antibodies used were mouse anti-HA (1:1000, sc-57592, Santa-Cruz), Mouse anti-Tubulin (1:10,000, T9026, Sigma) and goat-anti-mouse HRP (1:10,000, 115-

035-174, Jackson). Protein bands were visualized using Pierce ECL Western blotting substrate (Thermo Scientific).

Quantification and Statistical Analysis

Data was tested for normality using the Kolmorgorov-Smirnov test of normality. If data were normal, then a two-tailed t-test was performed. If data were not normal, then a Kolmorgorov-Smirnov two-tailed t-test was performed. For data comparing multiple brains at the same time, two-way ANOVA was performed. For these two-way ANOVA, reported p-values refer to the p-value associated with variation due to the differences in color within slices. P-values associated with variation due to differences between slices was not reported. Complete data is available upon request. All statistical tests were performed in Prism 8 (Graph Pad).

Data and Code Availability

The TRON program was designed to perform reproducible, high throughput and largely automated calculation of cell body location and distance from one or more user defined regions of interest. It was specifically designed for progenitor cells and migrating neurons, or neurons that have recently completed migration. We anticipate it will work well for most cell types, excluding highly branched and differentiated neurons. Most steps are automated, manual steps will be indicated. The TRON program largely utilizes ImageJ/Fiji tools. In short, images are processed via unsharp mask, gaussian blur, thresholding, erosion and watershedding to transform cells into reduced cell bodies. These cell bodies are then run through a modified 3D objects counter to determine which cells in a similar XY location in different slices are the same

or distinct cells. The distance from each cell to a user defined region of interest is then calculated. A downloadable program, complete instructions for use and a sample Double UP image file can be found here: https://go.wisc.edu/tron. Full code and associated instructions can be found here: https://go.wisc.edu/troncode

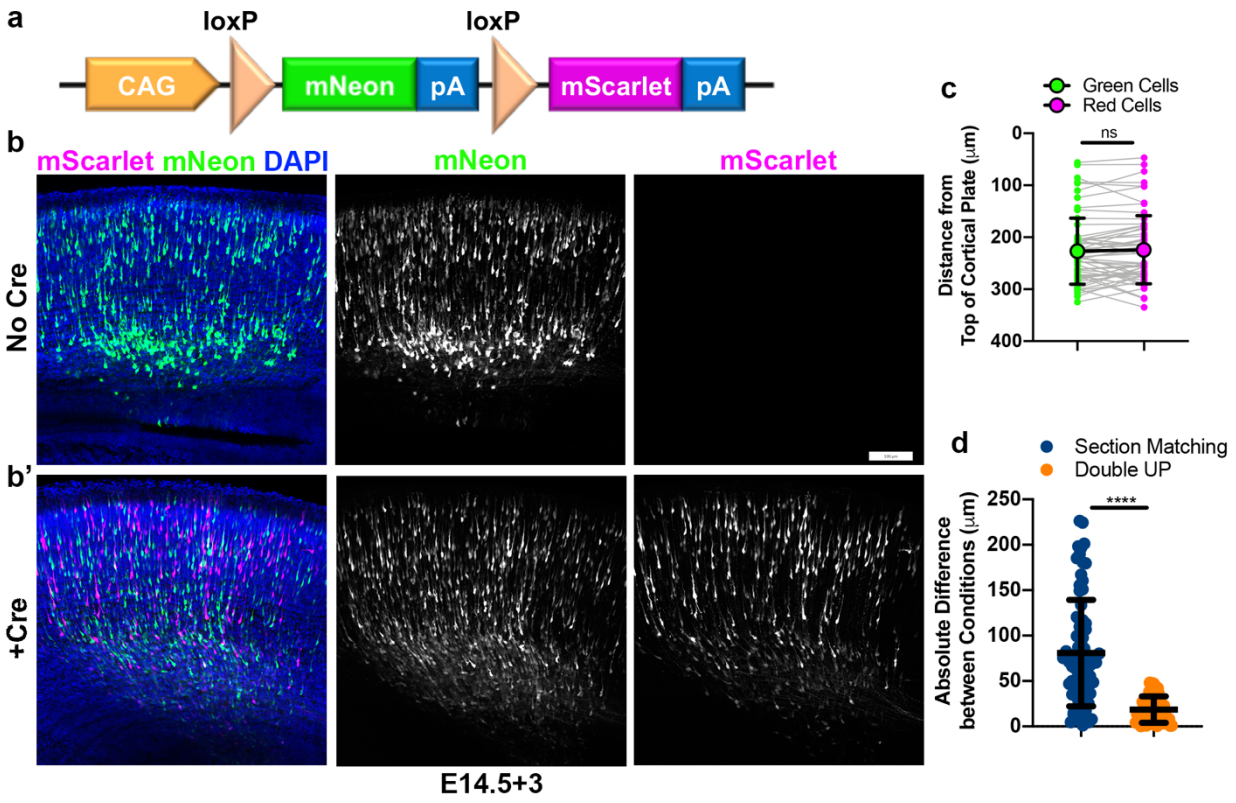

Figure 1: Construction and characterization of Double UP.

Double UP generates equivalent populations of red and green neurons within an individual slice. **(a)** Schematic of Double UP construct. **(b, b')** Representative IUE of 2 µg/µL Double UP without Cre **(b)** and with 15ng/µL pCAG-Cre **(b')**. Embryos were electroporated at E14.5 and allowed 3 days to mature (E14.5+3). Scale bar, 100µm. **(c)** Comparison of migration of mNeon-Green- and mScarlet-positive cells, E14.5+3. Each dot represents the mean distance of all cells within one cortical slice to the top of the cortical plate. Connected dots indicate measures from the same slice (n=61 slices). Large dots and black line indicate mean and SD of all 61 slices. No significant difference was detected between green and red populations (two-way ANOVA). Full data shown in Supplemental Figure 1. **(d)** Comparison of reliability of controls between section matching and Double UP. 76 comparisons were made for section matching and 61 comparisons were made for

Double UP. Only sections that had a perfect match in another brain were included for either analysis. **** $p<0.0001$., Kolmogorov-Smirnov t-test, two-tailed. Lines indicate mean and SD. See also Supplemental Figure 1.

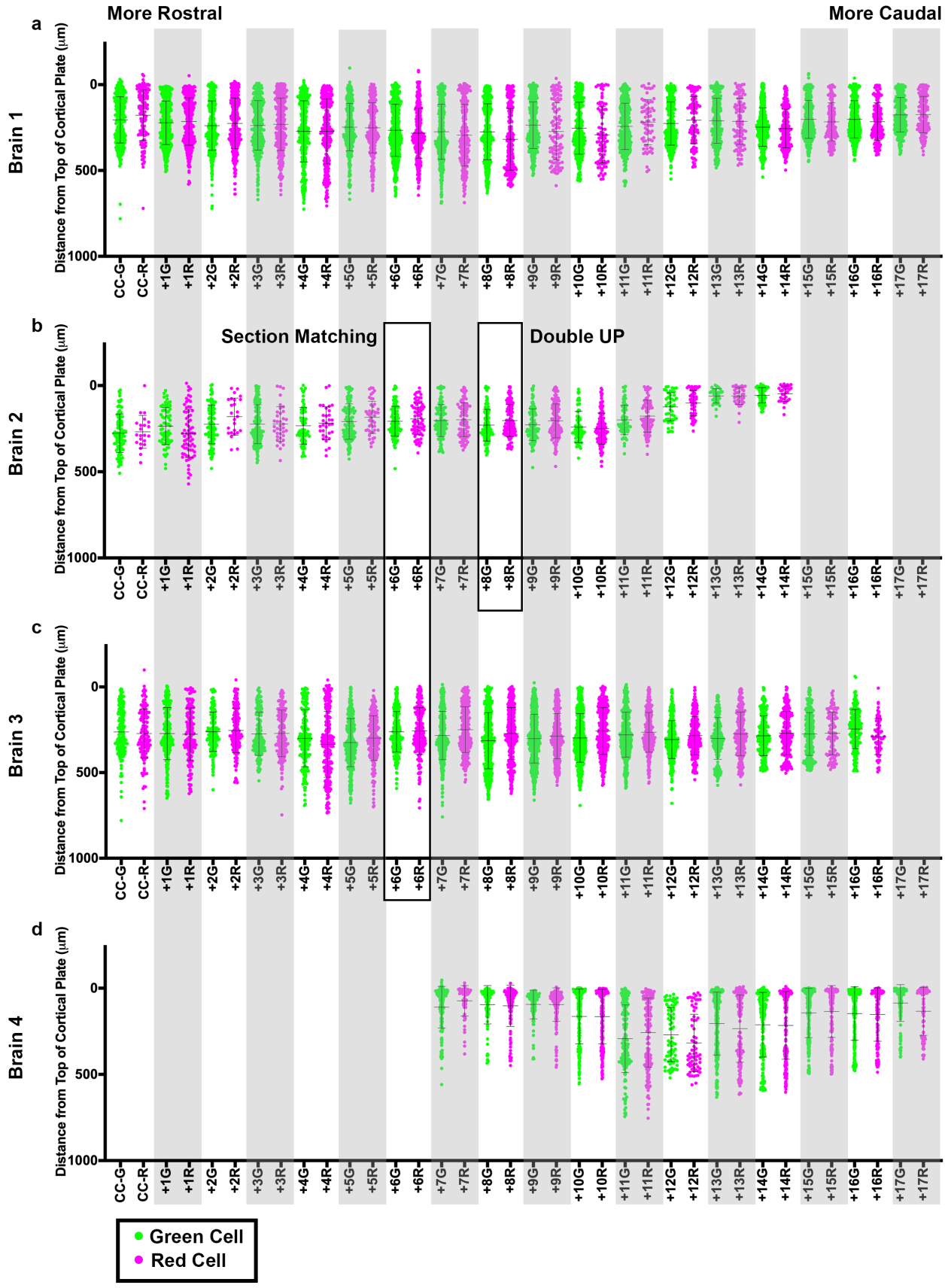
a
More Rostral
More Caudal
Brain 1
b
Brain 2
Section Matching
Double UP
c
Brain 3
d
Brain 4
Distance from Top of Cortical Plate (µm)
0
500
1000
CC-G
CC-R
+1G
+1R
+2G
+2R
+3G
+3R
+4G
+4R
+5G
+5R
+6G
+6R
+7G
+7R
+8G
+8R
+9G
+9R
+10G
+10R
+11G
+11R
+12G
+12R
+13G
+13R
+14G
+14R
+15G
+15R
+16G
+16R
+17G
+17R
Green Cell
Red Cell

Supplemental Figure 1: Full Data for Figures 1C and 1D.

Comparison of migration data between and across brains. **(a-d)** Results for cell location of four different brains, all relative to the top of the cortical plate. Each dot corresponds to the location of a single cell, either mNeon (green) or mScarlet (red) relative to the top of the cortical plate. One example of section matching is shown between corresponding sections 12 in brains **b** and **c** (large boxed region). An example of the Double UP comparison is highlighted by the boxed region in section 8 of brain **b**. Lines within each population of red and green cells indicate mean and SD. Along the x-axis, G and R refer to all green (G) or all red (R) neurons within a section, while +1, +2, +3, etc. refer to how many sections caudal of the CC the section is located. Each section is 100μm in thickness. (n=118-1026 cells per section, approximately half green, half red)

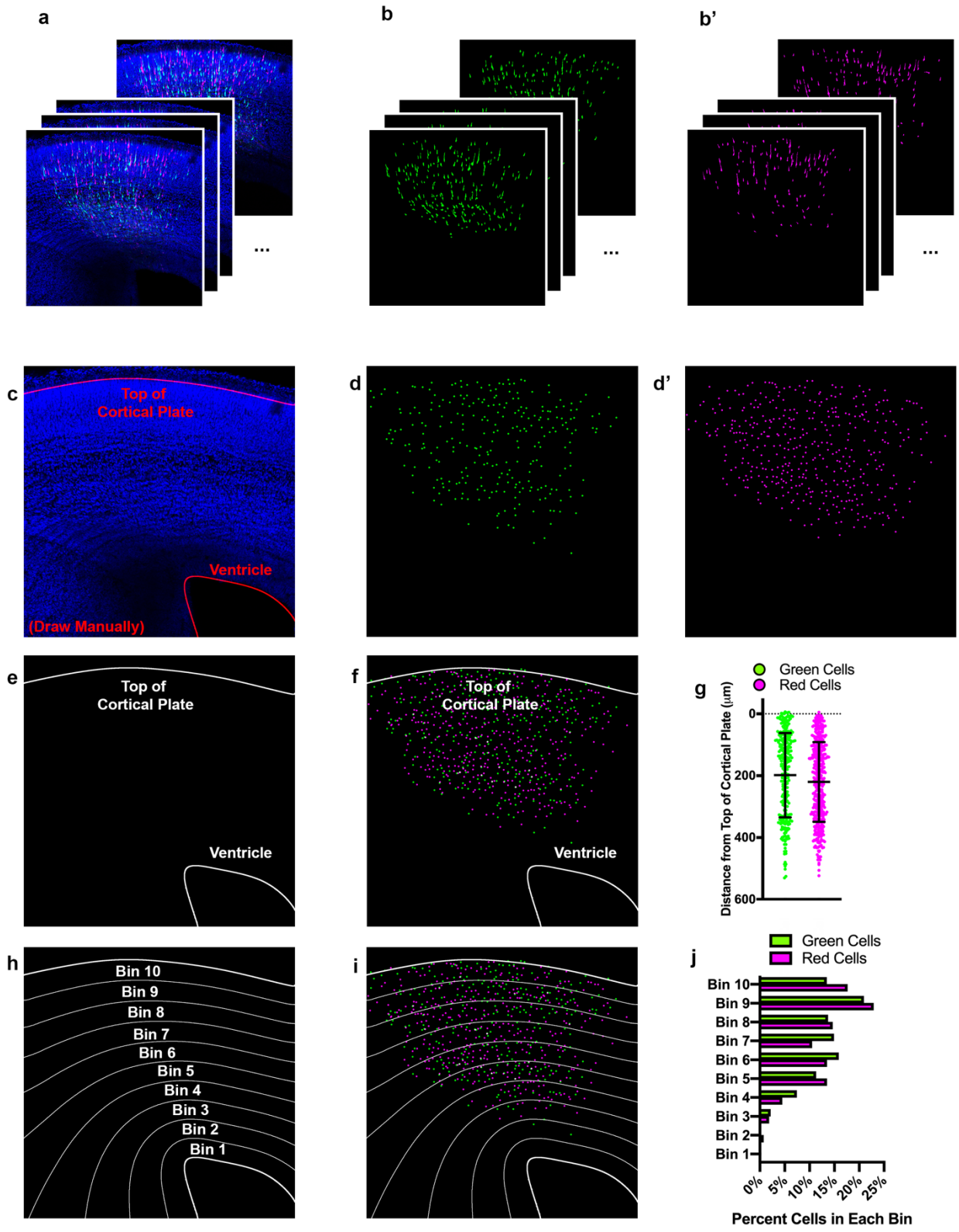
a
b
b'
...
...
...
c
Top of
Cortical Plate
Ventricle
(Draw Manually)
d
d'
e
Top of
Cortical Plate
Ventricle
f
Top of
Cortical Plate
Ventricle
g
Green Cells
Red Cells
Distance from Top of Cortical Plate (μm)
0
200
400
600
h
Bin 10
Bin 9
Bin 8
Bin 7
Bin 6
Bin 5
Bin 4
Bin 3
Bin 2
Bin 1
i
j
Green Cells
Red Cells
Bin 10
Bin 9
Bin 8
Bin 7
Bin 6
Bin 5
Bin 4
Bin 3
Bin 2
Bin 1
0%
5%
10%
15%
20%
25%
Percent Cells in Each Bin

Figure 2: Automated tracking of cellular location with TRON program.

Example of data analysis using the TRON program. **(a)** Example input. 12, 3-color confocal slices from a 100µm coronal brain slice from an E14.5+3 embryo after IUE. **(b)** Green and **(b')** red colors, processed independently and automatically via: unsharp mask, gaussian blur, conversion to 8-bit, automatic threshold, erode, watershed. **(c)** Manual drawing of regions of interest (ROIs – red lines at top of cortical plate and ventricle). This is the only manual step in the process. **(d, d')** Output of modified 3D Object Counter plugin from Fiji. Center of mass of each cell is identified and mapped; X, Y location and brightness of original is obtained and recorded. **(e)** Tracings of the top of the cortical plate and ventricle (ROIs). **(f)** Location of each cell mapped onto the ROIs. Distance from the center of each cell to the nearest point on each ROI is measured and recorded. **(g)** Graphical representation of distance each cell is from top of the cortical plate. Cells located above the top of the cortical plate are treated as having a "negative" distance. Lines indicate mean and SD. **(h)** Distance between ROIs can be split into bins, calculated to reflect the ROI to which they are closest. **(i)** Location of each cell mapped onto the bins. **(j)** Graphical representation of the data split into 10 equal-sized bins, each bar shows percentage of cells of that color in the respective bin.

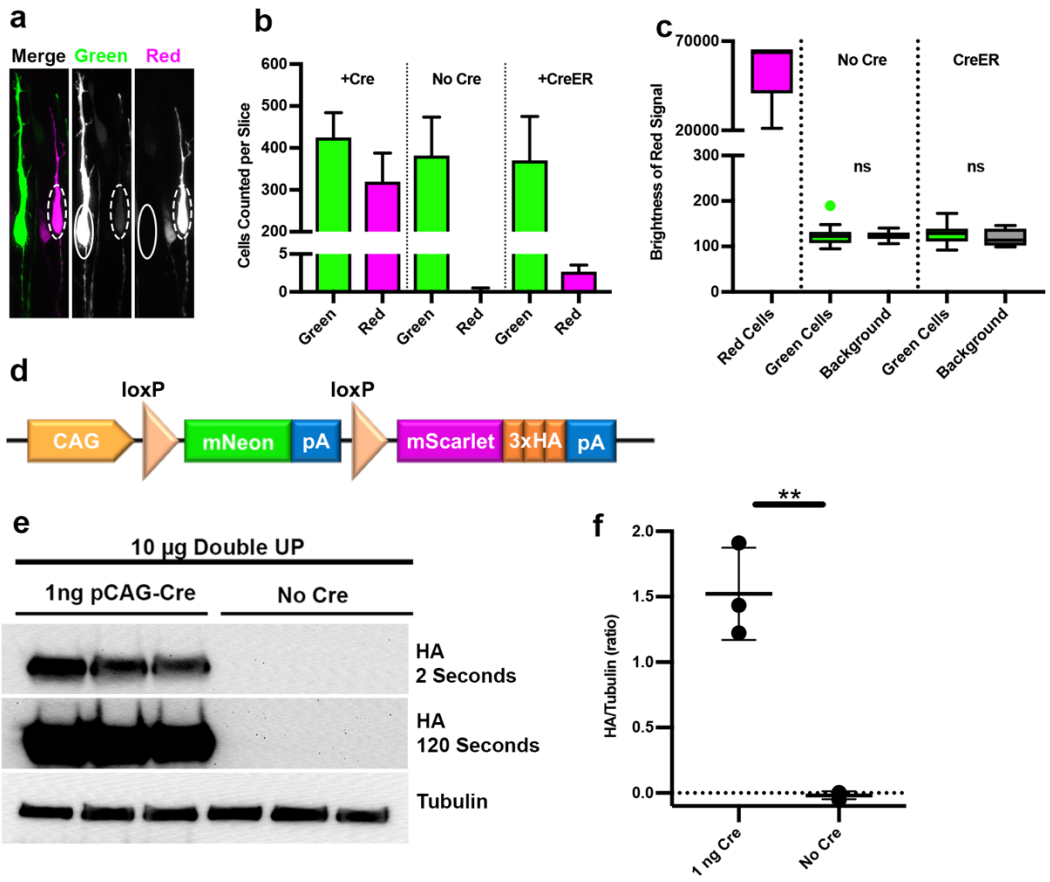

Figure 3: Double UP is not "leaky".

Three tests to determine if green cells express any red protein or associated manipulation. **(a)** High power image of two adjacent neurons, one green and one red, taken with a 63x/1.4NA oil objective. In the green neuron (solid oval), no signal is visible in the red channel. In the red neuron (dashed oval), a faint signal is visible in the green channel. **(b)** Number of green and red cells of greater than 1000 units of brightness per slice in Double UP +Cre (3 slices, mean=425 green/320 red cells), Double UP No Cre (4 slices, mean = 382 green /0.25 red cells) and Double UP +ERT2-Cre-ERT2 (3 slices, mean = 370 green/3 red cells). Error bars indicate SEM. All images acquired with identical settings. **(c)** Quantification of the brightness in the red channel of red neurons from 90 neurons across three brains for: red neurons from Double UP +Cre, as well as green neurons

from brains having received Double UP without Cre and Double UP +CreER. Dot above box and whiskers in “Green Cells” column with No Cre indicates an outlier, all other points are contained within the whiskers (Tukey). Boxes are 25%/75%, median is also shown. **(d)** Schematic of Double UP-HA. **(e)** Western blots of protein from CAD cells transfected with 10µg of Double UP and either 1ng/uL pCAG-Cre or no Cre. Quantification done on HA exposed for 2 seconds, 120 second exposure only shown for reference. **(f)** Amount of HA protein detected in each condition. The average HA signal in three experiments was slightly less than background. ** p=0.0017, unpaired two-tailed t-test of three experimental replicates. Lines indicate mean and SD.

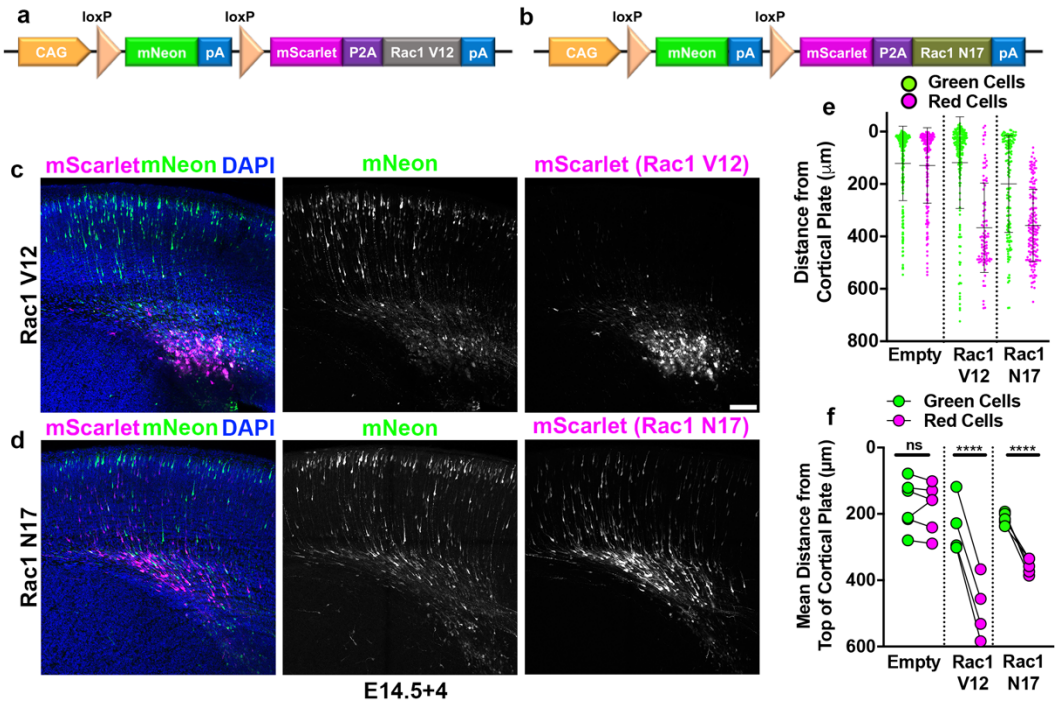

Figure 4: Double UP provides overexpression with an internal control.

Robust replication of previously discovered migration defects utilizing Double UP. **(a)** Schematic of Double UP Rac1-V12. **(b)** Schematic of Double UP Rac1-N17. **(c)** Representative image of Double UP Rac1-V12, E14.5+4. Scale bar, 100µm. **(d)** Representative image of Double UP Rac1-N17 E14.5+4. **(e)** Dot plot of three representative slices from Double UP, Double UP Rac1-V12 and Double UP Rac1-N17. Each dot represents distance from the top of the cortical plate to the center of mass for each neuron. **(f)** Dot plot of Double UP, Double UP Rac1-V12 and Double UP Rac1-N17 (n=6, 4 and 5 slices, respectively, each from a different brain). Each dot represents mean distance from the top of the cortical plate to the distance of all cortical neurons in a slice. Connected dots indicate measurements were made in the same brain. ns=not significant, **** $p<0.0001$, two-way ANOVA. Error bars not shown for clarity. See also Supplemental Figure 2.

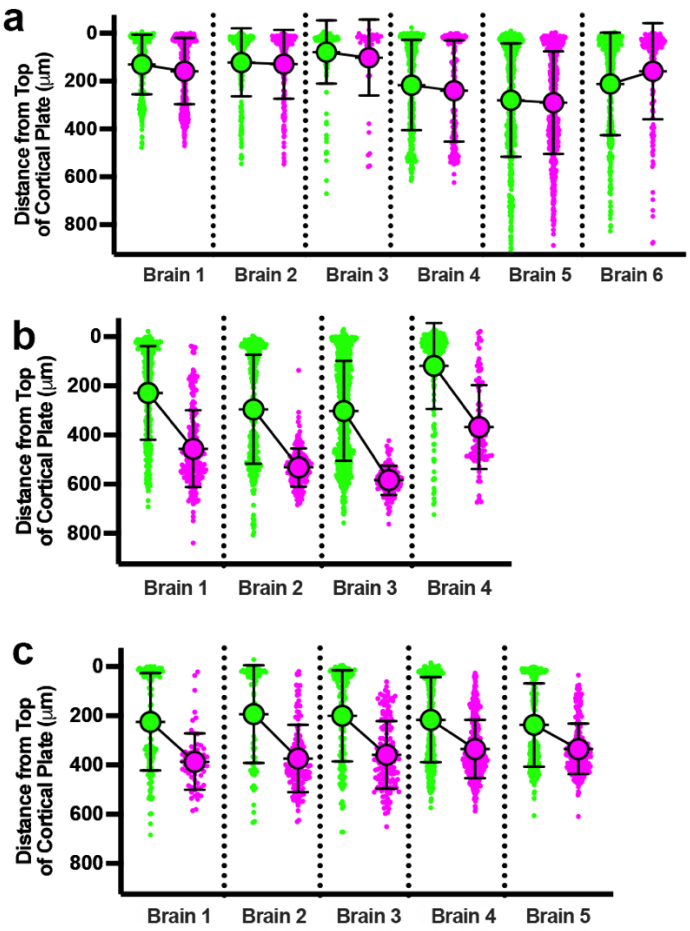

Supplemental Figure 2: Full Data of Figure 4f.

(a-c) Results for cell location for Double UP **(a)**, Double UP Rac1-V12 **(b)** and Double UP Rac1-N17 **(c)**, 6, 4 and 5 slices respectively, each from a different brain. Statistics were run only on the combined data presented in **Figure 4f**. Bars represent Mean and Standard Deviation.

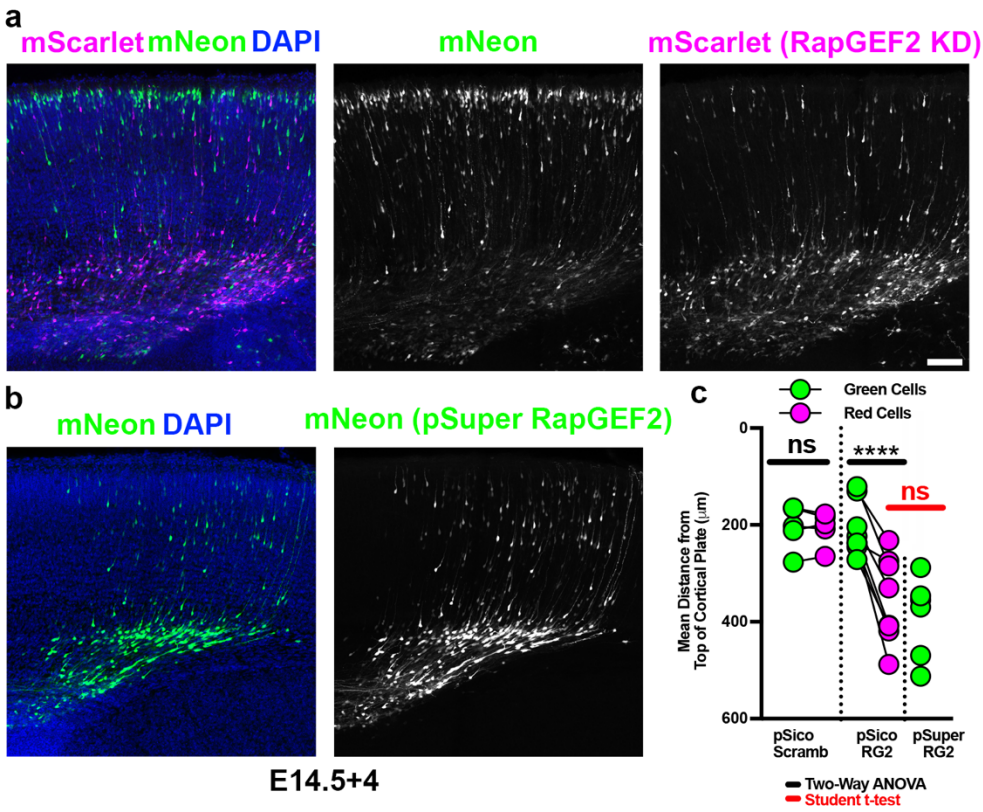

Figure 5: Double UP combined with pSico provides knockdown with an internal control.

Robust replication of previously discovered migration defects, utilizing Double UP and pSico. **(a)** Representative image of IUE with pSico RapGEF2 (2μg/μL), Double UP (1μg/μL) and pCAG-Cre (15ng/μL). Scale Bar 100μm. **(b)** Representative image of IUE with pSuper RapGEF2 (2μg/μL) and Double UP (1μg/uL). **(c)** Dot plot of Double UP and either pSico Scrambled (pSico Scramb), pSico RapGEF2 (pSico RG2) and pSuper RapGEF2 (pSuper RG2) (n=5, 8 and 5 slices, respectively, each from a different brain). Each dot represents mean distance from the top of the cortical plate to all cortical neurons in a slice. Connected dots indicate measurements were made in the same brain. ns=not significant, **** $p<0.0001$. Comparisons within samples (black bars) were two-way ANOVA, comparison between pSuper RapGEF2 and the red cells of pSico RapGEF2 (red bars) were

performed with a Student's t-test. Error bars not shown for clarity. See also Supplemental Figure 3.

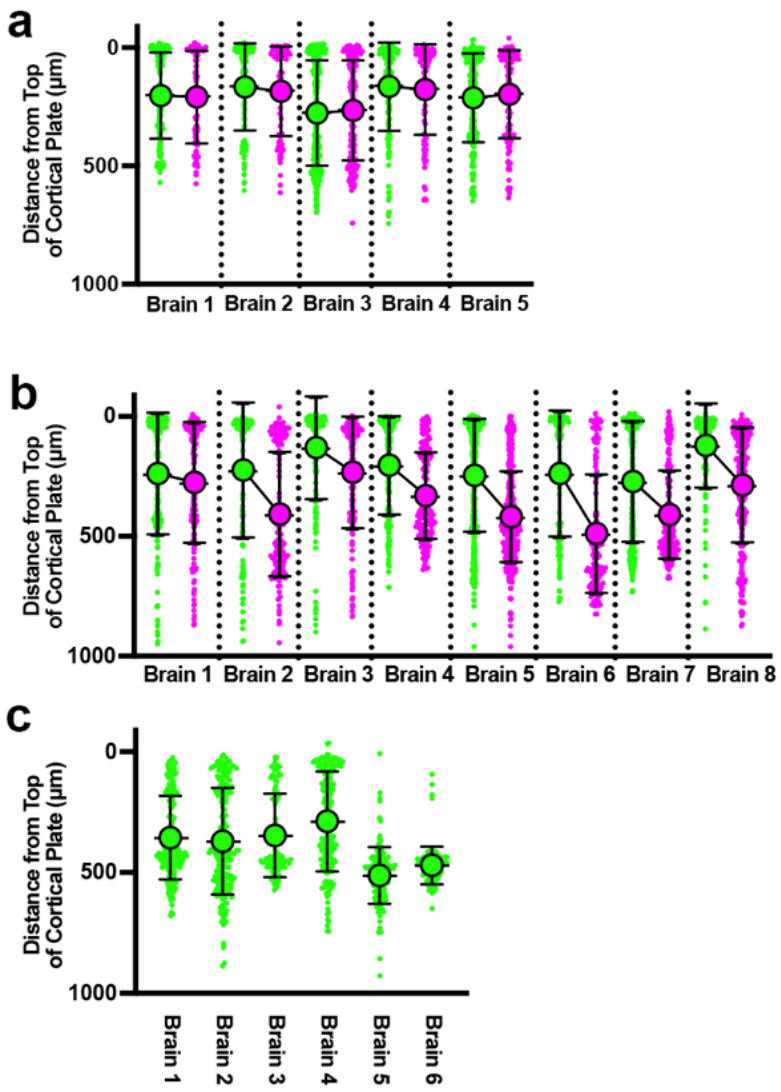

Supplemental Figure 3: Full Data of Figure 5

(a-c) Results for cell location for Double UP (1µg/µL) with pSico Scrambled (2µg/µL) and pCag-iCre (15ng/µL) **(a)**, pSico RapGEF2 (2µg/µL) and pCag-iCre (15ng/µL), **(b)** and pSuper RapGEF2 (2µg/µL) **(c),** 5, 8 and 6 slices respectively, each from a different brain. Statistics were run only on the combined data presented in **Figure 5c**. Bars represent Mean and Standard Deviation

Chapter 3:

CIP4 Regulates Neurite Initiation and Cortical Migration

These experiments and analysis have been done in cooperation with Lauren English, under the direction of Erik Dent.

Abstract

The morphology of a cell is essential for the it to engage in normal behaviors, and proper coordination of the cytoskeleton and plasma membrane are essential for a cell to control its morphology. CIP4, an F-BAR membrane bending protein that associates with the actin cytoskeleton, has been shown to have a strong effect on the morphology of cortical neurons *in vitro*. Overexpression of CIP4 results in cells extending prominent veils around the cell body, inhibiting filopodia formation and subsequent process formation. Here we present evidence that proper expression of CIP4 regulates process outgrowth *in vivo*, with CIP4 expression negatively correlated with both process number and length in newly differentiated pyramidal cortical neurons. Cortical neurons are especially sensitive to levels of CIP4 during radial migration. Disruption of normal CIP4 expression, either via overexpression or knockdown, leads to dysregulation of process number and length in early migrating neurons, which in turn markedly decreases neuronal migration. These results suggest that CIP4 expression levels are intimately tied to neuronal morphology and the capacity of cortical neurons to migrate radially in the cortex.

Introduction

The development of the mouse cerebral cortex requires precisely timed birth, migration and maturation of millions of neurons. Pyramidal excitatory neurons are born in the ventricular zone, adjacent to the lateral ventricles (Parnavelas, 2000). Newly born pyramidal cortical neurons then undergo a series of stereotyped morphological changes as they migrate dorsally from the ventricular zone to the cortical plate, taking their positions in a newly forming six layer cortex. Newly born pyramidal neurons start out as spherical cells. They begin their journey as a bipolar

neuron in the ventricular zone, but in the subventricular zone they pause and develop a multipolar morphology. Subsequently, they retract these extraneous processes, at which point they resume migration as a bipolar neuron, until they reach their destination in the cortical plate. Reaching their destination they extend an axon toward the ventricular zone and a dendrite toward the pial surface (Noctor, Martinez-Cerdeno, Ivic, & Kriegstein, 2004).

While regulation of morphological changes in cortical neurons has been studied extensively *in vitro,* relatively little is known about the molecules that control these morphological transitions *in vivo*. Importantly, changes to neuronal morphology happen concurrently with migration from the ventricle to the cortical plate, a process which cannot be recapitulated in a dish. This is a serious limitation of *in vitro* studies, as disruption of these steps during cortical migration can lead to problematic and even life-threatening disorders in humans, including lissencephaly, agyria and microcephaly (Moffat, Ka, Jung, & Kim, 2015).

The CIP4 family of proteins are a subgroup of the F-BAR family of proteins, known to sense and induce membrane curvature in cells (Henne et al., 2007). These proteins are typically understood to function in endocytosis, elongating endocytic vesicles (Henne et al., 2007; Itoh et al., 2005). However, we have previously shown that in dissociated neurons CIP4 does not appear to function in endocytosis, but instead localizes to the protruding, peripheral membrane of the neuron (Saengsawang et al., 2012; K. L. Taylor et al., 2019). Sustained overexpression of CIP4 prevents neurites from forming in dissociated neurons, and newly plated neurons from CIP4 knockout mice initiate neurites earlier than wildtype mice (Saengsawang et al., 2012). Additionally, CIP4 has been shown to be highly expressed in early embryonic cortex, with levels

decreasing until birth, at which point it is largely absent (Saengsawang et al., 2012). These findings suggest that CIP4 may have an important role to play in radial cortical neuron migration.

To investigate the role of CIP4 in neuronal migration we utilized *in utero* electroporation (IUE) to introduce plasmid DNA into newly born neurons in the embryonic mouse cortex (Saito & Nakatsuji, 2001; Tabata & Nakajima, 2001). We have enhanced these experiments using a technique we recently described, called Double UP (R. J. Taylor et al., 2020). Double UP generates green cells containing no manipulation, and red cells which are expressing a manipulation of interest (either overexpression or knockdown of a target gene) in the same electroporated region of cortex. This technique allows direct comparisons of control and manipulated neurons in the same section of cortex, as neurons dynamically migrate and change their morphology. Applying this technique, we show that radially migrating cortical neurons are very sensitive to CIP4 expression levels. Either increased or decreased levels of CIP4 inhibit migration, even though they result in opposing morphological changes in neurons.

Results

CIP4 Expression in prenatal cortex

Our previous studies, using western blots of prenatal and postnatal cortex, have demonstrated that CIP4 is expressed prenatally but decreases to undetectable levels soon after birth (Saengsawang et al., 2012). An important remaining gap in knowledge for understanding the role of CIP4 in neuronal development has been to identify which cells in the developing cortex express CIP4 protein. However, every antibody tested, including two generated within the lab, have detected similar signal in both knockout and wildtype tissue when used for

immunohistochemistry. Likewise, we have not been unable to use antibodies to detect endogenous CIP4 in dissociated neurons for the same reasons mentioned above.

To address these limitations, we have utilized CRISPR/Cas9 to generate a novel transgenic mouse, in which an mScarlet fluorophore is fused via a flexible linker to the C-terminus of endogenous CIP4. Using this CIP4-mScarlet mouse, we can for the first time examine expression of CIP4 within intact tissue. At embryonic day 12.5 (E12.5), before the cortical plate has been formed, CIP4 expression spans the cortex, from the ventricle to the pial surface **(Fig. 1 a, b)**. At embryonic day 14.5 (E14.5), a time when the cortical plate is first visible, CIP4 expression spans the cortex, but is diminished in the newly forming cortical plate **(Fig. 1 e, f)**. It therefore appears that CIP4 is present in neuronal progenitors and newly born neurons, but is depleted or otherwise removed prior to or as neurons enter the cortical plate. At embryonic day 16.5 (E16.5), CIP4 expression is decreased in both the cortical plate and intermediate zone, relative to the ventricular and subventricular zone (**Fig. 1 I, j)**. Because the endogenous CIP4-mScarlet signal is very dim, wildtype litter mates, collected and imaged using identical methods and settings are displayed as well **(Fig. 1 c, d, g, h, k, l)**. These data suggest that CIP4 is present in the cortex in a spatial and temporal manner consistent with a role in neuronal migration, but may not play a role in post-migratory neurons.

CIP4 overexpression inhibits neuronal migration and prevents neurite formation

To determine if CIP4 expression levels affect neuronal morphology and migration we began by overexpressing CIP4. The reasoning being that CIP4 is normally downregulated in prenatal development, so maintaining CIP4 in neurons would likely result in a stronger phenotype than

knock down. Sustained CIP4-overexpression has been shown to inhibit neurites in cortical neurons *in vitro* (Saengsawang et al., 2012; K. L. Taylor et al., 2019). Since neuronal development *in vitro* closely resembles neuronal development *in vivo*, we sought to determine the effects of sustained CIP4-overexpression *in vivo*. To accomplish this, we utilized IUE at E14.5 in combination with Double UP-CIP4.

CIP4 overexpression led to distinct morphological and migration defects even as early as two days after electroporation (E14.5+2) **(Fig. 2f)**. At this timepoint, CIP4 neurons (magenta) remained further from the top of the cortical plate than did control neurons (green) **(Fig. 2g)**. Although CIP4 overexpression resulted in a significant decrease in migration after two days, labeled neurons were still in relatively the same area of the cortex (ventricular/subventricular zone). Being that both CIP4 overexpressing and wildtype neurons were in similar locations we could compare their morphology to each other. CIP4 expressing neurons had greatly reduced complexity **(Fig. 2h, h')**, with very few processes **(Fig. 2i)**, including a majority of cells which contained no visible processes. Counting only cells that did produce processes, CIP4 expressing cells still had shorter processes than the control cells **(Fig. 2j)**. Importantly, using Double UP with no manipulation (termed Double UP Empty) **(Fig. 2a)**, green and magenta cells were comparable both in distance remaining to migrate **(Fig. 2b)**, as well as neurite number and length **(Fig. 2 c-e)**. Thus, CIP4 overexpression delays or prevents process initiation, consistent with our *in vitro* findings. Moreover, this failure to initiate processes correlates with a marked decrease in radial migration.

To further examine the effects of sustained CIP4 overexpression, we performed live slice imaging of cortical slices. IUE was performed at E14.5, collected 2 days later, and the brains were

sectioned on a vibratome. Confocal images of organotypic brain slices were collected every fifteen minutes for 17 hours. Following image acquisition, the brightest neurons were positionally tracked **(Fig. 3a)** and analyzed for somal translocations and new process formation over the course of 17 hours. Green cells (control) extended numerous processes **(Fig. 3d)**, and travelled via a series of somal translocations **(Fig. 3b)** towards the pial surface **(Fig. 3c)**, as has been previously described for cortical migration (Komuro & Rakic, 1995; Nadarajah, Brunstrom, Grutzendler, Wong, & Pearlman, 2001). Conversely, the large majority of magenta cells (CIP4 expressing) extended very few processes **(Fig. 3b)** and did not exhibit any somal translocations over the course of the time-lapse **(Fig. 3b)**. Thus, CIP4 expressing cells did not have sustained movement towards or away from the pial surface **(Fig. 3c)**.

Similar to reports by other groups, we observed some gradual spreading and sagging of either the cortical tissue or membrane in live slice cultures (Carter et al., 2017; Schwarz et al., 2019). By comparing movement of cells with changes in cortical slice spreading, we suggest most of the movement observed in the CIP4 expressing cells during the course of imaging is attributable to this tissue spreading. This can be seen most clearly in the video, as populations of magenta cells have very little/no movement compared with their neighbors. Importantly, use of Double UP Empty resulted in no difference between green or magenta cells for any measures **(Supplemental Fig. 1)**, suggesting that these findings are the result of CIP4 expression rather than some feature or failure of the Double UP system. Taken together, these results suggest that CIP4 actively prevents process initiation. A leading process is an essential component for saltatory migration, and so it follows that a lack of processes would result in a failure to migrate (Edmondson & Hatten, 1987; He, Zhang, Guan, Xia, & Yuan, 2010).

CIP4 knockdown inhibits neuronal migration while increasing neurite number and length

CIP4 is expressed early in cortical development, and dissociated neurons from CIP4 knockout animals initiate neurites earlier than wildtype *in vitro* (Saengsawang et al., 2012), but how this would translate *in vivo* and the consequences of CIP4 knockdown on radial neuronal migration are unclear. Utilizing Double UP in combination with a Cre-Dependent shRNA vector, "pSico" (Ventura et al., 2004), we knocked down CIP4 *in utero*, while maintaining control (green) and knockdown (magenta) cells in the same slice **(Fig. 4f)**. CIP4 knockdown significantly inhibited migration, though to a lesser extent than CIP4 overexpression **(Fig. 4g)**. Interestingly, there was a pronounced effect of CIP4 knockdown on neuronal morphology **(Fig 4h, h')**, resulting in both more processes **(Fig. 4i)**, and longer processes **(Fig. 4j)** relative to adjacent green cells. Control IUE with a scrambled sequence in pSico resulted in no difference between green and magenta neurons **(Fig. 4 a-e)**, indicating CIP4 knockdown was specific. Previous work *in vitro* has established that loss of CIP4 is associated with precocious neurite outgrowth, but no increase in the growth rate of neurites (Saengsawang et al., 2012). The finding that CIP4 knockdown generates neurons with more and longer processes is consistent with a role for CIP4 in inhibiting process initiation, as less repression of process initiation could result in more processes, and earlier forming processes could grow longer than processes of control neurons.

To better understand the effects of CIP4 knockdown, we performed live slice cultures, similar in scope to the CIP4 overexpression live slice cultures examined above. As expected from our fixed knockdown data **(Fig. 4)**, CIP4 knockdown neurons had a decreased ability to migrate, as seen both by somal translocations per hour **(Fig. 5b)** and movement towards the pial surface

(Fig. 5c). Surprisingly, knockdown neurons did not extend more processes over the course of the timelapse than control neurons **(Fig. 5d)**, but they did retract processes at a greater rate than control neurons **(Fig. 5e)**. This suggests that the role of CIP4 may be to retract processes, rather than to delay their initiation. Importantly, there was no alteration in process retraction with Double UP Empty (data not shown, p=.5186). I want to urge caution with these results, however. This is based off of one live slice experiment, and while these data fits with hypotheses generated before performing the experiment, this experiment will need to be repeated several times.

CIP4 overexpression and knockdown result in persistent migration defects

Both CIP4 overexpression and CIP4 knockdown resulted in very distinctive morphological phenotypes. To determine if these phenotypes had lasting consequences on migration, we performed IUE at E14.5 and collected brains four days later for imaging (E14.5+4). At this timepoint, many but not all control neurons will have reached the top of the cortical plate. CIP4 overexpression at E14.5+4 **(Fig. 6a)** very closely resembled results at E14.5+2, resulting in a robust reduction of migration **(Fig. 6b)**, with very few visible neurites or processes of any sort in the mScarlet/CIP4+ cells. CIP4 knockdown also resulted in a strong reduction of migration **(Fig. 6 g, h)**, though not to the same degree as CIP4 overexpression. CIP4 knockdown cells were disproportionately in the intermediate zone (61.9% of red cells vs 37.3% of green cells, p=.026, 5 brains), as opposed to cells containing the scrambled construct (44.7% of red cells vs 45.9% of green cells, p=.845, 4 brains). It broadly appears that neurons in both conditions have moved little between two and four days after electroporation, with CIP4-overexpressing neurons remaining near the boundary of the subventricular zone and the intermediate zone, and CIP4-

knockdown neurons remaining within the intermediate zone. Importantly, and consistent with our previous paper introducing and validating Double UP, both control conditions (Double UP Empty, as well as Double UP Empty combined with pSico-Scrambled) had equivalent levels of migration between magenta and green cells **(Fig. 6 a-b, e-f)**. These results suggest that not only does increasing or decreasing the expression of CIP4 rapidly disrupt migration of radially migrating cortical neurons, but these effects are lasting, at least for a few days. Furthermore, the finding that CIP4 knockdown neurons are delayed in the intermediate zone suggests that CIP4 has a role in exit from the multipolar phase, which neurons typically undergo in the intermediate zone.

Discussion

Evidence presented here suggests that CIP4 has an important role *in vivo* relating to delaying or otherwise preventing neurite formation. Loss of CIP4 results in more and longer neurites, and prolonged overexpression of CIP4 inhibits neurites almost entirely. Curiously, migration appears to be impeded by either extraneous neurites or by a lack of neurites. CIP4 seems to be specifically involved in the transition from the multipolar phase to the migratory bipolar phase, as knockdown cells fail to undergo this transition.

Previous *in vitro* findings have led us to describe a function of CIP4 in delaying process initiation (Saengsawang et al., 2012; Saengsawang et al., 2013; K. L. Taylor et al., 2019). Nothing presented here directly contradicts this finding, but the knockdown data suggests another hypothesis, that CIP4 acts to retract processes. Several findings make this a more appealing hypothesis than CIP4 acting solely to delay neurite initiation. First, CIP4 is present in the

subventricular zone at E14.5, when neurons are becoming multipolar, but absent from the upper intermediate zone at E16.5 where neurons are exiting the multipolar stage (Figure 1). Second, neurons lacking CIP4 becoming "stuck" in the intermediate zone can be directly explained by a loss of neurite retraction, leading to an inability to resume bipolar morphology (Figure 4). Finally, CIP4 is typically understood to function in endocytosis. Radial glia process retraction has been poorly studied, but it stands to reason that retraction of a long phospholipid membrane and accompanying cytoskeleton cannot occur without endocytosis. It is important to note that these two hypotheses (CIP4 delays neurites, CIP4 retracts neurites) are not mutually exclusive. A role for CIP4 in retracting neurites is a possible mechanism for delaying neurite initiation. Ongoing experimentation will attempt to clarify whether the primary function of CIP4 is to delay neurite formation or retract neurites.

Overexpression and knockdown of proteins of interest are both useful tools to discern the function of the protein. Together, they can give a much more complete picture of the processes involved, especially when the findings are complementary. The findings presented here are most certainly complementary. Overexpression of CIP4 generates cells with very few processes, and those cells with processes have very short processes. Knockdown of CIP4 generates cells with extra processes, and those processes are longer than typical. These data are also consistent with previous *in vitro* work (Saengsawang et al., 2012), showing that both *in vitro* and *in vivo* CIP4 is present in cortical neurons, and is acting to impede process formation. This manuscript provides additional information on the role of process formation with regard to migration. Specifically, proper control of processes is essential for normal migration and interference with the ability to initiate cellular processes inhibits cellular migration.

Timing of Expression

ShRNA targeting CIP4 has a pronounced effect in a short period of time, stalling cells in the intermediate zone that contain supernumerary processes. Additionally, from our endogenously tagged CIP4-mScarlet transgenic mouse, neurons in the cortical plate had little, if any, visible CIP4 protein. This presents a relatively tight window, wherein a neuron born at E14.5 has CIP4 transcripts that are still being used to translate protein (because knockdown has an effect), but no protein is present 3-4 days later when E14.5 cells will be entering the cortical plate. It is not clear at this time what processes could be controlling CIP4 expression, either at the genomic, mRNA or protein level. Similarly, it is unclear at exactly what point during radial neuron migration CIP4 levels decrease. Overexpression leads to cells stuck at the boundary of the SVZ and IZ, whereas knockdown results in cells unable to leave the IZ. We had hoped to address the issue of timing on a cellular level using the endogenous CIP4-mScarlet mouse, but the signal is too dim to visualize in any individual cell in the context of an intact cortex.

Most proteins known to be expressed in developing neurons and involved in process formation are pro-neurite genes (Dehmelt, Smart, Ozer, & Halpain, 2003; Dent et al., 2007; Krause et al., 2004; Yang et al., 2012), and expression of these proteins is required for process formation or extension. By contrast, both *in vitro* and *in utero*, CIP4 behaves to impede neurites. This is despite being present in early neurons, as evidenced both by the data from the transgenic mouse (Figure 1) and the effects caused by knockdown (Figures 4, 5 and 6). These data, taken with the clear and obvious inhibition of process formation by CIP4 overexpression, lead to a potential role of CIP4 acting as a gatekeeper for neuronal differentiation. However, it is unclear

whether CIP4 must be removed for a neuron to enter the cortical plate, or if a CIP4-negative cell acts as a signal indicating the cell has now entered the cortical plate. While these two hypotheses are mutually exclusive, both are consistent with our data at this time and will require further experimentation to determine which is occurring in the cortex.

One protein with a very similar phenotype to CIP4 is the small Rho GTPase Rnd2. Knockdown of Rnd2 results in neurons stuck in the intermediate zone with more and longer processes, and overexpression of Rnd2 results in neurons with fewer processes and a similarly decreased migration (Heng et al., 2008; Nakamura et al., 2006). Rnd2 has been described as an interactor of the very close family member FBP17 (Fujita, Katoh, Ishikawa, Mori, & Negishi, 2002), although the high degree of similarity between the phenotypes of Rnd2 and CIP4 suggest they may be acting together. More work will need to be done to determine if Rnd2 is upstream of CIP4, and may potentially be involved in defining a zone of action for CIP4 to operate within.

Contrasts with Published Work

Overexpression of CIP4 *in vitro* results in very round cells, with very few prominent filopodia or neurites (Saengsawang et al., 2012). This is reminiscent of triple knockout of the actin polymerase family of proteins, Ena/VASP/EVL (termed mmvvee), which similarly have very few prominent filopodia or neurites (Dent et al., 2007; Kwiatkowski et al., 2007). However, *in utero*, these two manipulations behave very differently. CIP4-expressing neurons fail to migrate, and live imaging of cortical neurons in organotypic slice cultures demonstrate that they move very little, if at all. Conversely, mmvvee neurons do not exhibit a migration phenotype (Kwiatkowski et al., 2007). Interestingly, knocking down these three proteins with a sequestration approach (FP4-Mito)

generated a differing phenotype, with neurons ultimately migrating to a higher cortical layer than control (Goh, Cai, Cepko, & Gertler, 2002). While these two effects seem contradictory amongst themselves and with CIP4, there are several potential explanations. Kwiatkowski used a transgenic knockout mouse, and there may be compensation resulting from a knockout compared with an acute knockdown, explaining the distinction between those two. To explain the difference between Goh and colleagues and the work presented here, the answer may be in the manner of process repression. CIP4 neurons produce large amounts of actin-rich ribs, which seem to actively inhibit any neurites from forming. In contrast, mmvvee neurons have a defect in actin bundling, which can be rescued by many different exogenous factors, including Myosin X and mDia2 (Dent et al., 2007). Indeed, neurons lacking Ena/VASP were still able to generate leading and trailing processes *in vivo* (Kwiatkowski et al., 2007). It is likely that *in vivo*, one or more factors were able to overcome the "passive" block caused by loss of Ena/VASP proteins and allowed these cells to produce neurites, whereas the more "active" block of CIP4 overexpression may be too much to overcome. This finding is consistent with other strong inhibitors of neurite formation, such as constitutively active Rac1 (Kawauchi, Chihama, Nabeshima, & Hoshino, 2003; R. J. Taylor et al., 2020).

Reliability of Double UP

Double UP was utilized heavily in this work, including numerous metrics not validated in the initial publication (R. J. Taylor et al., 2020). For each metric analyzed (migration at E14.5+2, number and length of processes at E14.5+2, as well as new processes per hour, somal translocations per hour and change in Y position per hour) control conditions were analyzed (Double UP alone as well as

Double UP with pSico Scrambled shRNA). For each of these measurements green cells and magenta cells were not significantly different from each other, further validating the quality and versatility of Double UP as a tool. Double UP proved to be especially advantageous for the organotypic live slice cultures. Variability in live slice culture results from the additive variabilities inherent to IUE (surgery inconsistencies, difference between embryos, difference between litters) and in live slice culture (speed of dissection, sectioning, whether or not the brain remains embedded in agarose, intensities of lasers required to visualize signal, “sagginess” of tissue, necessity to use embryos from different litters, and likely other sources impacting the relative health and “happiness” of the living cortical slice). Without internal controls, two live slice experiments might look radically different, even if both were electroporated with the same conditions. One live slice experiment does not behave like another, and we show data to that effect. However, in the absence of manipulation, green and magenta cells behave the same within an individual slice, regardless of whether that slice exhibits prolific migration (a “happy” slice) or lessened migration (an “unhappy” slice). This allows for green and magenta cells to be compared with each other, to great effect, within a single living slice during experiments in which magenta is associated with a manipulation.

References

Carter, R. N., Casillo, S. M., Mazzocchi, A. R., DesOrmeaux, J. S., Roussie, J. A., & Gaborski, T. R. (2017). Ultrathin transparent membranes for cellular barrier and co-culture models. *Biofabrication, 9*(1), 015019. doi:10.1088/1758-5090/aa5ba7

Dehmelt, L., Smart, F. M., Ozer, R. S., & Halpain, S. (2003). The role of microtubule-associated protein 2c in the reorganization of microtubules and lamellipodia during neurite initiation. *J Neurosci, 23*(29), 9479-9490. Retrieved from https://www.ncbi.nlm.nih.gov/pubmed/14573527

Dent, E. W., Kwiatkowski, A. V., Mebane, L. M., Philippar, U., Barzik, M., Rubinson, D. A., . . . Gertler, F. B. (2007). Filopodia are required for cortical neurite initiation. *Nat Cell Biol, 9*(12), 1347-1359. doi:10.1038/ncb1654

Edmondson, J. C., & Hatten, M. E. (1987). Glial-guided granule neuron migration in vitro: a high-resolution time-lapse video microscopic study. *J Neurosci, 7*(6), 1928-1934. Retrieved from https://www.ncbi.nlm.nih.gov/pubmed/3598656

Fujita, H., Katoh, H., Ishikawa, Y., Mori, K., & Negishi, M. (2002). Rapostlin is a novel effector of Rnd2 GTPase inducing neurite branching. *J Biol Chem, 277*(47), 45428-45434. doi:10.1074/jbc.M208090200

Goh, K. L., Cai, L., Cepko, C. L., & Gertler, F. B. (2002). Ena/VASP proteins regulate cortical neuronal positioning. *Curr Biol, 12*(7), 565-569. doi:10.1016/s0960-9822(02)00725-x

He, M., Zhang, Z. H., Guan, C. B., Xia, D., & Yuan, X. B. (2010). Leading tip drives soma translocation via forward F-actin flow during neuronal migration. *J Neurosci, 30*(32), 10885-10898. doi:10.1523/JNEUROSCI.0240-10.2010

Heng, J. I., Nguyen, L., Castro, D. S., Zimmer, C., Wildner, H., Armant, O., . . . Guillemot, F. (2008). Neurogenin 2 controls cortical neuron migration through regulation of Rnd2. *Nature, 455*(7209), 114-118. doi:10.1038/nature07198

Henne, W. M., Kent, H. M., Ford, M. G., Hegde, B. G., Daumke, O., Butler, P. J., . . . McMahon, H. T. (2007). Structure and analysis of FCHo2 F-BAR domain: a dimerizing and membrane recruitment module that effects membrane curvature. *Structure, 15*(7), 839-852. doi:10.1016/j.str.2007.05.002

Itoh, T., Erdmann, K. S., Roux, A., Habermann, B., Werner, H., & De Camilli, P. (2005). Dynamin and the actin cytoskeleton cooperatively regulate plasma membrane invagination by BAR and F-BAR proteins. *Dev Cell, 9*(6), 791-804. doi:10.1016/j.devcel.2005.11.005

Kawauchi, T., Chihama, K., Nabeshima, Y., & Hoshino, M. (2003). The in vivo roles of STEF/Tiam1, Rac1 and JNK in cortical neuronal migration. *EMBO J, 22*(16), 4190-4201. doi:10.1093/emboj/cdg413

Komuro, H., & Rakic, P. (1995). Dynamics of granule cell migration: a confocal microscopic study in acute cerebellar slice preparations. *J Neurosci, 15*(2), 1110-1120. Retrieved from https://www.ncbi.nlm.nih.gov/pubmed/7869087

Krause, M., Leslie, J. D., Stewart, M., Lafuente, E. M., Valderrama, F., Jagannathan, R., . . . Gertler, F. B. (2004). Lamellipodin, an Ena/VASP ligand, is implicated in the regulation of lamellipodial dynamics. *Dev Cell, 7*(4), 571-583. doi:10.1016/j.devcel.2004.07.024

Kwiatkowski, A. V., Rubinson, D. A., Dent, E. W., Edward van Veen, J., Leslie, J. D., Zhang, J., . . . Gertler, F. B. (2007). Ena/VASP Is Required for neuritogenesis in the developing cortex. *Neuron, 56*(3), 441-455. doi:10.1016/j.neuron.2007.09.008

Moffat, J. J., Ka, M., Jung, E. M., & Kim, W. Y. (2015). Genes and brain malformations associated with abnormal neuron positioning. *Mol Brain, 8*(1), 72. doi:10.1186/s13041-015-0164-4

Nadarajah, B., Brunstrom, J. E., Grutzendler, J., Wong, R. O., & Pearlman, A. L. (2001). Two modes of radial migration in early development of the cerebral cortex. *Nat Neurosci, 4*(2), 143-150. doi:10.1038/83967

Nakamura, K., Yamashita, Y., Tamamaki, N., Katoh, H., Kaneko, T., & Negishi, M. (2006). In vivo function of Rnd2 in the development of neocortical pyramidal neurons. *Neurosci Res, 54*(2), 149-153. doi:10.1016/j.neures.2005.10.008

Noctor, S. C., Martinez-Cerdeno, V., Ivic, L., & Kriegstein, A. R. (2004). Cortical neurons arise in symmetric and asymmetric division zones and migrate through specific phases. *Nat Neurosci, 7*(2), 136-144. doi:10.1038/nn1172

Parnavelas, J. G. (2000). The origin and migration of cortical neurones: new vistas. *Trends Neurosci, 23*(3), 126-131. doi:10.1016/s0166-2236(00)01553-8

Saengsawang, W., Mitok, K., Viesselmann, C., Pietila, L., Lumbard, D. C., Corey, S. J., & Dent, E. W. (2012). The F-BAR protein CIP4 inhibits neurite formation by producing lamellipodial protrusions. *Curr Biol, 22*(6), 494-501. doi:10.1016/j.cub.2012.01.038

Saengsawang, W., Taylor, K. L., Lumbard, D. C., Mitok, K., Price, A., Pietila, L., . . . Dent, E. W. (2013). CIP4 coordinates with phospholipids and actin-associated proteins to localize to the protruding edge and produce actin ribs and veils. *J Cell Sci, 126*(Pt 11), 2411-2423. doi:10.1242/jcs.117473

Saito, T., & Nakatsuji, N. (2001). Efficient gene transfer into the embryonic mouse brain using in vivo electroporation. *Dev Biol, 240*(1), 237-246. doi:10.1006/dbio.2001.0439

Schwarz, N., Uysal, B., Welzer, M., Bahr, J. C., Layer, N., Loffler, H., . . . Koch, H. (2019). Long-term adult human brain slice cultures as a model system to study human CNS circuitry and disease. *Elife, 8*. doi:10.7554/eLife.48417

Tabata, H., & Nakajima, K. (2001). Efficient in utero gene transfer system to the developing mouse brain using electroporation: visualization of neuronal migration in the developing cortex. *Neuroscience, 103*(4), 865-872. doi:10.1016/s0306-4522(01)00016-1

Taylor, K. L., Taylor, R. J., Richters, K. E., Huynh, B., Carrington, J., McDermott, M. E., . . . Dent, E. W. (2019). Opposing functions of F-BAR proteins in neuronal membrane protrusion, tubule formation, and neurite outgrowth. *Life Sci Alliance, 2*(3). doi:10.26508/lsa.201800288

Taylor, R. J., Carrington, J., Gerlach, L. R., Taylor, K. L., Richters, K. E., & Dent, E. W. (2020). Double UP: A Dual Color, Internally Controlled Platform for in utero Knockdown or Overexpression. *Front Mol Neurosci, 13*, 82. doi:10.3389/fnmol.2020.00082

Ventura, A., Meissner, A., Dillon, C. P., McManus, M., Sharp, P. A., Van Parijs, L., . . . Jacks, T. (2004). Cre-lox-regulated conditional RNA interference from transgenes. *Proc Natl Acad Sci U S A, 101*(28), 10380-10385. doi:10.1073/pnas.0403954101

Yang, T., Sun, Y., Zhang, F., Zhu, Y., Shi, L., Li, H., & Xu, Z. (2012). POSH localizes activated Rac1 to control the formation of cytoplasmic dilation of the leading process and neuronal migration. *Cell Rep, 2*(3), 640-651. doi:10.1016/j.celrep.2012.08.007

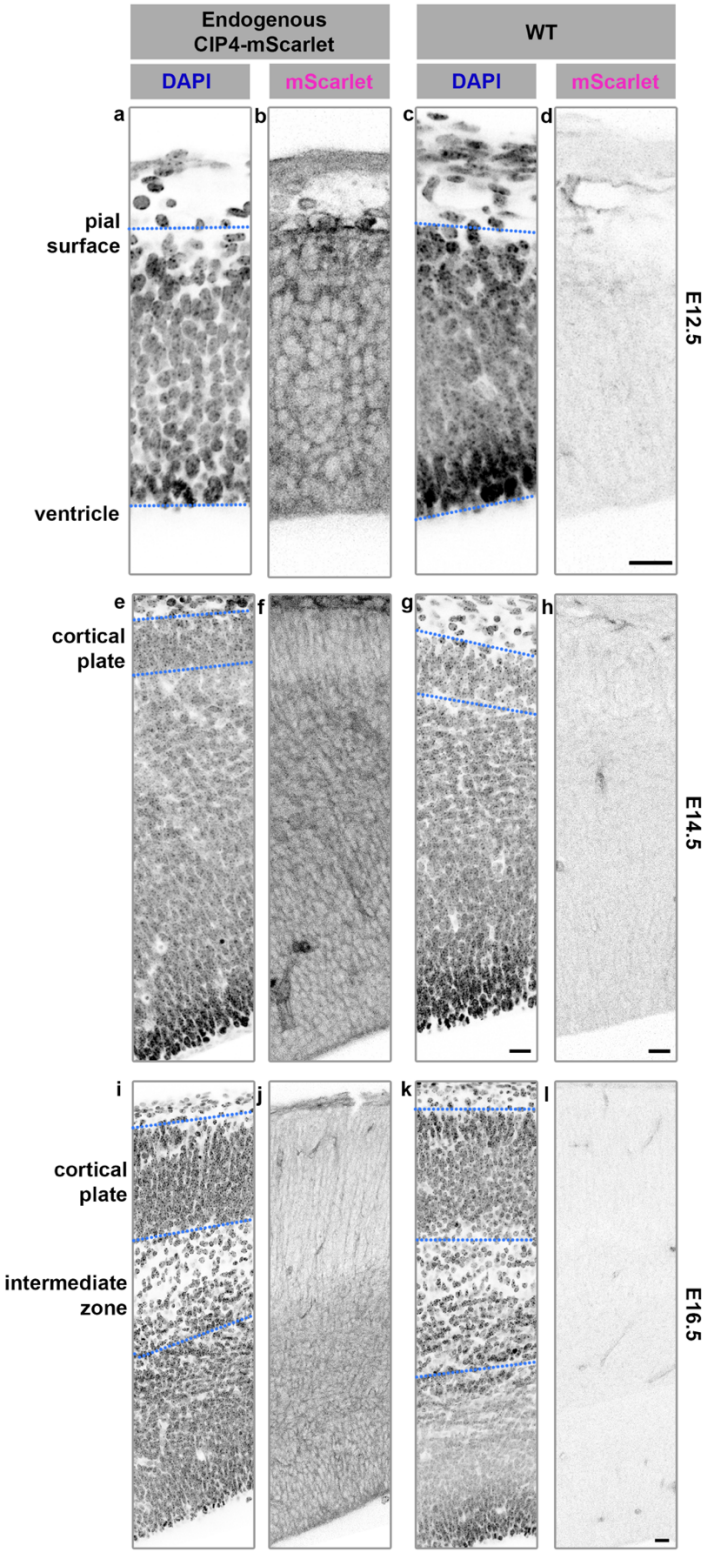
Endogenous CIP4-mScarlet
WT
DAPI
mScarlet
DAPI
mScarlet
a
b
c
d
pial surface
ventricle
E12.5
e
f
g
h
cortical plate
E14.5
i
j
k
l
cortical plate
intermediate zone
E16.5

Figure 1: Endogenous CIP4 in the developing brain

(a, c) Representative images of cortices from CIP4-mScarlet (a) and wildtype (WT) (c) littermates at embryonic day 12.5 (E12.5), stained for DAPI, with pial surface and ventricle indicated with dotted lines. **(b, d)** CIP4-mScarlet (red) signal inverted in black and white to show contrast. **(e, g)** Representative images of cortices from CIP4-mScarlet (e) and WT (g) littermates at E14.5, stained for DAPI, with cortical plate and ventricle indicated with dotted lines **(f, h)** CIP4-mScarlet (red) signal inverted in black and white to show contrast. **(i, k)** Representative images of cortices from CIP4-mScarlet (i) and WT (k) littermates at E16.5, stained for DAPI, with cortical plate, intermediate zone and ventricle indicated with dotted lines. **(j, l)** CIP4-mScarlet (red) signal inverted in black and white to show contrast. All scale bars 20μm. Images at each age acquired with the same settings and processed in the same manner.

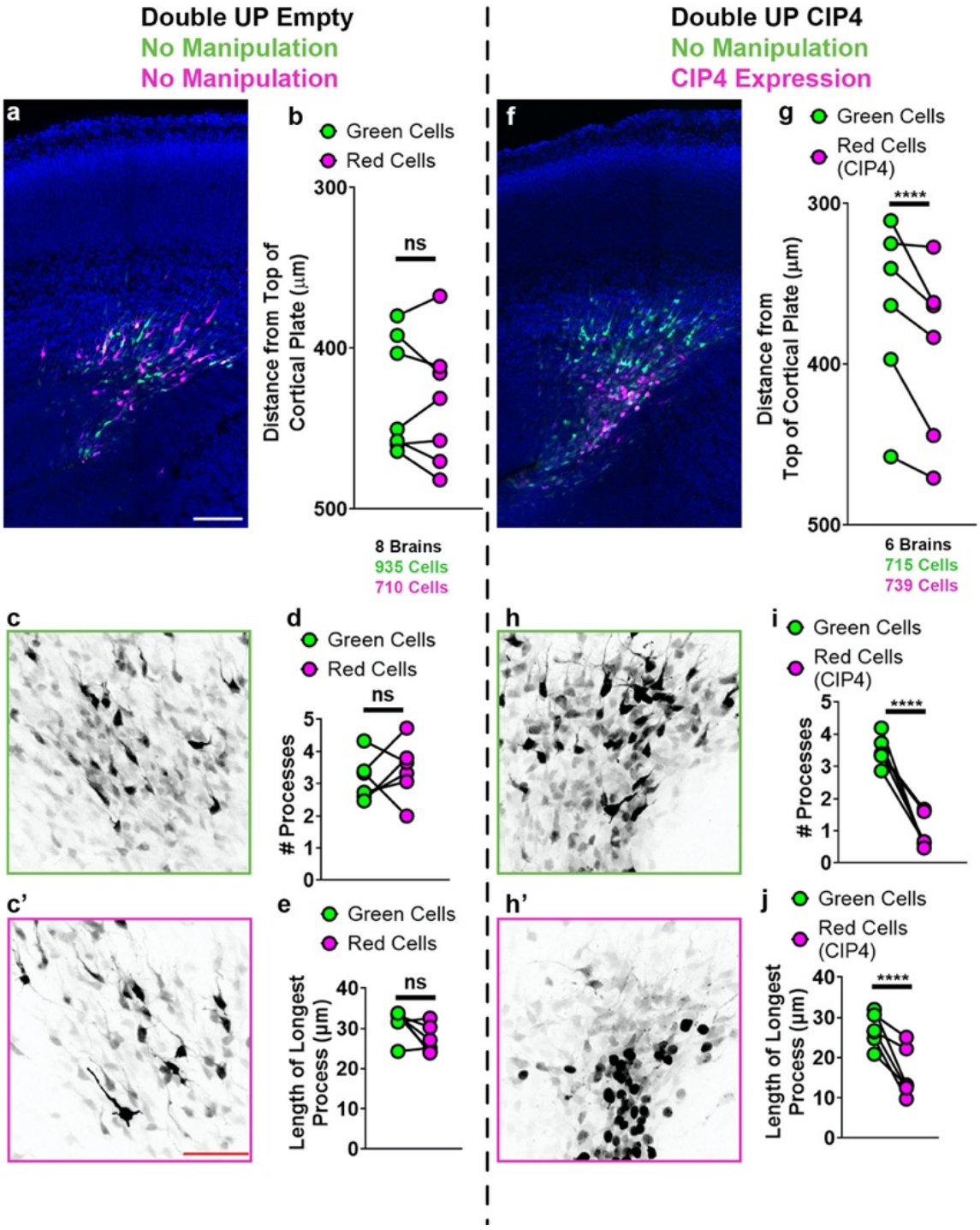
Double UP Empty
No Manipulation
No Manipulation
Double UP CIP4
No Manipulation
CIP4 Expression
a
b
Green Cells
Red Cells
Distance from Top of Cortical Plate (µm)
300
400
500
ns
8 Brains
935 Cells
710 Cells
f
g
Green Cells
Red Cells (CIP4)
****
Distance from Top of Cortical Plate (µm)
6 Brains
715 Cells
739 Cells
c
d
Processes
ns
h
i
****
c'
e
Length of Longest Process (µm)
h'
j

Figure 2: Sustained CIP4 overexpression decreases migration and processes

(a, f) Representative image of Double UP Empty (a) and Double UP CIP4 (f), E14.5+2. Scale bar 100µm. **(b, g)** Dot plot of migration of green and magenta cells. n=8 brains with 1655 cells for Empty (b) and n=6 brains with 1454 cells for CIP4 (g). Each dot represents mean distance from the top of the cortical plate to the distance of all cortical neurons in a slice. Connected dots indicate measurements were made in the same coronal slice. **(c, c', h, h')** Max project of cells green (c and h) and magenta (c' and h') cells from Double UP Empty and Double UP CIP4, displayed with inverted black and white to emphasize morphology. Scale bar=50 µm **(d, i)** Dot plot of number of number of processes of green and magenta cells. Each dot represents mean number of processes. n= 6 brains, 120 total cells for Empty (d) and also for CIP4 (i). **(e)** Dot plot of number of length of longest processes of green and magenta cells. Each dot represents mean number of length of the longest process. Cells with no processes were not included. n= 6 brains, 179 total cells for Empty (e) and n=6 brains, 143 cells for CIP4.

ns=not significant, **** p<0.0001, two-way ANOVA. Error bars not shown for clarity

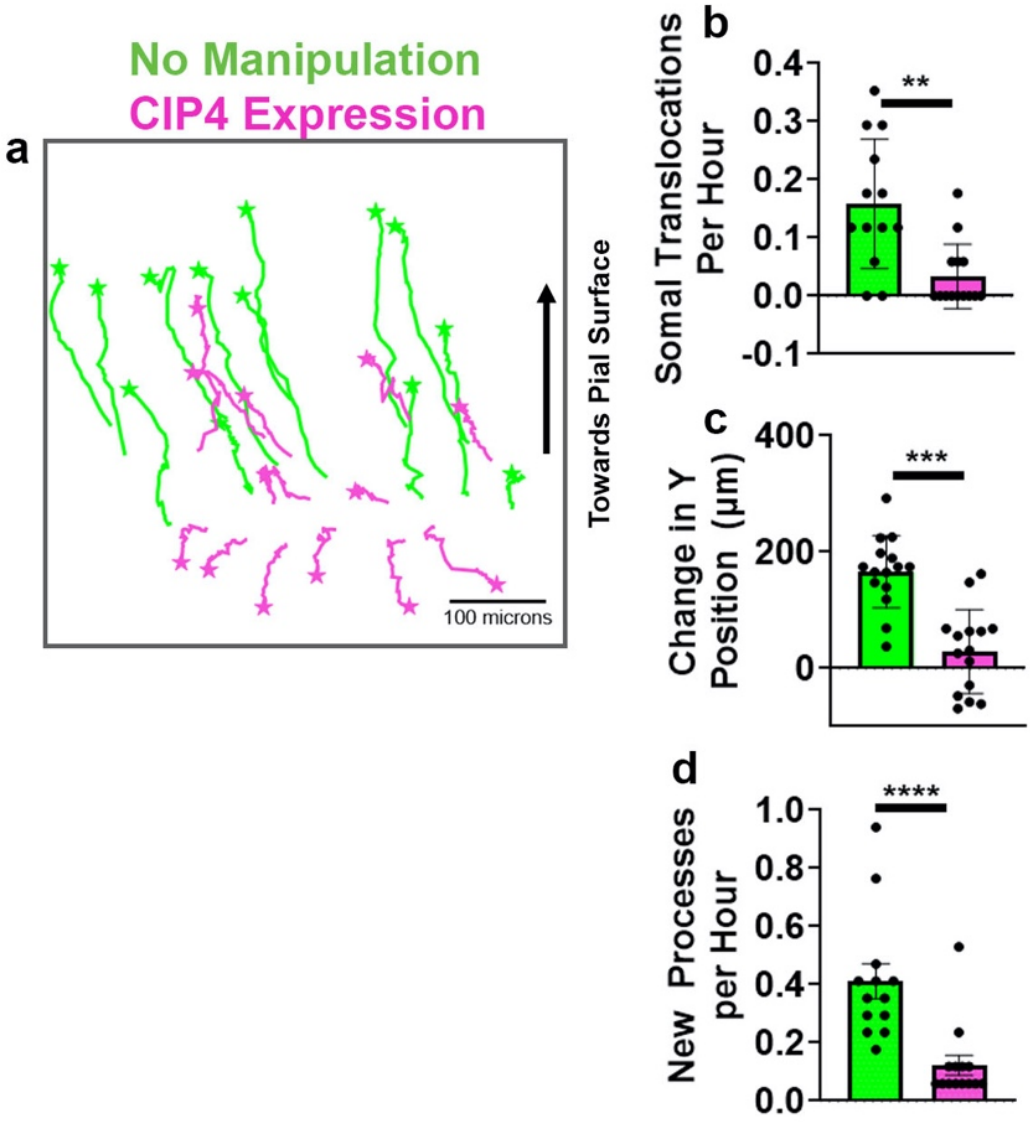
No Manipulation
CIP4 Expression
a
100 microns
Towards Pial Surface
b
Somal Translocations Per Hour
0.4
0.3
0.2
0.1
0.0
-0.1
**
c
Change in Y Position (µm)
400
200
0
***
d
New Processes per Hour
1.0
0.8
0.6
0.4
0.2
0.0
****

Figure 3: CIP4 overexpression in live slice culture

(See also Video 1 at go.wisc.edu/RussellTaylorThesis) **(a)** Trace of the brightest 12 green cells and 13 magenta cells taken during a 17 hour timelapse video of a living slice (n=1). Stars indicate position at the end of 17 hours, arrow indicates direction of normal migration (towards the pial surface). Prior to quantification, tissue movement was corrected using the "Correct 3D drift" plugin in Fiji. **(b)** Bar graph of somal translocations per hour over the course of the 17 hour timelapse. Each dot represents one cell. **(c)** Bar graph of change in Y position, after correction with the "Correct 3D drift" plugin in Fiji. **(d)** Bar graph of new processes per hour, over the course of the 17 hour timelapse. Each dot represents one cell

**** $p<0.0001$, *** $p<0.001$, ** $p<.01$, student's t-test, Mann-Whitney. The correction from the "Correct 3D drift" tool was generated using the video of magenta cells, but applied equally to both the magenta and green cells.

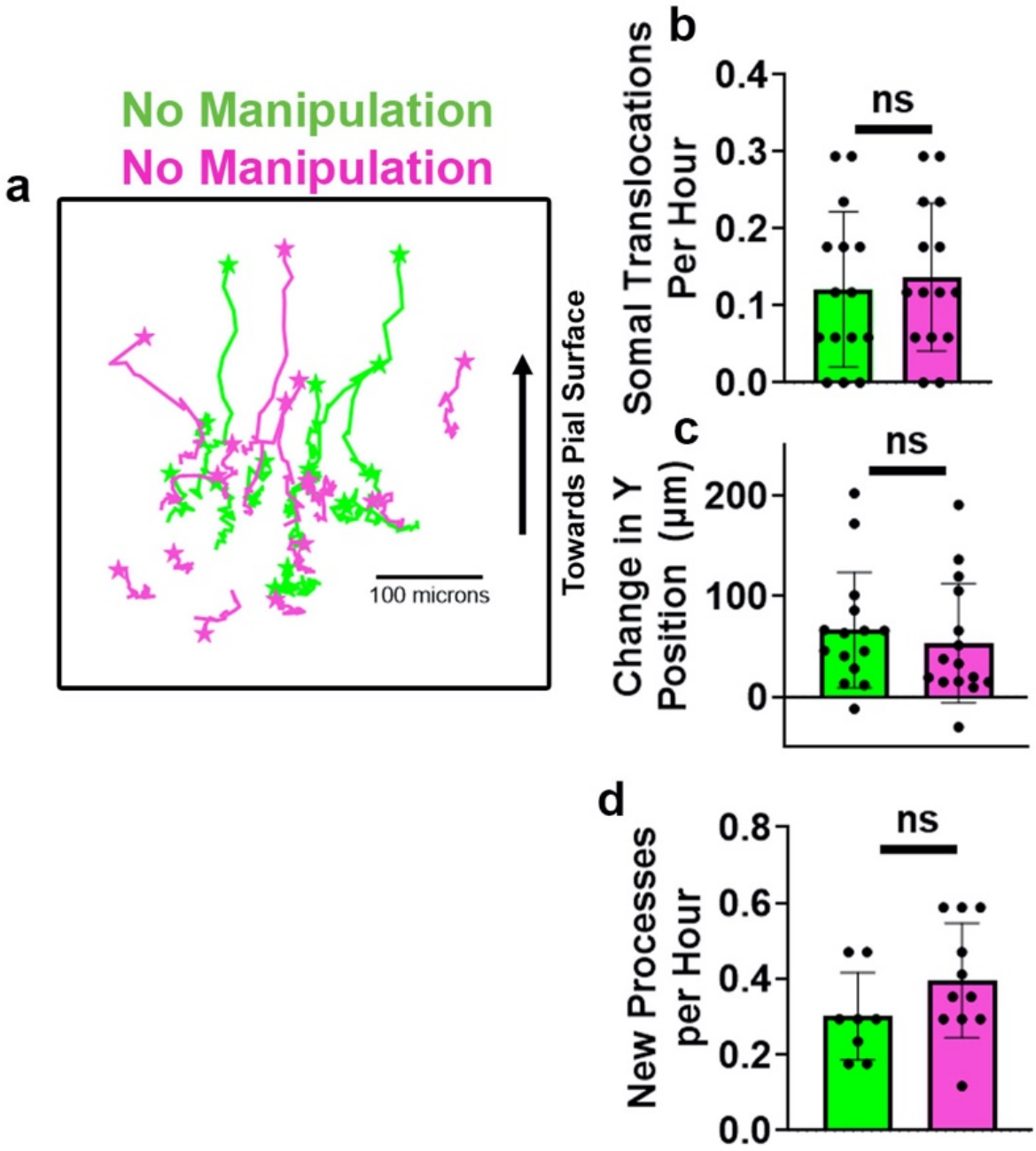

Supplemental Figure 1: Double UP in live slice culture (complementary to Figure 2)

(See also Video 2 at go.wisc.edu/RussellTaylorThesis) **(a)** Trace of the brightest 15 green cells and 15 magenta cells taken during a 17 hour timelapse video of a living slice (n=1). Stars indicate position at the end of 17 hours, arrow indicates direction of normal migration (towards the pial

surface). Prior to quantification, tissue movement was corrected using the “Correct 3D drift” plugin in Fiji. **(b)** Bar graph of somal translocations per hour over the course of the 17 hour timelapse. Each dot represents one cell. **(c)** Bar graph of change in Y position, after correction with the “Correct 3D drift” plugin in Fiji. **(d)** Bar graph of new processes per hour, over the course of the 17 hour timelapse. Each dot represents one cell **(e)** Bar graph of Processes Retracted per Hour, over the course of the 17 hour timelapse. Each dot represents one cell.

ns= not significant, student’s t-test, Mann-Whitney. The correction from the “Correct 3D drift” tool was generated using the video of magenta cells, but applied equally to both the magenta and green cells.

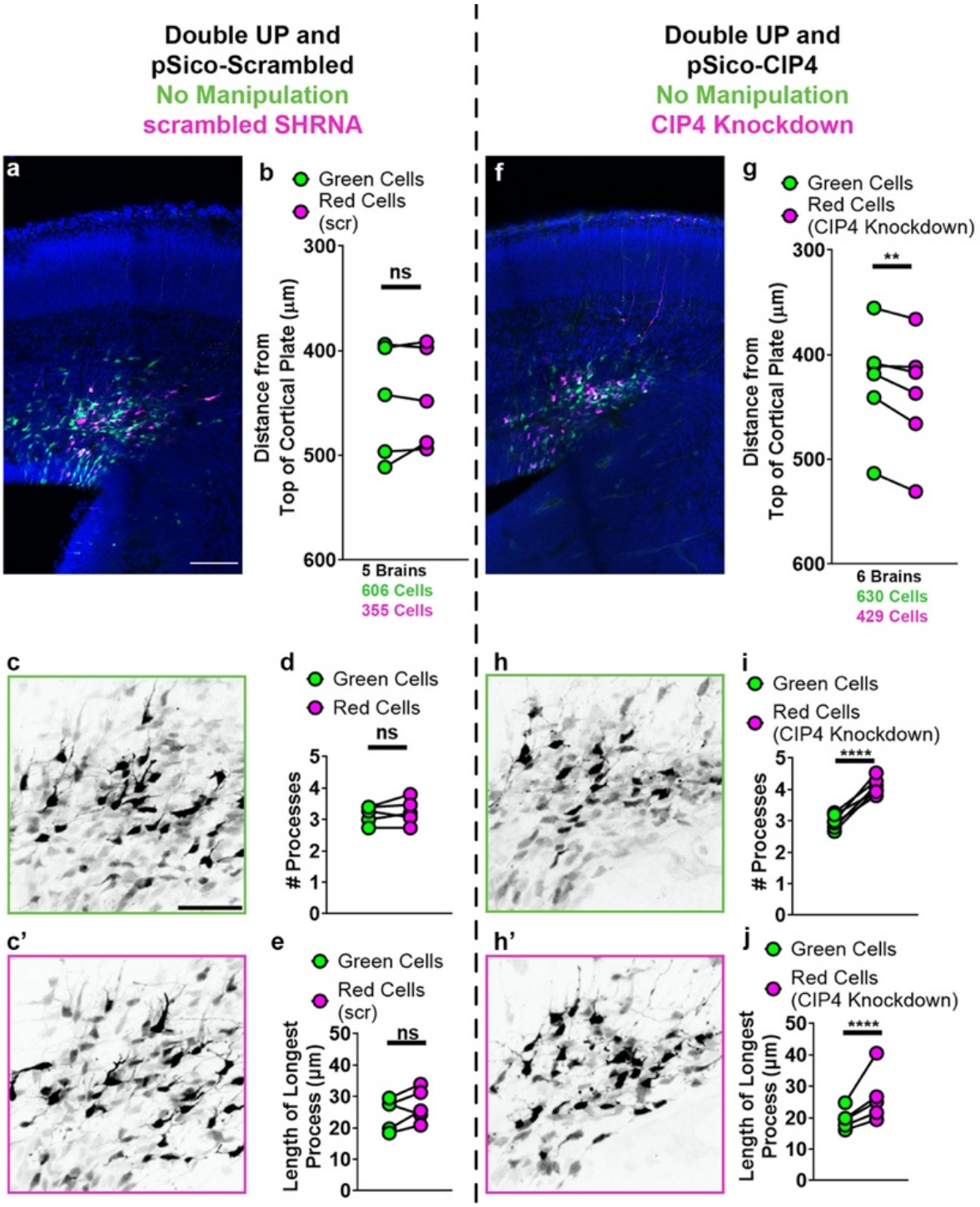
Double UP and
pSico-Scrambled
No Manipulation
scrambled SHRNA
Double UP and
pSico-CIP4
No Manipulation
CIP4 Knockdown
a
b
Green Cells
Red Cells
(scr)
ns
Distance from
Top of Cortical Plate (µm)
300
400
500
600
5 Brains
606 Cells
355 Cells
f
g
Green Cells
Red Cells
(CIP4 Knockdown)
**
6 Brains
630 Cells
429 Cells
c
d
Processes
0
1
2
3
4
5
h
i
****
c'
e
Length of Longest
Process (µm)
10
20
30
40
50
h'
j

Figure 4: CIP4 knockdown increases process length and number

(a, f) Representative image of Double UP Empty with pSico-Scrambled (a) and pSico-CIP4 (f), E14.5+2. Scale bar 100µm. **(b, g)** Dot plot of migration of green and magenta cells. n=5 brains, 961 total cells for pSico-Scrambled (scr) (b) and n=6 brains, 1059 total cells for pSico-CIP4 (g). Each dot represents mean distance from the top of the cortical plate to the distance of all cortical neurons in a slice. Connected dots indicate measurements were made in the same coronal slice. **(c, c', h, h')** Max project of cells green (c and h) and magenta (c' and h') cells from pSico Scrambled and pSico CIP4, displayed with inverted black and white to emphasize morphology. Scale bar=50 µm **(d, i)** Dot plot of number of number of processes of green and magenta cells. Each dot represents mean number of processes. n= 6 brains, 120 total cells for pSico-Scrambled (d) and also for pSico-CIP4 (i). **(e)** Dot plot of number of length of longest processes of green and magenta cells. Each dot represents mean number of length of the longest process. Cells with no processes were not included. n= 6 brains, 179 total cells for pSico-Scrambled (e) and n=6 brains, 143 cells for pSico-CIP4.

ns=not significant, **** p<0.0001, two-way ANOVA. Error bars not shown for clarity

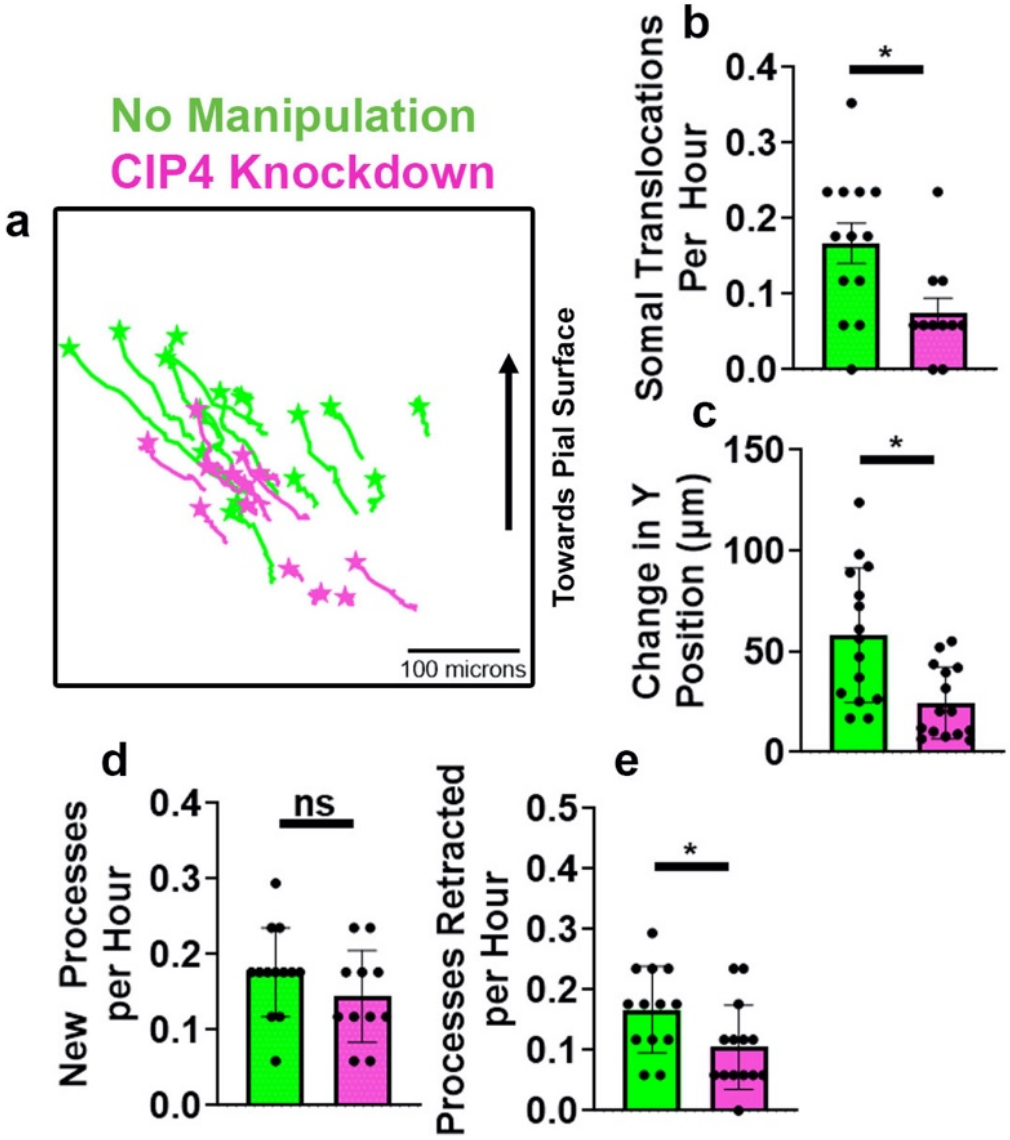
No Manipulation
CIP4 Knockdown
a
Towards Pial Surface
100 microns
b
Somal Translocations Per Hour
0.4
0.3
0.2
0.1
0.0
*
c
Change in Y Position (µm)
150
100
50
0
*
d
New Processes per Hour
0.4
0.3
0.2
0.1
0.0
ns
e
Processes Retracted per Hour
0.5
0.4
0.3
0.2
0.1
0.0
*

Figure 5: CIP4 knockdown in live slice culture

(See also Video 3 at go.wisc.edu/RussellTaylorThesis) **(a)** Trace of the brightest 15 green cells 15 magenta cells taken during a 17 hour timelapse video of a living slice. Stars indicate position at the end of 17 hours, arrow indicates direction of normal migration (towards the pial surface). Prior to quantification, tissue movement was corrected using the "Correct 3D drift" plugin in fiji. **(b)** Bar graph of somal translocations per hour over the course of the 17 hour timelapse. Each dot represents one cell. **(c)** Bar graph of change in Y position, after correction with the "Correct 3D drift" plugin in Fiji. **(d)** Bar graph of new processes per hour, over the course of the 17 hour timelapse. Each dot represents one cell **(e)** Bar graph of Processes Retracted per Hour, over the course of the 17 hour timelapse. Each dot represents one cell.

* $p<.05$ student's t-test, Mann-Whitney. The correction from the "Correct 3D drift" tool was generated using the video of magenta cells, but applied equally to both the magenta and green cells.

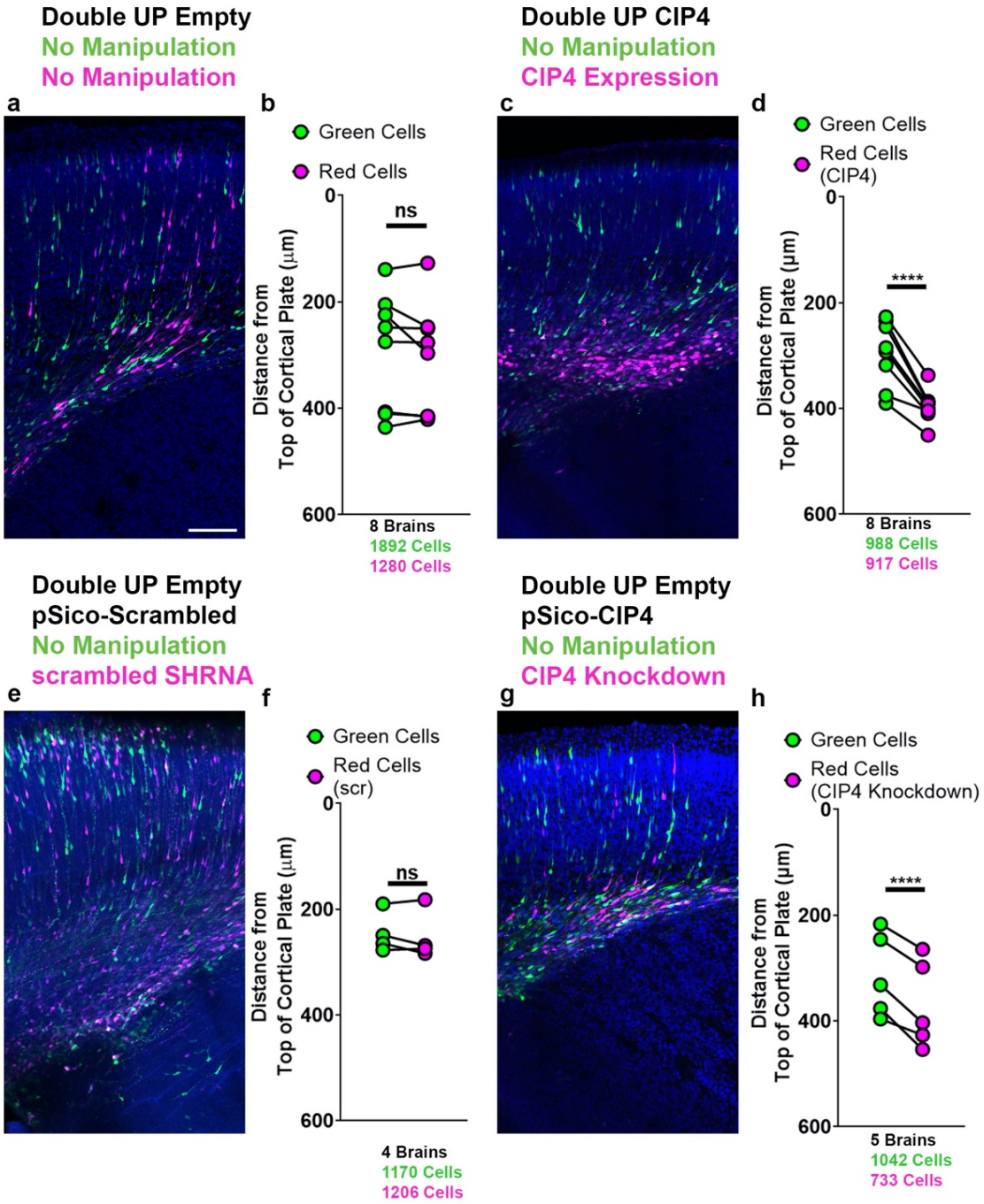
Double UP Empty
No Manipulation
No Manipulation
a
b
Green Cells
Red Cells
ns
Distance from Top of Cortical Plate (µm)
0
200
400
600
8 Brains
1892 Cells
1280 Cells
Double UP CIP4
No Manipulation
CIP4 Expression
c
d
Green Cells
Red Cells (CIP4)
****
8 Brains
988 Cells
917 Cells
Double UP Empty
pSico-Scrambled
No Manipulation
scrambled SHRNA
e
f
Green Cells
Red Cells (scr)
ns
4 Brains
1170 Cells
1206 Cells
Double UP Empty
pSico-CIP4
No Manipulation
CIP4 Knockdown
g
h
Green Cells
Red Cells (CIP4 Knockdown)
****
5 Brains
1042 Cells
733 Cells

Figure 6: CIP4 overexpression and CIP4 knockdown both stunt migration by E14.5+4

(a, c, e, g) Representative image of Double UP Empty (a) Double UP CIP4 (c), Double UP with pSico-Scrambled (e) and Double UP with pSico-CIP4 (g), E14.5+4. Scale bar 100µm. **(b, d, f, h)** Dot plots of migration of green and magenta cells. n=8 brains with 1655 cells for Empty (b) and n=6 brains with 1454 cells for CIP4 (g). Each dot represents mean distance from the top of the cortical plate to the distance of all cortical neurons in a slice. Connected dots indicate measurements were made in the same coronal slice. n=8 brains and 2572 cells for Double UP Empty, 8 brains and 1905 cells for Double UP CIP4, 4 brains and 2376 cells for Double UP and pSico-Scrambled, 5 brains and 1775 cells for Double UP and pSico-CIP4

ns=not significant, **** $p<0.0001$, two-way ANOVA. Error bars not shown for clarity

METHODS

Materials Availability

Double UP is available through Addgene (#125139)

pCAG-iCre was a gift from Wilson Wong (Addgene plasmid #89573). pSico PGK Puro was a gift from Tyler Jacks (Addgene plasmid #11586)

Double UP CIP4, pSico-CIP4 and pSico-Scrambled are available upon request. The sequence of the shRNA targeting CIP4 is GTCTGGAGCTGGCTAAGTA-TTCAAGAGA-TACTTAGCCAGCTCCAGAC. The sequence of the scrambled shRNA was GGCGGAGATTTCTGACTGA-TTCAAGAGA-TCAGTCAGAAATCTCCGCC. Human CIP4 (short) was utilized for these experiments, sequence and plasmid available upon request

Further information and requests for resources and reagents should be directed to and will be fulfilled by the Lead Contact, Erik Dent (ewdent@wisc.edu).

Animal Models

All mouse procedures were approved by the University of Wisconsin Committee on Animal Care and were in accordance with NIH guidelines. Timed matings were performed, and pregnant dams were used at embryonic day 14.5 (E14.5). Day E0.5 is the morning of sperm plug visualization. IUE was performed at E14.5, with embryos perfused either three or four days later, as specified in the text. Gender of embryos was not recorded. Pregnant females were housed individually. Prior to becoming pregnant, females were housed with 3-4 other females.

Generation of CIP4-mScarlet Transgenic Mouse

A cassette coding for Linker-LoxP-3xHA-Stop Codon-LoxP-mScarlet was cloned using Gibson Assembly. Genomic DNA was isolated from wild type mouse liver, and used to clone a 1.5kb 5' homology arm, and a 2.5kb 3' homology arm located immediately around the stop codon of CIP4. These three components were combined using Gibson Assembly, and the resulting plasmid DNA was used as a template for Crispr/Cas9. A guide RNA (GAACCCCACCAGAGGGGGACG(AGG)) was validated to cut genomic DNA, and then inserted with Cas9 protein and linearized homology plasmid into fertilized mouse oocytes. Animals were screened for presence or absence of a transgene via PCR, and a female was found to be mosaic for the insert. The transgene and surrounding 1KB of genomic DNA were sequence verified. The female was used as the founder of the colony. Once sufficient animals were positive for the transgene, a heterozygous female was crossed to a ß-Actin Cre Mouse (Jax 019099), to permanently recombine the transgene to code for CIP4-Linker-LoxP-mScarlet. Both lines (CIP4-Linker-LoxP-mScarlet and CIP4-Linker-LoxP-3xHA-Stop Codon-LoxP-mScarlet) are being maintained by the Dent Lab and are available upon request. Genotyping is performed using ACCAGGGGATGTAGCAGTTG (Forward) and CACGTGGGCAGGAATAAAGT (Reverse).

In Utero Electroporation (IUE)

Plasmid DNA was mixed before injection. 15ng/µL of pCAG-iCre was mixed with 2µg/µL of Double UP or Double UP CIP4. For knockdown studies, 15ng/µL pCAG-iCre was mixed with 1µg/µL Double UP and 2µg/µL of either pSico-CIP4 or pSico-scrambled. Plasmid DNA was then combined with Fast Green FCF to a final concentration of 0.05% Fast Green FCF, and loaded into pulled capillary

needles. The dam was anesthetized with isoflurane, and a laparotomy was performed, exposing the embryos. The embryos were gently pulled out of the abdominal cavity. The capillary needles were inserted into the lateral ventricles, and approximately 0.25-0.5 µL DNA/Fast Green FCF was injected using a PicoSpritzer II (Parker Instrumentation). Electrical current was passed across the head, in five pulses of 40 volts each lasting 100ms on and 900ms off using a CUY21 Electroporator (Bex Co. LTD). After the last embryo was electroporated, the embryos were inserted back into the mother, and the laparotomy was sutured closed. Embryos were allowed to develop normally for 2 or 4 days, depending on experiment (E14.5+2 or E14.5+4). Surgeries were performed on embryos from at least two different pregnant females for each experiment.

Tissue Collection

Embryos were again exposed via laparotomy on the mother after deep anesthesia with isoflurane. Embryos were removed from the uterus one by one, chest cavity was opened, a small incision was made in the right atrium and a needle was inserted into the left ventricle. Through this needle, the animal was perfused with approximately 1 mL of sterile saline and 3 mL of 4% paraformaldehyde (PFA) using an Instech perfusion pump, at the rate of approximately 1.25mL per minute. Following perfusion, heads were removed and left in PFA at 4°C overnight before dissection. After the last embryo was perfused, the dam was euthanized. Following dissection, embryos were screened for positive signal using the mScarlet signal, which is easily visible in an intact, dissected brain. All brains containing mScarlet signal were further processed.

Fixed Tissue Sectioning

After 16 hours in PFA at 4°C, heads were transferred to PBS and brains were dissected. Brains were placed in 3% low melt agarose for 10 minutes at 42°C, then moved into 6% low melt agarose and allowed to set on ice. After the agarose hardened, the brains were sectioned on a Leica VT1000S vibratome at 100µm in PBS. Sections were stored for less than one week in PBS+0.2% sodium azide before being stained with 4',6-diamidino-2-phenylindole (DAPI) and imaged.

Section Preparation

DAPI was diluted to a final concentration of 2.4 nM in 0.4% Triton/PBS, and left on sections for one hour on a gently rotating platform at room temperature. After one hour, the sections were washed three times in PBS before being mounted in Aqua-Poly Mount (Polysciences). Slides were allowed to dry for at least one hour and then imaged within two days.

Imaging

Confocal imaging was performed on a Zeiss LSM 800. Two imaging paradigms were used for IUE experiments, one for live slice experiments and one for endogenous CIP4 images. For fixed migration analysis (Figure 2: a, b, f, g, Figure 4: a, c, e, g, Figure 6: a, c, e, g) , 12 optical sections were obtained, each 1µm apart. 2x2 tiles were collected with a 20x/0.8NA Plan Apochromat objective, with 2x averaging, and presented as maximum projections. For fixed morphology analysis (Figure 2: c-e, h-j, Figure 4: c-e, h-j), 80-120 optical sections were obtained through the entirety of the 100µm section, each at .5 µm. This accounts for less than 100 µm, and is likely due to some tissue compression. These images were also collected with a 20x/0.8NA Plan

Apochromat objective, with 2x averaging, and presented as maximum projections. Live slice experiments, including imaging, are described below. For imaging of endogenous CIP4-mScarlet (Figure 1), 58 optical sections were obtained, each 1µm apart. Images were collected with a 20x/0.8NA Plan Apochromat objective, with 4x averaging, and presented as maximum projections of the three brightest continuous sections. For IUE experiments, gain/laser power were altered between each image set to optimize image quality. Tiles were stitched together using the stitching tool in Zen 2.3 (Zeiss), and resulting images were analyzed using the TRON Program software described elsewhere in this manuscript.

Live Slice Experiments

Live imaging was performed as described previously (Wiegreffe Jove). Somewhat briefly, embryos were exposed via laparotomy on the mother after deep anesthesia with isoflurane. Embryos were removed from the uterus one by one, and brains were immediately dissected in cold HBSS (+mg/+ca). Brains were quickly scanned for red fluorescence on a fluorescent microscope, and positive brains were embedded in 4% low melt agarose in HBSS. Agarose was allowed to harden on ice, then was superglued onto metal chucks and sectioned on a Leica VT1000S vibratome at 300µm in cold HBSS. Sections were quickly scanned for red fluorescence on a fluorescent microscope, and the best section was selected and mounted onto a ptfe membrane, pre-treated with 83µg/mL PDL and 8.3µg/mL laminin. Sections sit at the gas liquid interface above one mL of 5% CO2-equilibrated slice culture media (35mL BME, 12.9mL HBSS, 1.35mL of 1M D-Glucose, 0.5mL Pen Strep, 0.25mL L-Glutamine, sterile filter, add 2.5mL FBS). Slice can be imaged immediately, though there will likely be significant tissue “sagging” in the

first hour. Slices were then placed into an environmental chamber affixed to the confocal microscope, maintaining 37°C, 5% CO2 and high humidity. Images were taken using a 10x/0.3NA Plan-Neofluar objective, with 4x averaging, 5µm steps and presented as maximum projections. Images were taken every fifteen minutes for 17 hours.

Data Collection

Migration data was calculated using the TRON program, as described previously. Process number, process length, somal translocations per hour, new processes per hour and tracking of live migrating neurons was all done manually in either Zen 2.3 or Fiji, by experimenters blinded to condition.

Quantification and Statistical Analysis

For data comparing multiple brains at the same time, two-way ANOVA was performed. For these two-way ANOVA, reported p-values refer to the p-value associated with variation due to the differences in color within slices. P-values associated with variation due to differences between slices was not reported. Complete data is available upon request. All statistical tests were performed in Prism 8 (Graph Pad).

Chapter 4:

Discussion and Conclusions

Discussion and Conclusions

The radial migration of an individual cortical neuron is a highly complex process, which has been broadly described but may never be totally understood. The largest gap in our understanding of radial migration of cortical neurons surrounds the transition into and out of the multipolar phase of development. All radial migrating cortical neurons exhibit this behavior during their migration, but both the purpose and many of the factors involved in multipolar entry and exit are still being elucidated. The studies presented in this thesis suggest that CIP4 is necessary for retraction of unneeded neurites generated during the multipolar phase of cortical neuron migration.

Double UP

The use of Double UP in these studies might be easily overlooked, but it is critical to many of the findings presented here and should provide a more rigorous methodology to the greater scientific population. I have steady hands, high focus, and have performed *in utero* electroporation on greater than 2,000 embryos, and therefore consider myself to be an expert in this technique. However, variability has remained high between embryos, suggesting that expertise is insufficient to eliminate variability. Some embryos are physically larger than others, suggesting a differential level of development. Position along the uterus may play a role, as embryos near the cervix are much more crowded than those further from the cervix. There are additional variables present comparing between litters. Age and health of the mother, age and health of the father, time of copulation relative to time of surgery, are all likely contributors to variation. Double UP has thus far proven to be an excellent tool for mitigating this variability, by allowing comparison of cells within an individual cortical slice, from a single brain and a single

surgery. The ability to image control and experimental cells in the same slice, whether fixed or live, has allowed for an improved ability to not only discern broad migration defects, but also more subtle morphological distinctions between neurons in different conditions.

The rigor of IUE as traditionally performed is limited. “Section Matching” in combination with littermate controls is the broadly accepted methodology for comparing control and experimental conditions. However, many publications mention neither “section matching” nor “littermate controls” in their publications, so it is unclear which and whether these controls are in use. In fact, of the five most recent manuscripts published in well-known journals utilizing IUE, only one referenced littermates (Hu, Yang, & Wang, 2021) and none referenced the use of section matching (Fang, Bygrave, Roth, Johnson, & Huganir, 2021; Hamabe-Horiike et al., 2021; Morita et al., 2021; Nguyen & Bordey, 2021). From personal correspondence and interactions at conferences, section matching and littermates are both assumed to be the standard method of producing controls, but if major publications are not requiring acknowledgement of use of these controls it is unclear if they are used in common practice. This lack of reporting makes it impossible to know how rigorous past and present IUE experiments are, and further exemplifies the necessity of a tool like Double UP.

Additionally, before the introduction of the “Tron Machine” (Chapter 2, Figure 2), quantification of migration was very simplistic. Research groups would instead draw “binning lines”, separating tissue into either equally sized bins, or into bins according to biologically distinct regions of the cortex (ventricular zone, subventricular zone, intermediate zone, cortical plate), and then manually count cells present in each bin. While use of bins can be easier to implement, binning by equally sized regions should almost never be used (Flum, 2018), as it only

reduces the amount of available information, and increases the importance of “edge cases”- cells present at the border of two bins which can have an important impact on the significance of findings, depending on which bin cells are assigned. Use of bins according to biological regions of the cortex is better, but still reduces the power of the data, while over-emphasizing edge cases. Furthermore, the Tron Machine is largely automated, reducing the opportunity for user bias, and it creates a record of every cell counted and the exact positioning of areas of interest. By developing and using the Tron Machine, more cells can be counted in less time and in a less biased manner, while simultaneously avoiding the pitfalls of binning. Thus, the implementation of Tron machine results in data with more power and fewer problems than traditional methods of counting.

There were points of concern regarding the heavy dependence on Double UP for the work presented here. mScarlet is brighter than the mNeon, and there are always a higher number of dim green cells, as cells receiving less total plasmid are less likely to have received a Cre plasmid. It is a concern that these factors in combination would result in higher visibility of red processes, which could lead to the apparent detection of either more and/or longer processes. Additionally, it is possible that the presence of a Cre plasmid could lead to phenotypes on its own, or that a cell receiving more copies of plasmid would have a different phenotype than a cell receiving fewer copies. It is also possible that of the two types of cells at the ventricle, progenitors and neurons, one would be more amenable to transfection, taking in large numbers of plasmids. This could lead to a differential population of cells being labeled, even before any manipulation takes place. In Chapter Two, it was rigorously demonstrated that for cortical migration at E14.5+4, green and red cells behaved similarly. In Chapter Three, every single metric analyzed using

Double UP was first analyzed in the absence of manipulation, both with Double UP alone, and with Double UP and pSico Scrambled shRNA together. For every metric analyzed from control embryonic fixed or live slices (E14.5+4 migration, E14.5+3 migration, E14.5+2 migration, process number, process length, somal translocations, new processes/hour, processes retracted/hour, distance travelled) red and green cells have not been significantly different from each other. All of these data suggest that the use of Double UP in studies of cortical neuron migration will produce more rigorous and repeatable results. Thus, the implementation of Double UP in future studies will provide more accurate determinations of the cadre of proteins that actually play critical roles in neuronal migration.

The only instance of difference between green and red cells has come from observations of postnatal brains (data not shown). Postnatal brains have very high autofluorescence in the green spectrum, and very low autofluorescence in the red spectrum. This leads to Double UP, as currently constituted, being a poor tool for examining later postnatal effects, such as contralateral targeting/branching of axons, or dendritic branching. If Double UP is adopted by the wider scientific community, it will be important that each new metric being analyzed is validated first in the absence of manipulation.

CIP4 Modulation *in utero*

CIP4 overexpression *in utero* suggests that CIP4 expression may be a barrier for neurons to enter the intermediate zone and multipolar phase of development, but this statement has some serious caveats. CIP4 overexpression has been a useful tool for determining the contribution of various functional domains of CIP4 (Taylor et al., 2019), but may be too blunt of a tool to determine the true role of CIP4 *in vivo*. The exact level of overexpression is unclear, but

experiments performed in primary mouse cortical neuron cultures suggest that typical *in vitro* overexpression may exceed 40-fold of endogenous levels (data not shown). Furthermore, these western blots were performed in cultures with less than 50% of cells transfected. Therefore, the levels of bright/highly-expressing CIP4 cells could easily be 80-fold greater than endogenous levels, or even higher. Thus, CIP4 overexpression is likely not representative of "sustained CIP4 expression" and may be instead providing misleading information regarding the timing and nature of the relationship of CIP4 expression to migration.

CIP4 knockdown *in utero,* on the other hand, is likely much more physiologically relevant. Knockdown is a specific, targeted removal of a single protein from a cell. Based on our preliminary findings, we propose that CIP4 mRNA is still being actively translated into CIP4 protein in progenitors and newly born neurons present at the ventricular zone at the time of electroporation, and that loss of CIP4 leads to a neuron being unable to exit the multipolar phase of development. However, these data are from the use of an individual shRNA, and off-target effects remain a possibility. This will be addressed by looking for the same or similar phenotype using a different shRNA to CIP4 or rescue of the phenotype with the expression of low levels of CIP4 that is insensitive to the specific shRNA.

Novel Role for CIP4 in Process Retraction

Presented in Chapter 3 of this thesis is the hypothesis that CIP4 may be acting to retract neurites, and this could either be in contrast to a role of CIP4 inhibiting neurite initiation, or as a mechanism for this neurite inhibition. While either finding would lead to an interesting shift in research direction, it is important to note several things. First, this is based on fairly preliminary

data and basic pattern matching. It is clear that *in vivo*, CIP4 knockdown results in more and longer processes. This may be the result of a lack processes being retracted, as suggested in Chapter 3, Figure 5. Prior to this work, the dominant hypothesis, based on *in vitro* findings, was that CIP4 was acting to delay neurite initiation from the cell body (Saengsawang et al., 2012). These two hypotheses (CIP4 retracting neurites, CIP4 delaying neurite initiation) could be complementary or mutually exclusive. CIP4 could act as a continual retraction force, in an inconsistent equilibrium with a pro-neurite proteins such as FBP17 (Taylor et al., 2019). This could unify the two hypotheses, and lead to CIP4-mediated retraction being the mechanism for CIP4-mediated inhibition of neurite initiation. Alternatively, CIP4 could act only on neurites that have already been established. This would lead to mutually exclusive hypotheses. Determination of the exact role of CIP4 is discussed below (ongoing and future work).

The behavior of growth cone collapse, followed by neuronal process retraction is well studied in the field of neurobiology. Growth cones, first described by Santiago Ramon y Cajal 130 years ago (Cajal, 1890), have been shown to respond positively and negatively to signaling gradients and other cues (Kennedy, Serafini, de la Torre, & Tessier-Lavigne, 1994; Kolodkin & Tessier-Lavigne, 2011; Tessier-Lavigne, Placzek, Lumsden, Dodd, & Jessell, 1988). Many of these studies have focused on the actin cytoskeleton and associated proteins present in growth cones (Dent, Gupton, & Gertler, 2011). It is also clear that large amounts of endocytosis, in the form of macropinocytosis, also occurs during growth cone collapse and that this endocytosis is dependent upon dynamic actin (Fournier et al., 2000; Kabayama et al., 2009). It seems like a logical fit that CIP4 could be involved in growth cone collapse, but at this point it is only speculation. There is not even preliminary data specifically related to growth cones to support

this hypothesis. Experiments are ongoing, relatively straightforward, and addressed in detail in the "ongoing and future work" section below.

While the purpose of neurons undergoing a multipolar phase is still unclear, failure to exit this phase of migration can result in lissencephaly, epilepsy and intellectual disability (Stouffer, Golden, & Francis, 2016). An increasing number of proteins are found to be important for exit from the multipolar stage, including Lis1 (Tsai, Chen, Kriegstein, & Vallee, 2005), Doublecortin (Bai et al., 2003), Filamin A (Nagano, Morikubo, & Sato, 2004), Lamellipodin (Pinheiro et al., 2011) and Nyap1 (Wang et al., 2020). All of these proteins are cytoskeletal-associated proteins, suggesting that remodeling of the cytoskeleton is essential for this morphological transition from multipolar to bipolar morphology. CIP4, another cytoskeletal-associated protein, also appears to have a role in this process, as knockdown results in cells developing more and longer processes, and being stuck in the intermediate zone. In addition to being a cytoskeletal-associated protein, CIP4 is also known to function in endocytosis. CIP4 would be the first endocytic protein identified to be required for exit from the multipolar stage of neuronal migration.

One process in early cortical development that has received little attention is the normal retraction of radial glial processes during cortical maturation. This may be because radial glial retraction is a largely an *in vivo* phenomenon, and therefore more difficult to study. Radial glia can be cultured (Varga & Nagy, 2017), but lacking the tissue structure of the brain will not have long processes to retract following their final division. Retraction *in vivo* has been described but not directly studied, and findings are mixed. Electron microscopy studies published in the 1960s and 1970s describe the retraction (Hinds & Ruffett, 1971; Rakic & Sidman, 1968; Stensaas & Stensaas, 1968), but with the cloning of GFP (Prasher, Eckenrode, Ward, Prendergast, & Cormier,

1992) and the resulting widespread use in the 1990s and onwards, single cell and lineage tracing studies indirectly studied process retraction. Models of glial division have differing findings regarding whether and when radial glial processes retract (Cayouette & Raff, 2003; Miyata et al., 2004; Noctor, Flint, Weissman, Dammerman, & Kriegstein, 2001; Tabata, Kanatani, & Nakajima, 2009). These studies have used different animal models, different timing and different approaches, which may account for some of the distinctions. Based on images of endogenous CIP4 in cortical tissue (Chapter 3 Figure 1), CIP4 is likely present in radial glial processes. Moreover, from the CIP4-knockdown live slice experiments, CIP4 appears to be involved in retraction of radial glial processes. Control cells have either stable radial glial processes, or no radial glial processes to be observed. In contrast, cells lacking CIP4 have highly dynamic, motile processes. Additionally, there may also be a non-autonomous effect. Green cells (control) in brains receiving CIP4 knockdown label a higher percentage of radial glia than red or green cells in control conditions (data not shown). This frustrates analysis, but is potentially an interesting lead to follow up on. Testing for cell autonomous/non autonomous effects of CIP4 loss on radial glia requires further validation and development of a reliable method for quantification, but CIP4 would be the first protein shown to be necessary for retraction of radial glial processes.

Ongoing and Future work

The hypothesis that CIP4 may be involved in neurite retraction was formulated recently and is a work in progress. There are still some very basic questions that need addressing and experiments that need to be performed to test key components and assumptions to increase confidence in this hypothesis.

Cortical migration data presented in this thesis relies upon knockdown of CIP4 over a period of days during mid-gestation. How does this compare with data from CIP4 knockout mice (Feng…Corey, 2010, JBC 285:4348, Saengsawang et al, 2012)? Published data on cortical development in CIP4 knockout mice is lacking. Nevertheless, previous work in our lab demonstrated that CIP4 knockout mice have normal migration, but a defect in neuronal proliferation (data not shown) (Taylor, 2019), as determined by EdU labeling (a thymidine analog which labels dividing cells) (Chehrehasa, Meedeniya, Dwyer, Abrahamsen, & Mackay-Sim, 2009). However, IUE presented here demonstrates that acute knockdown of CIP4 results in both a morphological and migration defect. The primary discrepancy between knockout and IUE data is that CIP4 knockout does not affect migration by one metric (EdU), while acute knockdown of CIP4 does affect migration by another metric (IUE). This inconsistency will need addressing to determine the role of CIP4 and neurite inhibition/retraction in radial migration. In the knockout animals it could be an issue of compensation, as is suspected with DCX (Reiner, Gorelik, & Greenman, 2012). It could also be an issue of off-target effects of the shRNA used in IUE, as results are currently derived from one single shRNA. Determining which result is causing a distinction is critical, but addressable. Potential off-target effects of shRNAs can be addressed by using other shRNAs targeting CIP4 and/or rescuing the effects of knockdown by inclusion of a low concentration of CIP4 that is not sensitive to the shRNA. To address both potential issues simultaneously, IUE can be performed in CIP4 knockout animals. IUE of GFP alone will allow for determination of morphology of individual neurons, to test if the morphological effects of CIP4 knockout neurons is similar to that of acute CIP4 knockdown neurons. Additionally, IUE of CIP4

shRNA should not generate any phenotype in CIP4 knockout animals beyond that seen with GFP alone, if CIP4 shRNA is faithfully targeting CIP4.

If CIP4 is retracting neurites *in vivo*, it is most likely having a similar effect *in vitro*, and this should be relatively simple to determine. The more interesting finding would still be the *in vivo* findings, but if this phenomenon can be studied *in vitro* it allows for greater access to easier experiments, thus increasing the power of analysis. Neurons can be plated from either knockout animals (which we have) or from wildtype animals with endogenous CIP4 knocked down via transfection with shRNA. These neurons will be allowed to develop, while timelapse imaging occurs. This experiment will allow for simple quantification of neurite initiation and retraction events for many neurons. Comparison with wildtype neurons (if using knockout) or neurons transfected with scrambled shRNA will allow for knowing what is “normal”, and whether CIP4 knockout/knockdown neurons do indeed have delayed neurite initiation, reduced neurite retraction, both or neither.

After neurons have been allowed to develop, we will perform growth cone collapse assays on wildtype and CIP4 knockdown/knockout neurons. If CIP4 is involved in growth cone collapse, neurons lacking CIP4 should have reduced or eliminated growth cone collapse in response to a repulsive cue, such as Sema3a (Luo, Raible, & Raper, 1993), which is present in early developing cortex (Polleux, Giger, Ginty, Kolodkin, & Ghosh, 1998). It will also be interesting to determine if CIP4 is involved in responses of cortical neurons to attractive cues, such as BDNF (Paves & Saarma, 1997).

Neurons exiting the multipolar phase re-enter a bipolar phase, with a leading process directed radially towards the pial surface, and a trailing process directed into the intermediate

zone and the corpus callosum (Noctor, Martinez-Cerdeno, Ivic, & Kriegstein, 2004). If CIP4 is acting to retract neurites, it may be involved in controlling orientation of a neuron, by restricting neurite outgrowth in incorrect directions. This can be tested using the iLid/Lov2 system (Guntas et al., 2015) to allow for targeted sequestration and inactivation of CIP4, to test the hypothesis that CIP4 is restricting neurite/process initiation in certain directions. CIP4 would be overexpressed in neurons, and then sequestered to mitochondria in differing sized regions of the neuron. If CIP4 is acting to control directionality of neurite initiation, inactivating in one quadrant of the neuron should lead to neurite initiation in that portion. If these experiments are fruitful *in vitro*, it should be feasible to attempt to replicate them *in vivo*, although admittedly with lower spatial and temporal resolution. This would allow further testing to determine if CIP4 is acting to delay/retract neurites and to select neurites growing in the optimal directions.

The transgenic mouse introduced in Chapter three was initially constructed with the mScarlet dependent upon Cre for activation. The intent was to introduce Cre-Dependent mNeon (flox-stop mNeon) along with Cre plasmid, to recombine the genomic locus within individual cells. This was to allow for visualization of the entirety of a cell using the mNeon, and localize CIP4 within that cell using mScarlet. These experiments have failed entirely and repeatedly. The flox-stop mNeon works well, but there are two likely points of failure. It could be that transcription of CIP4 is largely or completely finished by the time a neuron is born, and therefore the Cre is reaching the cell too late. Cre will only recombine genomic DNA, and not have an effect on already transcribed mRNA. It is also possible that the CIP4-mScarlet is too dim to be visualized at the level of a single cell in a cortex with relatively low background.

The transgenic mouse was designed with an easily utilized HA-tag to allow for pull-down and mass spectrometry experiments, and preliminary work is being undertaken in that direction. This work could identify the proteins CIP4 interacts with, specifically in neurons, that lead to the unique neuronal phenotype of CIP4. We have hypothesized that CIP4 may compete for binding partners with "pro-neurite" proteins, and that this competition underlies the equilibrium of extending and retracting neurites during multipolar morphology. Further testing of this hypothesis relies on identifying with which proteins CIP4 is typically interacting. Work is currently being performed to identify a non-neuronal tissue that can operate as a suitable control for immunoprecipitation and mass spectrometry analysis of CIP4-HA binding partners. A more ideal option would be to generate an FBP17-3x Flag mouse, and compare CIP4 and FBP17 binding partners in developing cortical tissue, because they have such different localization patterns in neurons, with CIP4 localized to protruding plasma membrane and FBP17 localized to elongated, endocytosed vesicles.

Studies on CIP4 localization in dissociated neurons have relied upon overexpression of CIP4, resulting in strong phenotypes (Saengsawang et al., 2012; Saengsawang et al., 2013; Taylor et al., 2019). These have been useful for determining the necessity of various domains of CIP4 in localization and function (Taylor et al., 2019), but as the neurons do not differentiate normally it has not been possible to determine the localization and expression of CIP4 in normally developing neurons. Based on our hypothesis that CIP4 is involved in neurite retraction, we expect to see CIP4 localizing to neurites prior/during retraction, but absent from neurites that prove to be more permanent. These hypotheses are now possible due to the endogenously labelled CIP4-mScarlet mice.

Conclusion

Work presented here clearly demonstrates a role for CIP4 in neuronal migration. CIP4 is an unusual protein, as it is only expressed prenatally in the brain and seems to function to delay neuronal differentiation and process outgrowth (Saengsawang et al., 2012). *In vivo*, overexpression of CIP4 represses neurite formation and stalls neurons prior to entering the intermediate zone, where the bipolar-to-multipolar transition would take place. Examining the effects of knockdown *in utero* suggest that CIP4 is critical for exit of the multipolar stage of neuronal migration and development. Together, these findings indicate that CIP4 expression is critical to allow for normal migration of the neuron. Too much, or too little CIP4 results in neurons that fail to migrate. The knockdown data in particular suggests neurons must properly downregulate CIP4 expression to undergo migration, and the mechanism of this downregulation is of great interest and will be determined in future studies.

It is still unclear exactly which step or steps of neuritogenesis CIP4 is involved. It could be functioning to delay entrance into the multipolar phase, until cells reach the intermediate zone. This hypothesis is supported by the overexpression and knockdown data. Cells with overexpressed CIP4 fail to enter the intermediate zone, and cells with CIP4 knocked down have more and longer processes, which may occur from premature initiation of processes. CIP4 could also function at the end of the multipolar phase, restricting new processes from initiating once the cell is ready to exit the multipolar phase, or retracting minor processes to allow the cell to resume the bipolar morphology that accompanies further neuronal migration. This is especially supported by the knockdown studies, as cells lacking CIP4 seem unable to exit the multipolar

phase and resume bipolar morphologies. Careful experimentation, and further analysis of the CIP4 knockdown phenotype should continue to shed light on this issue. As more and more cells can be followed through their development, it should become clear at which stages the timing is altered by a lack of CIP4. Understanding the role of CIP4 in neuronal development and migration will help clarify the role of neurite formation and retraction in cortical development, especially with regards to the still mysterious multipolar phase of cortical migration.

References

Bai, J., Ramos, R. L., Ackman, J. B., Thomas, A. M., Lee, R. V., & LoTurco, J. J. (2003). RNAi reveals doublecortin is required for radial migration in rat neocortex. *Nat Neurosci, 6*(12), 1277-1283. doi:10.1038/nn1153

Cajal, S. R. (1890). Sobre la aparición de las expansiones celulares en la médula embrionaria. *Gac. Sanit. Barc., 12*, 413–419.

Cayouette, M., & Raff, M. (2003). The orientation of cell division influences cell-fate choice in the developing mammalian retina. *Development, 130*(11), 2329-2339. doi:10.1242/dev.00446

Chehrehasa, F., Meedeniya, A. C., Dwyer, P., Abrahamsen, G., & Mackay-Sim, A. (2009). EdU, a new thymidine analogue for labelling proliferating cells in the nervous system. *J Neurosci Methods, 177*(1), 122-130. doi:10.1016/j.jneumeth.2008.10.006

Dent, E. W., Gupton, S. L., & Gertler, F. B. (2011). The growth cone cytoskeleton in axon outgrowth and guidance. *Cold Spring Harb Perspect Biol, 3*(3). doi:10.1101/cshperspect.a001800

Fang, H., Bygrave, A. M., Roth, R. H., Johnson, R. C., & Huganir, R. L. (2021). An optimized CRISPR/Cas9 approach for precise genome editing in neurons. *Elife, 10*. doi:10.7554/eLife.65202

Flum, P. (2018). Why binning continuous data is almost always a mistake. *medium.com*.

Fournier, A. E., Nakamura, F., Kawamoto, S., Goshima, Y., Kalb, R. G., & Strittmatter, S. M. (2000). Semaphorin3A enhances endocytosis at sites of receptor-F-actin colocalization during growth cone collapse. *J Cell Biol, 149*(2), 411-422. doi:10.1083/jcb.149.2.411

Guntas, G., Hallett, R. A., Zimmerman, S. P., Williams, T., Yumerefendi, H., Bear, J. E., & Kuhlman, B. (2015). Engineering an improved light-induced dimer (iLID) for controlling the localization and activity of signaling proteins. *Proc Natl Acad Sci U S A, 112*(1), 112-117. doi:10.1073/pnas.1417910112

Hamabe-Horiike, T., Kawasaki, K., Sakashita, M., Ishizu, C., Yoshizaki, T., Harada, S. I., . . . Kawasaki, H. (2021). Glial cell type-specific gene expression in the mouse cerebrum using the piggyBac system and in utero electroporation. *Sci Rep, 11*(1), 4864. doi:10.1038/s41598-021-84210-z

Hinds, J. W., & Ruffett, T. L. (1971). Cell proliferation in the neural tube: an electron microscopic and golgi analysis in the mouse cerebral vesicle. *Z Zellforsch Mikrosk Anat, 115*(2), 226-264. doi:10.1007/BF00391127

Hu, S., Yang, T., & Wang, Y. (2021). Widespread labeling and genomic editing of the fetal central nervous system by in utero CRISPR AAV9-PHP.eB administration. *Development, 148*(2). doi:10.1242/dev.195586

Kabayama, H., Nakamura, T., Takeuchi, M., Iwasaki, H., Taniguchi, M., Tokushige, N., & Mikoshiba, K. (2009). Ca2+ induces macropinocytosis via F-actin depolymerization during growth cone collapse. *Mol Cell Neurosci, 40*(1), 27-38. doi:10.1016/j.mcn.2008.08.009

Kennedy, T. E., Serafini, T., de la Torre, J. R., & Tessier-Lavigne, M. (1994). Netrins are diffusible chemotropic factors for commissural axons in the embryonic spinal cord. *Cell, 78*(3), 425-435. doi:10.1016/0092-8674(94)90421-9

Kolodkin, A. L., & Tessier-Lavigne, M. (2011). Mechanisms and molecules of neuronal wiring: a primer. *Cold Spring Harb Perspect Biol, 3*(6). doi:10.1101/cshperspect.a001727

Luo, Y., Raible, D., & Raper, J. A. (1993). Collapsin: a protein in brain that induces the collapse and paralysis of neuronal growth cones. *Cell, 75*(2), 217-227. doi:10.1016/0092-8674(93)80064-l

Miyata, T., Kawaguchi, A., Saito, K., Kawano, M., Muto, T., & Ogawa, M. (2004). Asymmetric production of surface-dividing and non-surface-dividing cortical progenitor cells. *Development, 131*(13), 3133-3145. doi:10.1242/dev.01173

Morita, K., Matsumoto, N., Saito, K., Hamabe-Horiike, T., Mizuguchi, K., Shinmyo, Y., & Kawasaki, H. (2021). BMP signaling alters aquaporin-4 expression in the mouse cerebral cortex. *Sci Rep, 11*(1), 10540. doi:10.1038/s41598-021-89997-5

Nagano, T., Morikubo, S., & Sato, M. (2004). Filamin A and FILIP (Filamin A-Interacting Protein) regulate cell polarity and motility in neocortical subventricular and intermediate zones during radial migration. *J Neurosci, 24*(43), 9648-9657. doi:10.1523/JNEUROSCI.2363-04.2004

Nguyen, L. H., & Bordey, A. (2021). Convergent and Divergent Mechanisms of Epileptogenesis in mTORopathies. *Front Neuroanat, 15*, 664695. doi:10.3389/fnana.2021.664695

Noctor, S. C., Flint, A. C., Weissman, T. A., Dammerman, R. S., & Kriegstein, A. R. (2001). Neurons derived from radial glial cells establish radial units in neocortex. *Nature, 409*(6821), 714-720. doi:10.1038/35055553

Noctor, S. C., Martinez-Cerdeno, V., Ivic, L., & Kriegstein, A. R. (2004). Cortical neurons arise in symmetric and asymmetric division zones and migrate through specific phases. *Nat Neurosci, 7*(2), 136-144. doi:10.1038/nn1172

Paves, H., & Saarma, M. (1997). Neurotrophins as in vitro growth cone guidance molecules for embryonic sensory neurons. *Cell Tissue Res, 290*(2), 285-297. doi:10.1007/s004410050933

Pinheiro, E. M., Xie, Z., Norovich, A. L., Vidaki, M., Tsai, L. H., & Gertler, F. B. (2011). Lpd depletion reveals that SRF specifies radial versus tangential migration of pyramidal neurons. *Nat Cell Biol, 13*(8), 989-995. doi:10.1038/ncb2292

Polleux, F., Giger, R. J., Ginty, D. D., Kolodkin, A. L., & Ghosh, A. (1998). Patterning of cortical efferent projections by semaphorin-neuropilin interactions. *Science, 282*(5395), 1904-1906. doi:10.1126/science.282.5395.1904

Prasher, D. C., Eckenrode, V. K., Ward, W. W., Prendergast, F. G., & Cormier, M. J. (1992). Primary structure of the Aequorea victoria green-fluorescent protein. *Gene, 111*(2), 229-233. doi:10.1016/0378-1119(92)90691-h

Rakic, P., & Sidman, R. L. (1968). Supravital DNA synthesis in the developing human and mouse brain. *J Neuropathol Exp Neurol, 27*(2), 246-276. Retrieved from https://www.ncbi.nlm.nih.gov/pubmed/5646196

Reiner, O., Gorelik, A., & Greenman, R. (2012). Use of RNA interference by in utero electroporation to study cortical development: the example of the doublecortin superfamily. *Genes (Basel), 3*(4), 759-778. doi:10.3390/genes3040759

Saengsawang, W., Mitok, K., Viesselmann, C., Pietila, L., Lumbard, D. C., Corey, S. J., & Dent, E. W. (2012). The F-BAR protein CIP4 inhibits neurite formation by producing lamellipodial protrusions. *Curr Biol, 22*(6), 494-501. doi:10.1016/j.cub.2012.01.038

Saengsawang, W., Taylor, K. L., Lumbard, D. C., Mitok, K., Price, A., Pietila, L., . . . Dent, E. W. (2013). CIP4 coordinates with phospholipids and actin-associated proteins to localize to the protruding edge and produce actin ribs and veils. *J Cell Sci, 126*(Pt 11), 2411-2423. doi:10.1242/jcs.117473

Stensaas, L. J., & Stensaas, S. S. (1968). An electron microscope study of cells in the matrix and intermediate laminae of the cerebral hemisphere of the 45 mm rabbit embryo. *Z Zellforsch Mikrosk Anat, 91*(3), 341-365. doi:10.1007/BF00440763

Stouffer, M. A., Golden, J. A., & Francis, F. (2016). Neuronal migration disorders: Focus on the cytoskeleton and epilepsy. *Neurobiol Dis, 92*(Pt A), 18-45. doi:10.1016/j.nbd.2015.08.003

Tabata, H., Kanatani, S., & Nakajima, K. (2009). Differences of migratory behavior between direct progeny of apical progenitors and basal progenitors in the developing cerebral cortex. *Cereb Cortex, 19*(9), 2092-2105. doi:10.1093/cercor/bhn227

Taylor, K. L. (2019). Opposing functions of F-BAR proteins CIP4 and FBP-17 in neuronal membrane protrusion, tubule formation and cortical neuronal development (Thesis).

Taylor, K. L., Taylor, R. J., Richters, K. E., Huynh, B., Carrington, J., McDermott, M. E., . . . Dent, E. W. (2019). Opposing functions of F-BAR proteins in neuronal membrane protrusion, tubule formation, and neurite outgrowth. *Life Sci Alliance, 2*(3). doi:10.26508/lsa.201800288

Tessier-Lavigne, M., Placzek, M., Lumsden, A. G., Dodd, J., & Jessell, T. M. (1988). Chemotropic guidance of developing axons in the mammalian central nervous system. *Nature, 336*(6201), 775-778. doi:10.1038/336775a0

Tsai, J. W., Chen, Y., Kriegstein, A. R., & Vallee, R. B. (2005). LIS1 RNA interference blocks neural stem cell division, morphogenesis, and motility at multiple stages. *J Cell Biol, 170*(6), 935-945. doi:10.1083/jcb.200505166

Varga, B., & Nagy, A. (2017). Isolation, Propagation, and Differentiation of Radial Glia-Like Neural Progenitor Cells in Adherent Cultures. *Cold Spring Harb Protoc, 2017*(9), pdb prot094177. doi:10.1101/pdb.prot094177

Wang, S., Li, X., Zhang, Q., Chai, X., Wang, Y., Forster, E., . . . Zhao, S. (2020). Nyap1 Regulates Multipolar-Bipolar Transition and Morphology of Migrating Neurons by Fyn Phosphorylation during Corticogenesis. *Cereb Cortex, 30*(3), 929-941. doi:10.1093/cercor/bhz137